Widi Sunaryo

Secondary growth in the *Arabidopsis* hypocotyl

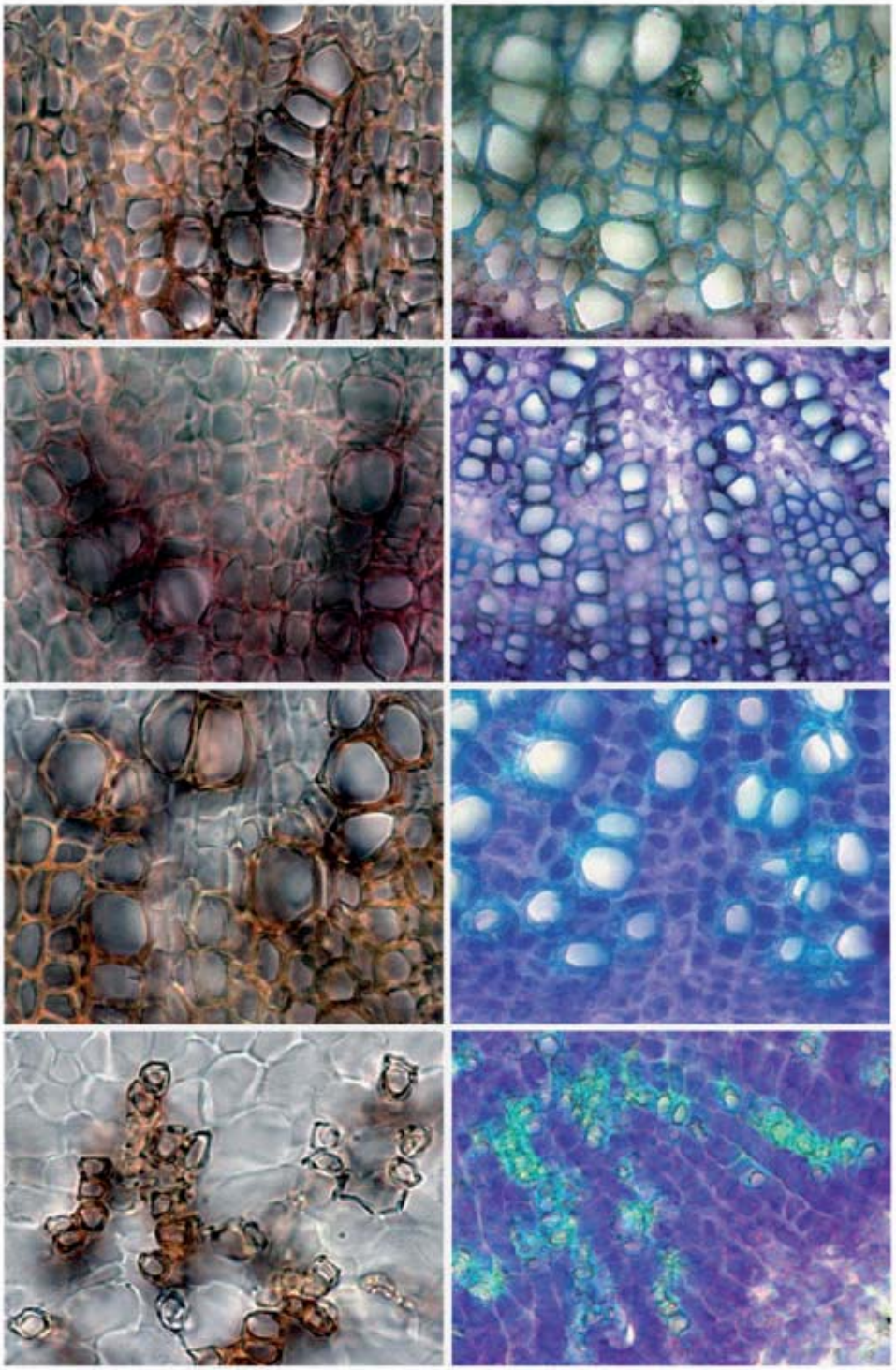

Cuvillier Verlag Göttingen
Internationaler wissenschaftlicher Fachverlag

Secondary growth in the *Arabidopsis* hypocotyl

Dissertation

In Partial Fulfillment of the Requirements for the Degree Doctor of Philosophy (PhD)

of the Faculty of Forest Sciences and Forest Ecology

Georg-August-University Göttingen

Submitted by

WIDI SUNARYO

born in Blitar, Indonesia

Göttingen, November 2010

Bibliografische Information der Deutschen Nationalbibliothek
Die Deutsche Nationalbibliothek verzeichnet diese Publikation in der Deutschen Nationalbibliografie; detaillierte bibliografische Daten sind im Internet über http://dnb.d-nb.de abrufbar.
1. Aufl. - Göttingen : Cuvillier, 2010
Zugl.: Göttingen, Univ., Diss., 2010

978-3-86955-588-1

D7

1. Referee: Prof. Dr. Andrea Polle
2. Referee: PD Dr. Thomas Teichmann

Date of Oral Examination: 19 November, 2010

Nonnenstieg 8, 37075 Göttingen
Telefon: 0551-54724-0
Telefax: 0551-54724-21
www.cuvillier.de

1. Auflage, 2010
Gedruckt auf säurefreiem Papier

978-3-86955-588-1

Dedicated to:

My beloved late grandmother “Mbah Jami”

Declaration

I declare on oath, that I have done the thesis with the title "Secondary growth in the *Arabidopsis* hypocotyl" in the department Forest Botany and Tree Physiology under the supervision of Prof. Dr. Andrea Polle without any other help and I did not use any unlicensed subjects. I did not present the thesis to any other examination procedure before. Up to now I did not get the aspired grade anywhere and did not fail in any earlier doctoral exam.

Göttingen, 19 November 2010

Widi Sunaryo

Table of contents

List of tables

List of figures

List of gene abbreviations

ARF4	:	*AUXIN RESPONSE FACTOR 4*
AtCL1	:	*Arabidopsis thaliana 4-COUMARATE:COA LIGASE 1*
ATHB-8	:	*ARABIDOPSIS THALIANA HOMEOBOX GENE 8*
BELL	:	*BELLINGER*
BP	:	*BREVIPEDICELLUS*
CAD1	:	*CINNAMYL ALCOHOL DEHYDROGENASE 1*
CesA4 (IRX5)	:	*CELLULOSE SYNTHASE 4 (IRREGULAR XYLEM 5)*
CesA7 (IRX3)	:	*CELLULOSE SYNTHASE 7 (IRREGULAR XYLEM 3)*
CesA8 (IRX1)	:	*CELLULOSE SYNTHASE 8 (IRREGULAR XYLEM 1)*
COBL4 (IRX6)	:	*COBRA-LIKE 4 (IRREGULAR XYLEM 6)*
CTL2 (GH19)	:	*CHITINASE-LIKE PROTEIN 2 (GLYCOSIDE HIDROLASE FAMILY 19)*
FLA11	:	*FASCICLIN-LIKE ARABINOGALACTAN-PROTEIN 11*
GAUT12(IRX8)	:	*GALACTURONOSYLTRANSFERASE 12 (IRREGULAR XYLEM 8)*
GH28	:	*GLYCOSIDE HIDROLASE FAMILY 19*
IAA27	:	*INDOLE-3-ACETIC ACID 27*
KNAT1	:	*KNOTTED-LIKE FROM ARABIDOPSIS THALIANA 1*
KNAT2	:	*KNOTTED-LIKE FROM ARABIDOPSIS THALIANA 2*
KNAT3	:	*KNOTTED-LIKE FROM ARABIDOPSIS THALIANA 3*
KNAT4	:	*KNOTTED-LIKE FROM ARABIDOPSIS THALIANA 4*
KNAT5	:	*KNOTTED-LIKE FROM ARABIDOPSIS THALIANA 5*
KNAT6	:	*KNOTTED-LIKE FROM ARABIDOPSIS THALIANA 6*
KNAT7	:	*KNOTTED-LIKE FROM ARABIDOPSIS THALIANA 7*
LAC4 (IRX12)	:	*LACCASE 4 (IRREGULAR XYLEM 12)*
LTP4	:	*LIPID TRANSFER PROTEIN 4*
NST1	:	*NAC SECONDARY WALL THICKENING PROMOTING FACTOR 1*
PAL1	:	*PHENYLALANINE AMMONIA-LYASE 1*
PAL4	:	*PHENYLALANINE AMMONIA-LYASE 4*
PME61	:	*PECTIN METHYLESTERASE 61*
PRX	:	*PEROXIDASE*
SND1	:	*SECONDARY WALL-ASSOCIATED NAC DOMAIN 1*
SND2	:	*SECONDARY WALL-ASSOCIATED NAC DOMAIN 2*
STM	:	*SHOOT MERISTEMLESS*

Summary

Secondary growth results from cell division and differentiation in the vascular cambium and gives rise to secondary xylem and phloem. Xylem of trees, commonly referred to as wood, is an important carbon source used for woody materials and industrial purposes such as timber, pulp, furniture, fibers, and also as a energy source. Although abundant data has been collected to address the genetic control of cambial activity and differentiation, the mechanism behind is still little known. The *Arabidopsis* hypocotyl has previously been shown to be a suitable model for secondary growth and xylem differentiation similar as it occurs in angiosperm trees.

Plant development requires a tightly controlled balance between undifferentiated dividing cells and cells, which are subjected to undergo differentiation. In the shoot apical meristem of *Arabidopsis*, this process is governed by a complex signaling network involving several classes of transcription factors, which are often expressed in highly distinct patterns. Key-players of differentiation control are the *KNOX* genes (*Knotted-1* like genes; e.g. *KNAT1*, *KNAT2*, *STM*), which comprise a small gene family with eight members in *Arabidopsis thaliana*. This project was aimed to investigate the role of *KNOX* genes in secondary growth and differentiation of xylem using the *Arabidopsis* hypocotyl as a model.

T-DNA insertion mutants for all *Arabidopsis KNOX* genes were isolated. Mutants of *stm* and *knat1* showed reduced xylem diameter and xylem fiber formation. The double mutant *stm-GK;knat1*$^{bp-9}$ had a strongly enhanced phenotype. *STM* and *KNAT1* were expressed in the cambial zone and their expression was not dependent on each other. Taken together this shows that *STM* and *KNAT1* have overlapping function and act synergistically on cambial activity and differentiation of xylem derivates.

Neither constitutive nor inducible overexpression of *KNAT1* led to overproduction of xylem. Moreover, overexpression of *KNAT1* could not complement the effects of *stm-GK* on xylem formation. This points to a requirement of optimal concentration for both genes, as it is often observed for physically interacting proteins.

KNAT1 and *STM* function are required for *ATHB-8* expression, a marker of early vascularization, in early xylem fiber derivates. *CyclinB1;1::GUS*, a cell divison reporter, showed that parenchymatic cells, which occurred instead of xylem fibers are no longer mitotically active. Hence, they are blocked in an early step of differentiation.

By co-expression analysis and qRT-PCR *STM*/*KNAT1* were found to regulate various genes, which are required for or associated with secondary cell wall formation, as the cellulose synthases (*IRX1, IRX3* and *IRX5*), *COBRA-LIKE4* (*IXR6*), *PECTIN METHYLESTERASE61 (PME61)*, and *FASICLIN-LIKE ARABIONGALACTAN11* (*FLA11*). Furthermore, *STM* and *KNAT1* were upstream of transcription factors, which determine xylem fiber (*SND1* and *NST1*) and vessel (*SND2*) identity. In contrast key-genes of lignin biosynthesis were not expressed differentially in the mutants. Together this indicates that *STM* and *KNAT1* promote early differentiation of xylem derivates but are not directly involved in later steps of secondary cell wall formation, i.e. in lignification.

In stark contrast to this work, *KNAT1* has previously been described as a repressor of lignification in the inflorescences stem of *Arabidopsis*. Further experiments will be required in order to resolve this contradiction.

1 Introduction

1.1 Secondary growth in plant stems and the activity of vascular cambium

Secondary growth is additional growth that thickens the stem and root after primary growth, usually elongation growth, is completed (Evert, 2006). In trees, secondary growth is represented by the stem or root diameter. Secondary growth is a result of cell division and differentiation in the vascular cambium. The vascular cambium consists of a mantle of cells between the phloem and xylem to which it gives rise. In contrast to the shoot apical meristem (SAM) that occupies the shoot tip, the cambium is displaced towards the outer side of the plant axis and is therefore considered as a lateral meristem. Vascular cambial cells are derived mostly from procambial cells which develop during vascularization in the primary stem (Raven et al. 1999). The cambial cells divide periclinally to produce xylem and phloem. Daughter cells of the cambium differentiate to the outer side into phloem and to the inner side into xylem to produce radial files of cells that meet at the cambial zone (Figure 1A). The phloem ensures the transport of photoassimilates from source leaves to sink tissues such as the shoot apical meristem and the stem; whereas the xylem transports mainly water and mineral solutes from the root to the shoot. Xylem of trees, commonly referred to as wood, is an important source of fixed carbon used for woody materials and industrial purposes such as timber, pulp, furniture, fibers, and also as energy source or for other products (films, adhesives, etc).

During secondary growth, cambial daughter cells develop and specialize to xylem cells (Figure 1 B). Xylem cells undergo progressive stages of differentiation; (1) elongation/ enlargement, (2) secondary cell wall deposition, and (3) programmed cell death before being mature xylem (Turner et al. 2008). The hallmark of mature xylem is secondary cell wall deposition. Secondary cell wall formation contributes to a large extent to the biomass of wooden tissues. The major compounds of secondary cell walls are cellulose, hemicelluloses and lignin. The wood of economically important poplar trees typically consists of 45 % of cellulose, 25 % hemicelluloses and 20 % of lignin (Timell et al. 1969; McDougall et al. 1993).

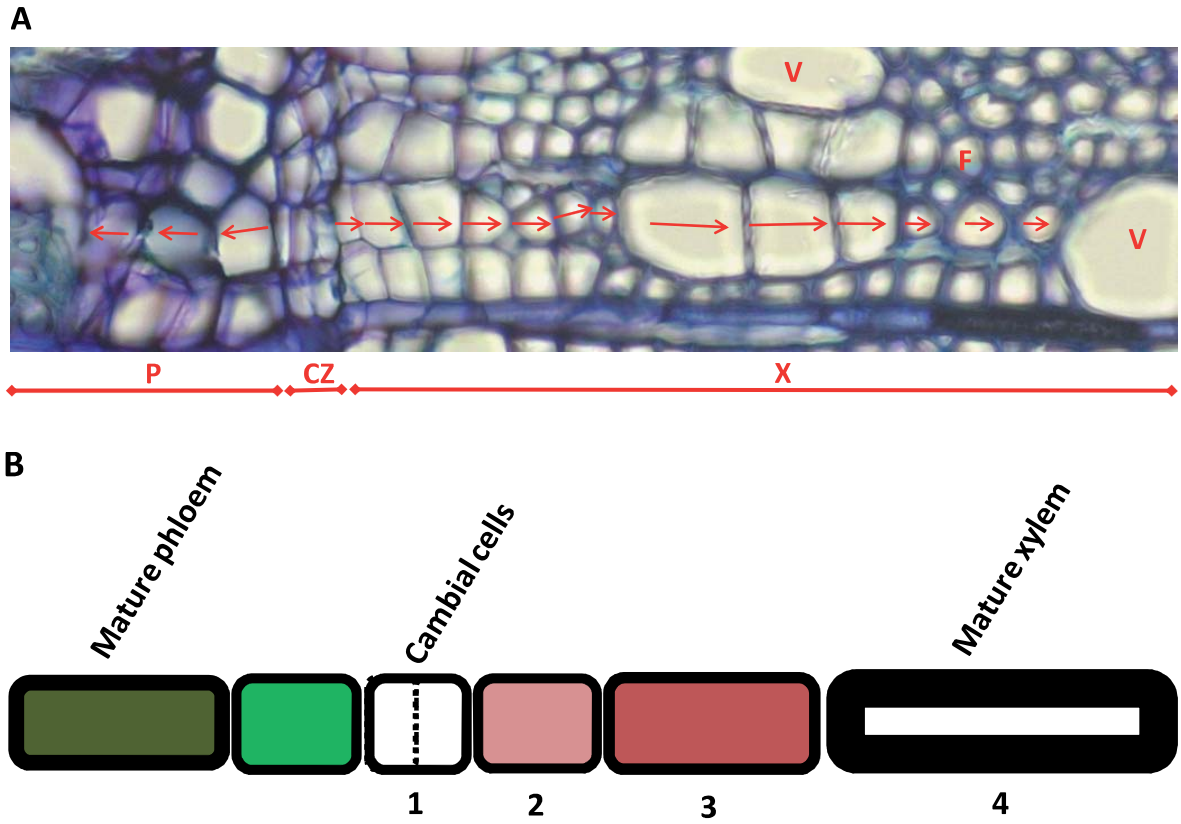

Figure 1. (A) Formation of xylem and phloem from cambial cell divisions in poplar (*Populus x canescens*). (CZ) Cambial zone, (X) xylem, (P) phloem, (V) vessel elements, (F) fibers and (red arrows) radial files of cambial derivates. (B) Differentiation and maturation of cambial daughter cells, schematically. (1) Cell division, (2) cell enlargement, (3) secondary cell wall deposition, (4) programmed cell death.

1.2 *KNOX* (*Knotted-1 Like homeobox*) gene function in plant development

KNOTTED1-like homeobox (*KNOX*) genes are families of homeobox genes identified in all monocot and dicot species and subsets of these genes regulate meristem function in all higher plant (Scofield and Murray, 2006). Homeobox genes encode proteins containing a conserved DNA-binding homeodomain motif that is found in transcription factors from all eukaryotes. Most homeobox genes encode transcription factors, which function in developmental processes. The first homeobox gene identified by mutation is *ANTENNAPEDIA* in *Drosophila melanogaster*. Mutations in *ANTENNAPEDIA* cause a homeotic conversion of organs, with antennae replaced by legs (Gehring, 1987). After that, many homeobox genes were found to play an important role in eukaryote development.

In plants, the first homeobox gene was identified in maize and called *ZmKN1* (*Zea mays KNOTTED1*) (Vollbrecht et al. 1991). Dominant mutations in *ZmKN1* inhibit leaf differentiation and cause the formation of knot-like meristematic structures in the vicinity of leaf veins suggesting *ZmKN1* to play an important role in regulation of meristematic fate (Smith et al. 1992; Sinha et al. 1993). Homologues homeobox genes were therefore termed as *KNOTTED1-like* or *KNOTTED1-like* homeobox (*KNOX*) genes (Lincoln et al. 1994; Long et al. 1996). Thereafter different classes of homeobox genes have been identified in plants like the *WOX (WUSCHEL* related homeobox*)* gene family members involved in early embryonic patterning in *Arabidopsis* (Haecker et al. 2004), the *BELL* family genes (Reiser et al. 1995) and the *HD-ZIP* (homeodomain protein containing a leucine zipper) (Sessa et al.1993).

Based on phylogenetic analyses of amino acid and nucleotide sequences, there are eight members of *KNOX* genes divided into two sub families in *Arabidopsis* (Scofield and Murray, 2006). The subfamily *KNOX* I comprises *STM, KNAT1, KNAT2* and *KNAT6* and the subfamily *KNOX* II comprises *KNAT3, KNAT4, KNAT5* and *KNA7* (Figure 2).

A well-characterized member of the class I *KNOX* genes is *SHOOT MERISTEMLESS* (*STM*), which is expressed in the centre of the shoot apical meristem (SAM) but not in the newly formed leaf primordia and in the incipient leaf (Long et al. 1996). Loss-of-function mutations in *STM* lead to premature differentiation of meristematic cells and eventually to cessation of the SAM (Long et al. 1996); but its simultaneous over-expression together with the homeodomain transcription factor *WUSCHEL* induces meristem formation at ectopic places (Lenhard et al. 2002). These findings indicate that *STM* is a critical regulator of differentiation, whose expression is required to keep cells in an undifferentiated state. The other characterized members of the class I *KNOX* genes fulfill partly redundant functions to *STM* and are generally suggested to be involved in preventing differentiation of the tissue where they are expressed (Scofield and Murray, 2006). In contrast to class I *KNOX* genes, the members of class II *KNOX* genes are only scarcely described and functional data is mostly lacking.

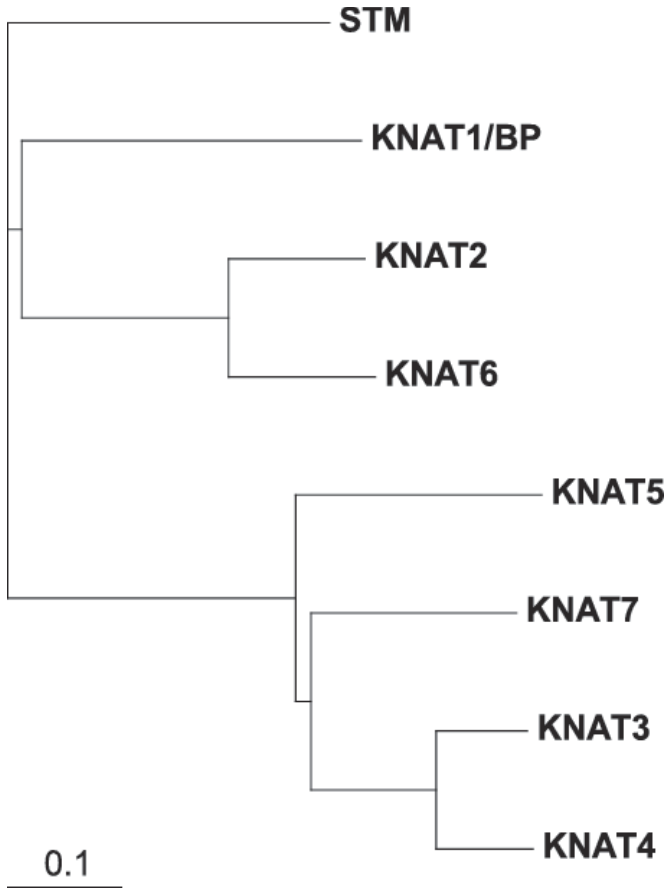

Figure 2. Phylogenetic relationship of the eight *Arabidopsis* KNOX proteins. Tree is consistant with published data (Scofield and Murray, 2006). Tree was drawn by using Treview (Sunaryo and Fischer, 2009)

1.3 Molecular and genetic control of secondary growth, xylem differentiation and secondary cell wall deposition

Although abundant data has been collected to address the genetic control of cambial activity and differentiation, the mechanism behind is still little known. In the model tree poplar however, evidence for an involvement of *KNOX* genes in controlling differentiation of cambial daughter cells has been recently found. High resolution transcript analyses of the poplar cambium had been exploited and showed several *KNOX* genes with strong cambial expression (Hertzberg et al. 2001; Schrader et al. 2004). Furthermore, the current understanding of the regulation of differentiation in vascular development was greatly enhanced by the study of the poplar *KNOX* gene *ARBORKNOX1* (*ARK1*) and *ARBORKNOX2* (*ARK2*), which are close homologues of the *Arabidopsis STM* and *BREVIPEDICELLUS(BP/KNAT1)*, respectively. *ARK1* was shown to be expressed in the cambium and over-expression of *ARK1* leads to inhibition of differentiation of vascular

cells (Groover et al. 2006). This is in line with the proposed role for *KNOX* genes in keeping cells undifferentiated. The *KNAT1* homolog, *ARK2*, was also shown to be expressed in the cambial zone and to be involved in cambial daughter cell differentiation, since downregulation of the endogenous gene by artificial miRNA-suppression led to additional secondary growth and premature secondary xylem formation (Du et al. 2009). Despite this progress, the functional analysis of gene families in poplar is strongly restricted by the long regeneration time of transgenic poplar, by the difficulty to construct loss-of-function alleles and by a steep developmental apical-basal gradient in the young stem.

The *Arabidopsis* hypocotyl has previously been shown to be a suitable model for secondary growth and xylem differentiation similar as it occurs in angiosperm trees and has therefore been suggested as a model for wood formation (Chaffey et al. 2002; Nieminen et al. 2004). Importantly, the hypocotyl does not have an apical-basal developmental gradient, as it occurs in stems (Sibout et al. 2008). However functional studies of *KNOX* gene function in regard to secondary growth of the vascular cambium in the hypocotyl have not yet been performed. In contrast to the hypocotyl, *KNOX* gene function has been addressed in the *Arabidopsis* inflorescence. Ko and Han (2004) reported that *STM* is expressed in the inflorescence stem harvested from three different stages of development: immature, intermediate, and mature. *KNAT7* was also observed to be expressed in the same tissues. Mele et al (2003) investigated the regulation of differentiation in vascular development in inflorescence stems by studying mutants of *KNAT1*/*BP* (*BREVIPEDICELLUS*). *knat1* mutants show an increase in lignification among various developmental defects of the cambial daughter cells; whereas over-expression of *KNAT1* leads to a decrease in lignin deposition (Mele et al. 2003). Other homeodomain transcription factors from class III *HD-ZIP* and *KANADI* gene family members such as *NAC, AP2, MADS*, and *MYB* have been reported to regulate cambial cell differentiation and activity in *Arabidopsis* (Zhao et al. 2005). Moreover, a leucine zipper (HD-ZIP) gene family, comprising amongst others, *ATHB-8*, *ATHB-9*, and *ATHB-14*, has been reported to play an important role in vascular development (Roberts and McCann, 2000).

Xylem cells comprise xylem vessels, fibers, parenchyma cells, and radial ray cells (Evert, 2006). One of the most studied type of xylem cells concerning cell differentiation in plants are the tracheary elements. Using the *Zinnia* model system the specification of xylem vessels has being studied and environmental factors and hormones such as light,

auxin, cytokinin, ethylene, brassinosteroids and phytosulfokine (Robert and McCann, 2000) have been shown to influence xylem vessel fate.

The formation of secondary cell wall in the xylem involves various biochemical processes including cellulose biosynthesis and lignin formation. The *Arabidopsis IRREGULAR XYLEM1 (IRX1*) and *IRX3* were reported to be secondary cell wall–specific cellulose synthase genes (Brown et al. 2005). In recessive mutants of those genes, collapsed vessel elements can be found in the inflorescence, which are likely due to reduced cellulose biosynthesis in the secondary cell wall. Other genes including *IRX5, 6, 7, 8, 9, 10, 11, and 12* also showed a distinct *irx*-like phenotype (Brown et al. 2005). Additionally, *MYB58* and *MYB63* have been reported to play an important role in lignin formation (Zhou et al. 2009). Previously, Zhong et al (2008) also reported that some MYB and NAC transcription factors, as *SECONDARY WALL ASSOCIATED NAC DOMAIN PROTEIN1* (*SND1*), as well as *KNAT7* are involved in secondary cell wall formation in the inflorescence, especially required for fiber differentiation. Furthermore, *NAC SECONDARY WALL THICKENING PROMOTING FACTOR1 (NST1)* and *SND1* were reported to play a redundant role in fiber differentiation (reviewed by Zhong and Ye, 2007).

1.4 Working hypothesis

In the vascular cambium similar decisions as in the SAM have to be taken; an equally tight balance between meristematic cells and cells, which undergo differentiation, is required. Some daughter cells of the cambial meristem differentiate into xylem or phloem, whereas others stay undifferentiated and maintain the pool of meristematic cells. *KNOX* genes might be also key players of cambial cell division and differentiation in *Arabidopsis* hypocotyls.

1.5 Objectives

The objectives of this work are:

1. To address the involvement of *KNO*X genes in secondary growth of *Arabidopsis* hypocotyls.

2. To figure out the action of *KNO*X genes on cambial cell divisions and differentiation during secondary growth of the *Arabidopsis* hypocotyls.

3. To address the function of *KNOX* genes in secondary wall formation, e.g. cellulose biosynthesis and lignin deposition, in the *Arabidopsis* hypocotyls.

4. To identify downstream targets of *KNOX* function.

2 Materials and Methods

2.1 Plant material and growth conditions

The *Arabidopsis* lines of *stm-GK, knat2, knat2-5, knat3, knat4, knat5, knat6, knat7, stm4, stm5, stm6, knat1*$^{bp-1}$, *KNAT1::GUS,* Columbia-0 (Col-0), Nossen-0 (No-0), Landsberg erecta (Ler) and C24, were obtained from the Nottingham *Arabidopsis* Stock Centre (NASC; http://nasc.nott.ac.uk). Seeds of *knat1*$^{bp-9}$ and *35S::KNAT1-GR* were provided by Dr. A. Hay (Department of Plant Sciences, Oxford University, UK), seeds of *35S::STM-GR* by Prof. R. Sablowski (John Innes Centre, UK) and seeds of *STM::GUS* by Prof. W. Werr (University of Cologne, Germany). Plant materials used in this experiment and detailed information are presented in the Appendix 7.1.

Plants were grown in long days (16 h light, 8 h dark) on soil and fertilized by 1/2 Murishage and Skoog (MS; Appendix 7.2) nutrients the first week after planting.

2.2 Identification and production of homozygous single and double *knox* mutants

To identify homozygous *knox* mutants carrying T-DNA insertions, seeds were surface sterilized using 70% ethanol for 1 minute, 5% calcium hypochlorite for 30-40 minutes and washed by sterile water three times. The sterilized seeds were then stored at 4°C for 3-5 days for seed stratification and put on a selective agar plates containing 1/2 MS nutrients and 35 µg/ml kanamycin (Sigma, Steinheim, Germany). The kanamycin resistant seedlings which had greener cotyledons and longer primary roots compared to sensitive wild-type (Figure 4), were transferred to soil and grown in long day conditions. Leaves of resistant plants were collected for genomic DNA extraction. DNA was extracted using a simple and rapid method (Edwards et al. 1991). PCR genotyping was performed with specific primers designed against the T-DNA insertion and the wild-type allele. Primer design was performed at http://signal.edu/tdnaprimers.2.html. Primer positions and location of T-DNA insertions in a respective *KNOX* gene are presented in Figure 3. The exact locations of the insertions can be seen in Appendix 7.3.

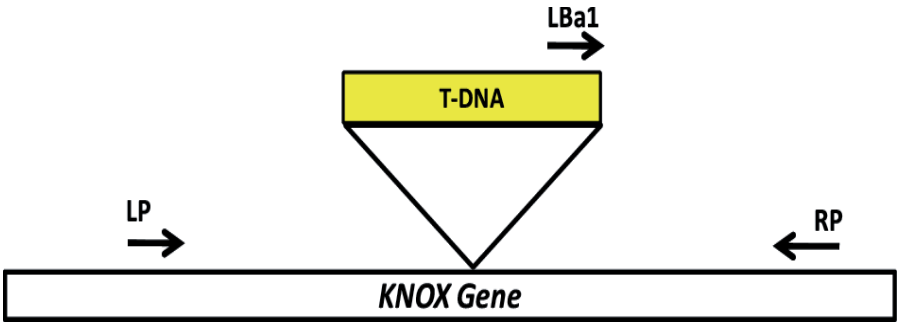

Figure 3. Primer construction for homozygous mutant identification using PCR genotyping. (LP) Left primer, (RP) right primer, and (LBa1) primer of T-DNA insertion.

PCR was run for 35 cycles; denaturation at 94°C for 40 seconds, annealing at 55°C for 40 seconds, and extension at 72 °C for 1 minute 20 seconds. The PCR products were loaded on a 1 % agarose electrophoresis gel and run at 70-100 volt for 20-30 min. PCR reagents and procedures were provided by Fermentas (St. Leon-Rot, Germany) (Appendix 7.4). An example for the identification of a homozygous *knox* T-DNA mutant is shown in Figure 4.

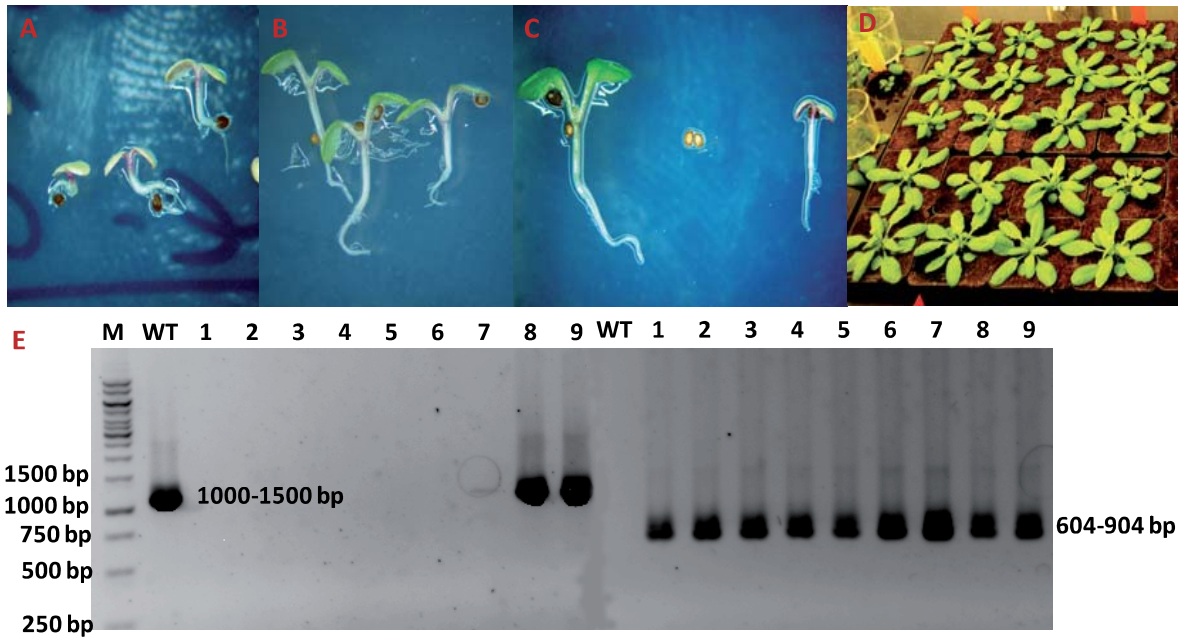

Figure 4. Identification of homozygous *knox* mutants. (A, B, C) Seedlings growing on kanamycin selective medium, (A) sensitive seedlings (wild-type, Col-0), (B) resistant seedlings (heterozygous or homozygous *knat5*), (C) resistant and sensitive seedling of segregating seeds (*knat5*). (D) Resistant seedlings were transferred to the soil. (E) A typical gel of PCR genotyping (*knat5*), the wild-type shows a discret band of approximately 1200 bp when amplified by LP/RP primers. No amplicon was detected for wild-type when using the Lba1/RP primer combination. In contrast, in plants homo- or heterozygous amplification with Lba1/RP resulted in a specific band of 750 bp. Line 1- 7 were homozygous for the insertion, while line 8 and 9 were heterozygous (also the willd-type band could be amplified). Marker (M): 1 Kb DNA Ladder (Fermentas, Germany).

Selection of homozygous *knat1*$^{bp-9}$ and *knat1*$^{bp-1}$ was based on the phenotype of downward pointing siliques (Venglat et al. 2002) and for *stm-GK* on the delayed initiation of a functional shoot apical meristem (SAM) (Barton and Poethig, 1993). Mutant phenotypes from segregating seedlings are shown in Figure 5.

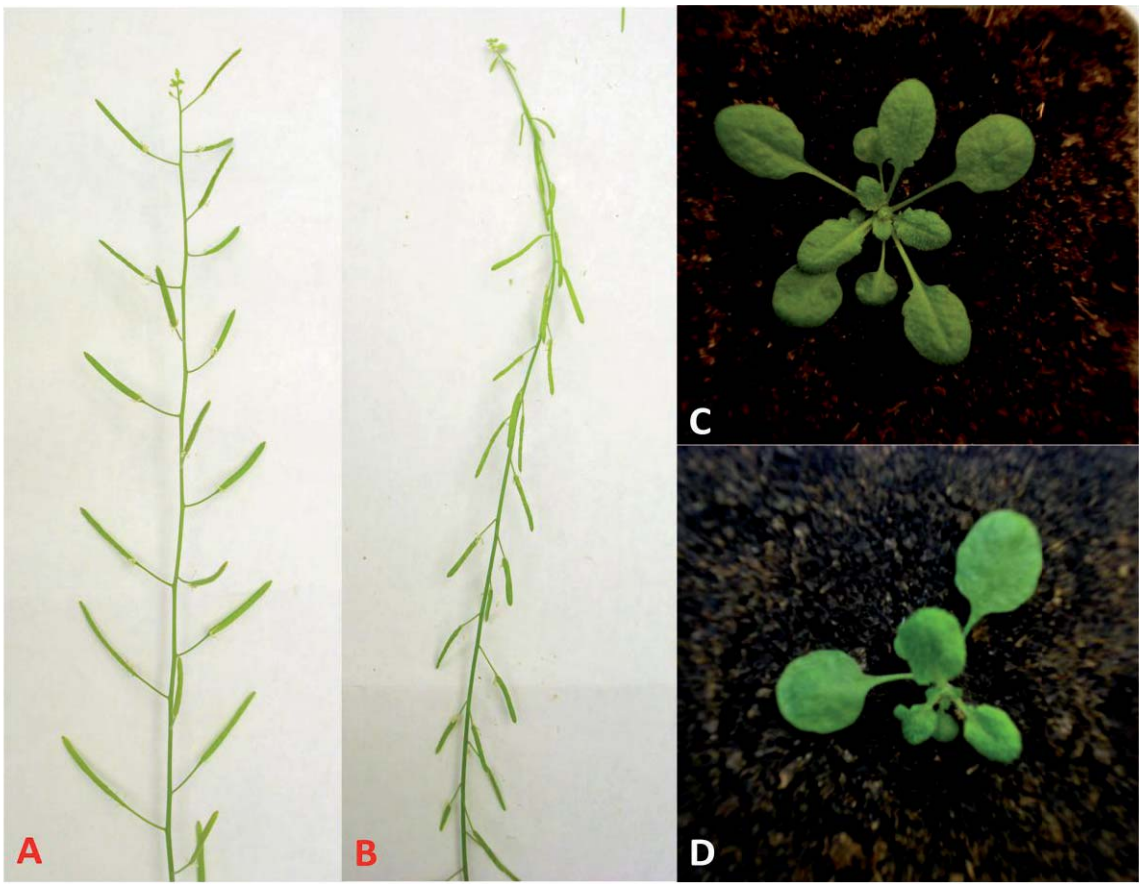

Figure 5. Identification of *knat1*$^{bp-9}$ and *stm-GK* mutants based on phenotype. (A) Wild-type inflorescence, (B) *knat1*$^{bp-9}$ inflorescence with downward pointing siliques, (C) wild-type shoot (2 weeks), (D) a delayed initiation of shoot apical meristem in *stm-GK* (2 weeks).

To generate double mutants, immature flowers of homozygous *knox* mutants were emasculated and manually cross-pollinated with the pollens from other *knox* mutants of interest. F1 seeds were grown on soil to generate the F2 generation. Kanamycin, phenotypic and PCR genotyping were performed to identify double homozygous *knox* mutants as described previously. The same procedure was used to produce reporter lines in mutant background, e.g. *STM::GUS, KNAT1::GUS, ATHB-8::GUS*, and *CyclinB1;1::GUS* in *stm* and *knat1*. In this case, F2 plants were selected using phenotype and GUS assays (part 2.6).

2.3 KNAT1-GR induction

To induce overexpression of *Arabidopsis 35::KNAT1-GR*, seeds were sown on the soil for germination and grown in long days (16 h light, 8 h dark) conditions and fertilized by ½ MS nutrients. After 1 week, the seedlings were transferred individually to a new pot. The plants were sprayed with 60 µM Dexamethazone (Dex) (Sigma, Germany) in 0.02 % Silwet L-77 surfactant (Lehle Seeds, USA). The treatment was repeated every week until plants were 6 weeks old.

Dexamethasone (Dex) and cycloheximide (Cyc) were employed on *35S::KNAT-GR* transgenics to test if *KNAT1* is sufficient to trigger expression of its downstream targets. For the experiments either 2 week old seedlings or isolated hypocotyls of 6 week old plants were used. For seedlings: seeds of *35S::KNAT-GR* were surface-sterilized (as described in part 2.2) and were inoculated on 1/2 MS medium. Seedlings then were harvested after two weeks on the plate and always 4 seedlings were inoculated in a scintillation vials containing 1 ml 1/2 liquid MS medium and treated with: (1) + 10 µl DMSO (control), (2) 5 µl Dex (50 µM), (3) 5 µl Cyc (10 µM) (4) 5 µl Dex (50 µM)+ 5 µl Cyc (10 µM). The vials were incubated for 3.5 hours at room temperature by gently shaking. The seedlings were removed one by one and dipped on a filter paper and immediately snap frozen in liquid nitrogen. The seedlings were then ready for RNA extraction (see part 2.4) and for expression analyses of downstream targets of *KNAT1*. For six week old plants: the same procedure performed for seedlings was employed, except that hypocotyls were separated from root and shoot previous to the treatments.

2.4 RNA extraction and cDNA synthesis

Total RNA was isolated from fresh hypocotyls or other tissues using RNeasy Plant Mini Kit (Qiagen, Hilden, Germany) following the manufacture's guidelines. The RNA was quantified by UV spectrophotometry and the quality was tested by running an aliquot on a 1.5 % agarose gel. A typical gel of total RNA extraction represented 28s and 18s rRNA in distinct bands with a smear of mRNA in between and above those bands (Figure 6).

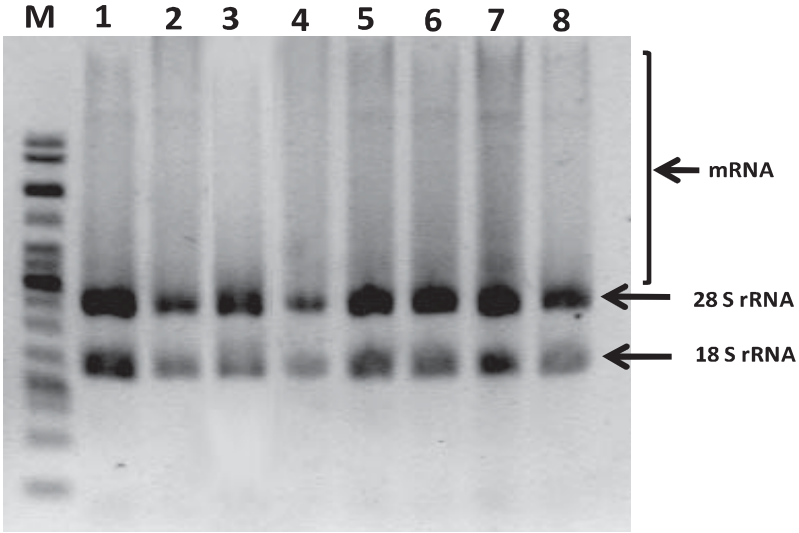

Figure 6. A typical gel of total RNA extraction. Distinct bands representing 28s and 18s rRNA. M: 1 Kb DNA Ladder. (Lane 1-5) Total RNA of various *knox* mutants.

Reverse-transcription (RT) was performed to generate first strand cDNA from total RNA using Quantitec ® Reverse Transcription (Qiagen) according to the manufacture's guidelines, including gDNA digestion previous to the RT reaction. 1 µg of total RNA was used for first strand cDNA synthesis. To evaluate the quality of first strand cDNA, cDNA was PCR amplified using a house keeping gene primer pair (*ACTIN2*) and run on a 1.5% agarose gel. PCR amplification was run for 30 cycles; denaturation at 94°C for 30 seconds, annealing at 55°C for 30 seconds, and extension at 72 °C for 1 minute. The PCR reaction procedure is presented in Appendix 8.4, using 0.5 µl cDNA instead of 2 µl DNA template (as for qRT-PCR). An example for such a cDNA quality evaluation is shown in Figure 7.

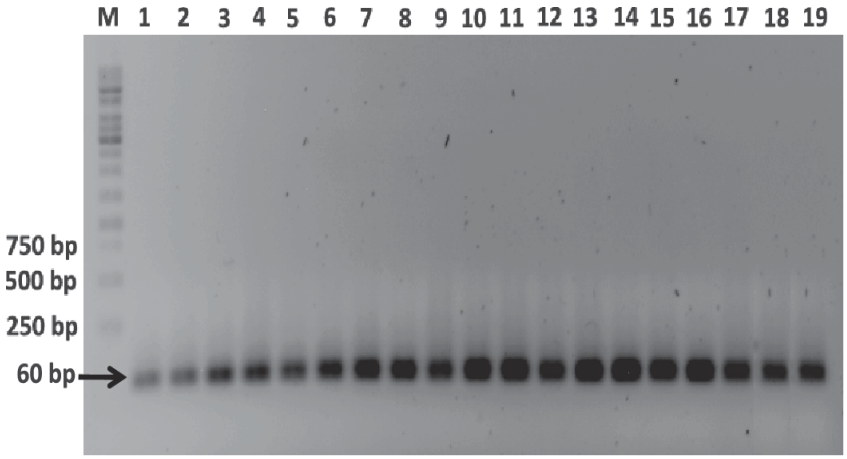

Figure 7. PCR amplification of *ACTIN2* from cDNAs of various *knox* mutants (lane 1-19). M: 1 Kb DNA Ladder.

2.5 Quantitative real time RT-PCR

The Universal ProbeLibrary Design Center (http://www.roche-applied-science.com/sis/rtpcr/upl/ezhome.html) was used to design specific primers for qRT-PCR. Primers were designed to amplify flanking sequences that are located downstream of or spanning the T-DNA/transposon insertion and spanning an intron if possible. This design allows to study the impact of an insertion on its own insertion site, as well as for classical expression analysis. Locations of flanking sequences and insertions in *KNOX* genes is shown in Figure 8. A list of primers used for this analysis is presented in Appendix 7.5.

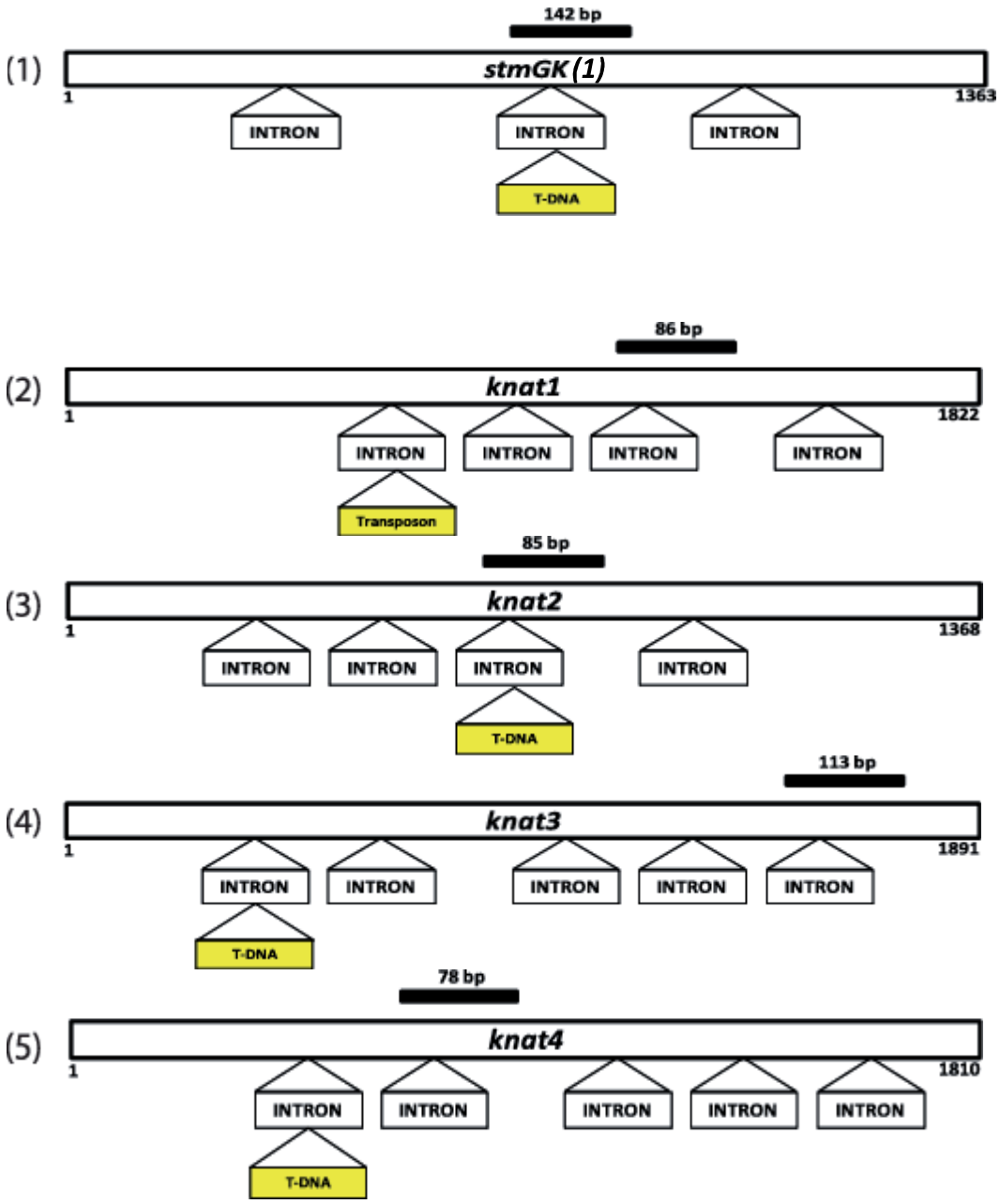

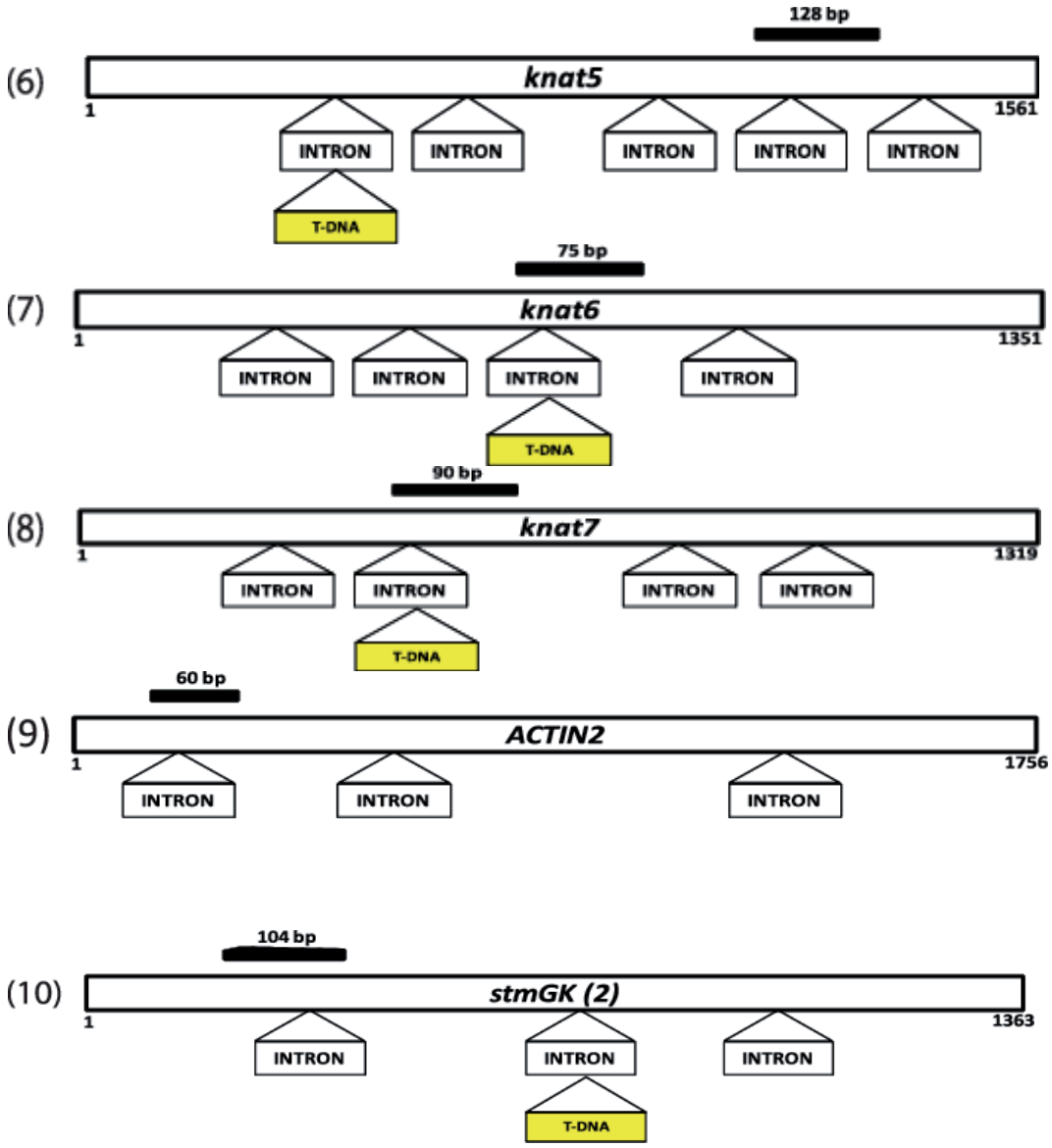

Figure 8. Location of flanking sequences and insertions in the *knox* mutants. Flanking sequences are shown by black boxes and transposon and T-DNA insertions by yellow boxes.

qRT-PCR was carried using the ROCHE qRTPCR SYBR green kit (Roche, Grenzach-Wyhlen, Germany) and reactions were run on a LightCycler®480 (Roche, Grenzach-Wyhlen, Germany) according to the protocol below:

Preincubation : 95ºC for 5 minutes

Amplification : 95ºC for 10 second

61ºC for 10 second

72ºC for 10 second

Melting curve : 95ºC for 5 second

65ºC for 60 second

67ºC – Acqu. 5

Cooling : 40ºC

Data were analyzed using LightCycler®480 Software Release1.5.0 (Roche Grenzach-Wyhlen, Germany). Values for crossing points (Cp) were obtained directly from the software and subsequently transformed to absolute concentration values using following formula:

$$Cp = Slope \cdot Log\,[x] + Y\ intercept$$

$$X = 10^{\left[\frac{Cp - Y\ intercept}{Slope}\right]}$$

Note:

(Cp) Crossing point, (X) concentration of amplified cDNA at time point 0, (slope and Y intercept) slope and intercept obtained from running standard curves generated by template dilution (Supplemental data 6.5).

The absolute concentration values then were normalized to the expression of *ACTIN2* by dividing the absolute expression value of the gene of interest by the absolute expression value of *ACTIN2* in the corresponding samples. All experiments were performed by using three biological and three technical replicates unless otherwise stated.

To determine slope (efficiency) and intercept, standard curves from dilution series were calculated. The initial first strand cDNA (1 µg of total RNA) was diluted 5x, corresponding to standard 1. Subsequently a series of 5x dilutions starting from standard 1 was made. For the standard curve dilutions from 5^0 to 5^{-7} were used. This procedure was performed for all primer pairs employed (Appendix 7.5 and 7.12).

2.6 GUS assays

6-week-old fresh hypocotyls were harvested and cut about 3-4 mm in length and directly immersed into GUS (ß-glucuronidase) staining solution (Appendix 7.6) and placed on ice. The hypocotyls were vacuum-infiltrated with the GUS solution two times, for approximately 3 seconds and then incubated at 37º C on a shaker for 2.5 hours. The hypocotyls were subsequently fixed in formaldehyde-acetic acid-ethanol (FAE, Appendix 7.7) for 1 hour and stored in 70% ethanol. The GUS-stained hypocotyls were then hand-sectioned using double sided razor blades and mounted on slides using chloralhydrate-glycerol solution (Appendix 7.8).

2.7 Histologic analysis and quantitative measurement of secondary growth

Fresh hypocotyls were harvested from 6-week-old plants and stored in 70% ethanol. The hypocotyls were then hand-sectioned using double sided razor blades to obtain cross sections. The sections were incubated in 70% ethanol for 1 minute and then directly transferred to phloroglucinol (in 20% HCl) lignin staining solution for about 3-5 minutes. The lignin-stained sections highlighted the area of secondary growth by dark red color. The sections were mounted on slides using chloral hydrate-glycerol solution. Hand sectioning and lignin staining were also performed to obtain tangential sections to observe more detailed of cell structures composing the xylem.

Secondary growth of *Arabidopsis* hypocotyls was measured using a stereomicroscope (Carl Zeiss Imaging Solutions, Jena, Germany) and AxioVision rel 4.7. Software (Carl Zeiss Imaging Solutions, Jena, Germany). Measurements comprised the diameter and area of hypocotyls, total xylem, and phase I of xylem development. Figure 9 shows schematically the different measurement on an *Arabidopsis* hypocotyl stained with phloroglucinol-HCl. The diameter was determined by calculating the mean value of two independent measurements of the longest and the shortest diameter per plant.

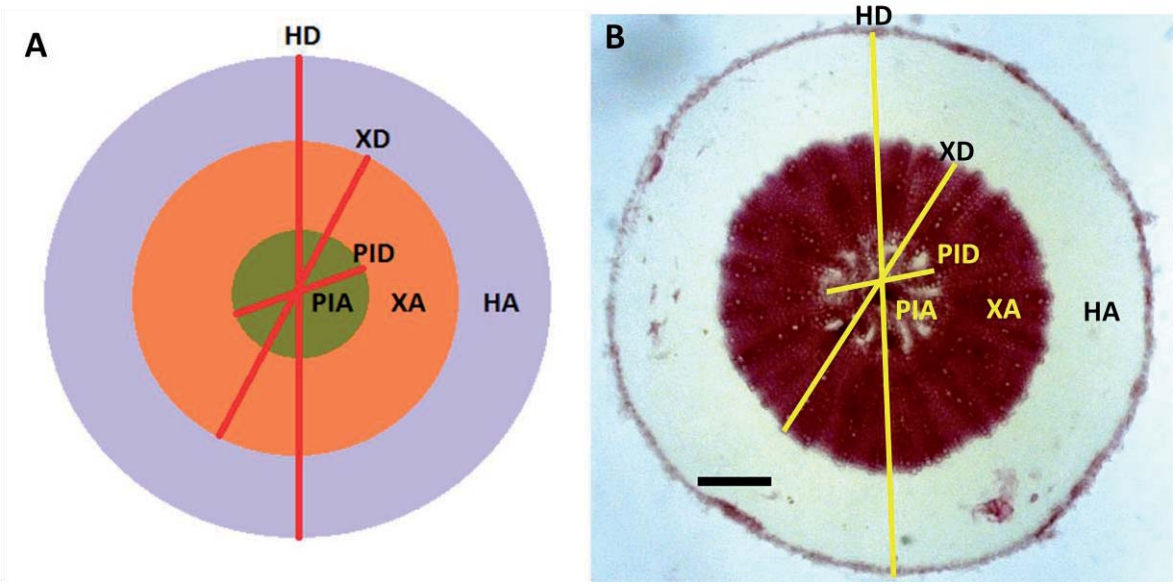

Figure 9. (A) Measurements of secondary growth in *Arabidopsis* hypocotyls. (HD) Hypocotyl diameter, (XD) xylem diameter, (PID) phase I of xylem diameter, (HA) hypocotyl area, (XA) xylem area, (PIA) phase I of xylem area. (B) Secondary growth of a hypocotyl of 6-week-old plant. Bar corresponds to 200 µm.

Xylem diameter or area ratio (XDR or XAR) were calculated by dividing the xylem diameter or area by the hypocotyl diameter or area. Phase II of diameter or area (PIID or PIIA) was calculated by subtracting the xylem diameter or area by the phase I of xylem diameter or area. The phase II of xylem diameter or area ratio (PIIDR or PIIAR) was calculated by dividing the phase II of xylem diameter or area with xylem diameter or area ratio.

2.8 Embedding and toluidine blue staining

Hypocotyls were fixed in a mixture of formaldehyde-acetic acid-ethanol (FAE, Appendix 7.7), treated in a series of increasing concentrations of ethanol, isopropanol, Roti-Histol (Roth Laborbedarf, Karlsruhe, Germany) and increasing paraffin (Rotiplast, Roth Laborbedarf, Karlsruhe, Germany) concentrations (Appendix 7.9) and finally embedded in a paraffin block. The blocks were then sectioned using a sliding microtome (Reichert, Vienna, Austria) into 30µm thick sections. The sections were directly placed on a drop of water onto gelatinized slides (Appendix 7.10) which were placed on a 60°C hot plate. The slides were then dried for about 3 hours and washed using 2 x Roti-Histol (Roth

Laborbedarf, Karlsruhe, Germany), 1 x isopropanol/Roti-Histol (1:1), and 1 x isopropanol, 1-3 minutes for each to remove the paraffin from the sections. The sections were stained using 1 % toluidine blue O (TBO, Sigma, Steinheim, Germany) in 1% sodium chloride (Appendix 7.11) for a minute and mounted in chloralhydrate -glycerol.

2.9 Light microscopy

Cross sections of hypocotyls from the GUS assays, lignin stainings, and toluidine blue stainings were observed under a stereomicroscope (Axioplan, Carl-Zeiss, Jena, Germany) and analyzed using AxioVision rel 4.7. Software (Carl Zeiss Imaging Solutions, Jena, Germany).

2.10 Identification of genes co-expressed with *STM* and *KNAT1*

To identify genes co-expressed with *STM* and *KNAT1* the *Arabidopsis* Co-expression Tool (ACT) was employed, a internet based tool for microarray experiment analysis, that is freely available at www.Arabidopsis.leeds.ac.uk/ACT (Manfield et al. 2006). For *STM* and *KNAT1*, the 100 best matches of co-expressed genes were extracted from a database of more than 300 microarray chips. Subsequently, overlapping gene models between genes coexpressed with *STM* and *KNAT1* were identified and selected according to their putative role in secondary growth. To verify co-expression experimentally qRT-PCR was performed. Primers were designed from selected genes by using The Universal ProbeLibrary Design Center (http://www.roche-applied-science.com/sis/rtpcr/upl/ezhome.html).

To study the relationship between *Arabidopsis STM* and *KNAT1* genes and lignin biosynthesis, an expression study using genes associated with lignin biosynthesis was performed (genes listed in Appendix 7.12). Primers were designed against these genes according to Mele et al (2003). The list of primers for co-expression and expression analysis is presented in Appendix 7.12. The qRT-PCR was run as described in 2.5.

3 Results

3.1 Isolation of insertional alleles as tool for functional analyses of *Arabidopsis KNOX* genes

T-DNA and stable transposon insertion lines became recently a popular tool in *Arabidopsis* for functional analyses of genes. While insertions in exons often result in the expression of non-functional truncated proteins, insertions into introns might be spliced out and leave gene expression unaltered. In some cases however, intron insertions may down- or up-regulate gene expression, e.g. insertions in gene regulating sequences in introns or insertions, which interfere with the efficiency of splicing.

Surprisingly, most of the publicly available insertion mutants for *KNOX* genes locate to introns. Therefore, after isolation of homozygous mutants, qRT-PCR was performed in order to identify mis-expression of the mutated *KNOX* genes. Primers (Appendix 7.5) were designed to either span or to locate 3' downstream of the T-DNA/transposon insertion site (Figure 8). qRT-PCR showed that the transcript level of the mutated genes were strongly downregulated in PCR selected-homozygous mutants of *stm-GK, knat1*$^{bp-9}$*, knat2, knat3, knat6,* and *knat7*. In case of *knat4* such a decrease of *KNAT4* expression was not observed and for *knat5* even increased expression was detected (Table 1).

Table 1. Mis-expression of *knox* insertional alleles. Negative fold changes correspond to a decrease of expression compared to wild-type (Col-0), positive fold changes to an increase. (*) p-value calculated based on t-test (Supplemental data 6.8). Data were analyzed from 3 biological and 3 technical replicates.

***knox* mutants**	**Insertion/location**	**Fold Change of Expression**	***P* Value***
stm-GK	T-DNA, 1st intron	- 746 x	0.0017
knat1^{bp-9}	*dSpm* transposon, 1st intron	- 243 x	0.0008
knat2	T-DNA, 3rd intron	- 319 x	0.0040
knat3	T-DNA, 1st intron	- 42 x	0.0085
knat4	T-DNA, 1st intron	+ 1 x	0.4989
knat5	T-DNA, 1st intron	+ 17 x	0.0001
knat6	T-DNA, 3rd intron	-1967 x	0.0088
knat7	T-DNA, 2nd intron	-140 x	0.0047

The strongest effect on the transcript level reduction of intron-insertion mutants was detected for *knat6*, followed by *stm-GK*, *knat2*, *knat1*$^{bp-9}$ and *knat3,* respectively. The location of T-DNA insertion determines its efficiency to inactivate the function of a target gene. In *knat4* the T-DNA is most likely spliced out from the hnRNA (heteronucleon- or

pre-RNA) and therefore does not affect gene expression. In the case of *knat5* the elevated gene expression might be due to insertion into a negative gene regulatory element or due to increased stability of the hnRNA.

For *stm-GK* the effect of the intron-insertion on the expression of the 5' upstream compared to the 3' downstream sequence was examined. Two different primer pairs for *STM* were designed; either upstream or downstream of the T-DNA insertion (Figure 8, No. 1 and 10). The downstream flanking sequence was very poorly expressed (746 x lower in *stm-GK*), whereas the upstream sequence was significantly more strongly expressed than in the wild-type (Col-0) (Table 2).

Table 2. Differential expression of truncated upstream compared to downstream *STM* transcript in *stm-GK*. Negative fold changes correspond to a decrease of expression compared to wild-type, positive fold changes to an increase. (*) p-value calculated based on t-test. Data were analyzed from 3 biological and 3 technical replicates.

Primer name	**Location toward T-DNA insertion**	**Fold Change of Expression**	***P* Value***
STM-1	Downstream	-746 x	0.0017
STM-2	Upstream	+4 x	0.0000

In general lower expression of the *KNOX* genes did not result in an effect on the leaf rosette phenotype compared to wild-type, except for *stm-GK* (Figure 10). *Shoot meristemless (stm)* mutants, as reported by Barton and Poethig (1993), are blocked in the initiation of the shoot apical meristem (SAM). A complete lack of SAM was found for strong alleles like *stm4* and *stm5* (Figure 11). In addition, fused-cotyledons were frequently observed (Figure 11B). On the other hand, a mild *stm* phenotype could be detected for *stm-GK* and as previously noted for *stm6* and stm^{wam1-1}. Those weak mutants were characterized by a "stop and go" development of SAM (Figure 11), with the SAM producing a few leaves before cessation and subsequent outgrowth of leaves from other SAMs.

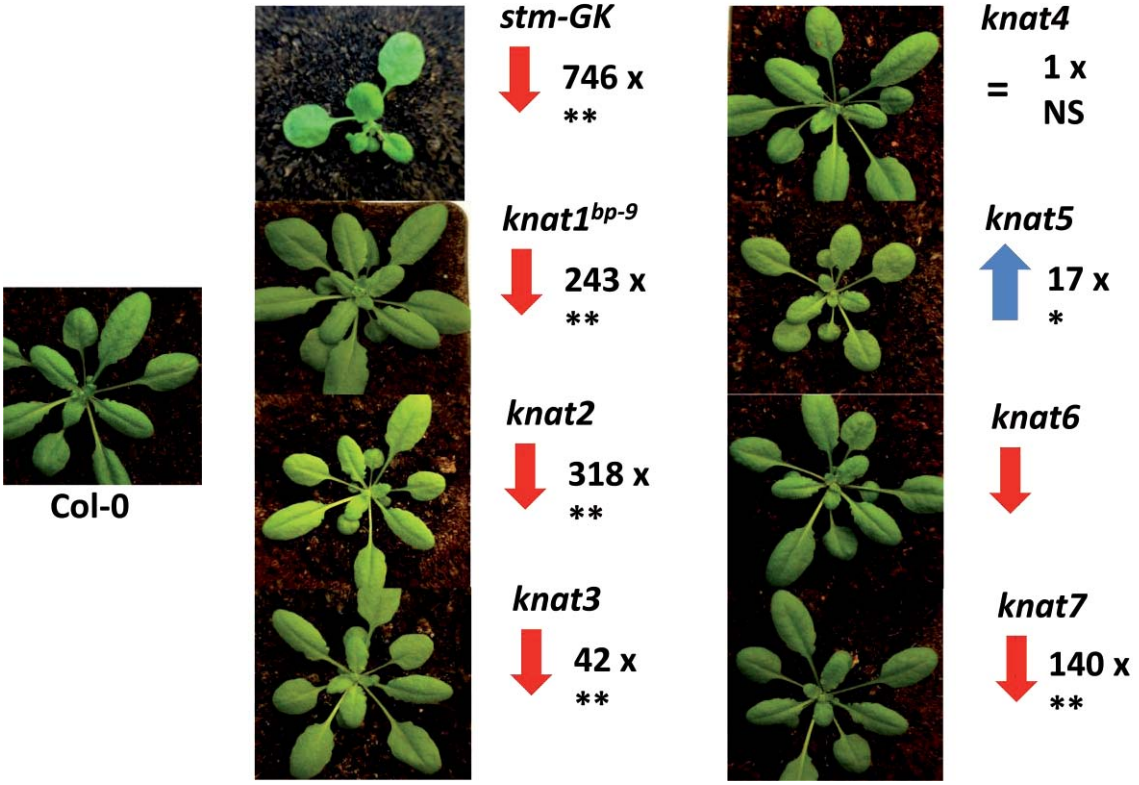

Figure 10. Leaf rosettes of *knox* mutants compared to wild-type (Col-0) in 4-week-old plants. (**) Significant $p \leq 0.01$, t-test, compared to wild-type, (*) significant $0.01 < p \leq 0.05$. (NS) not significant.

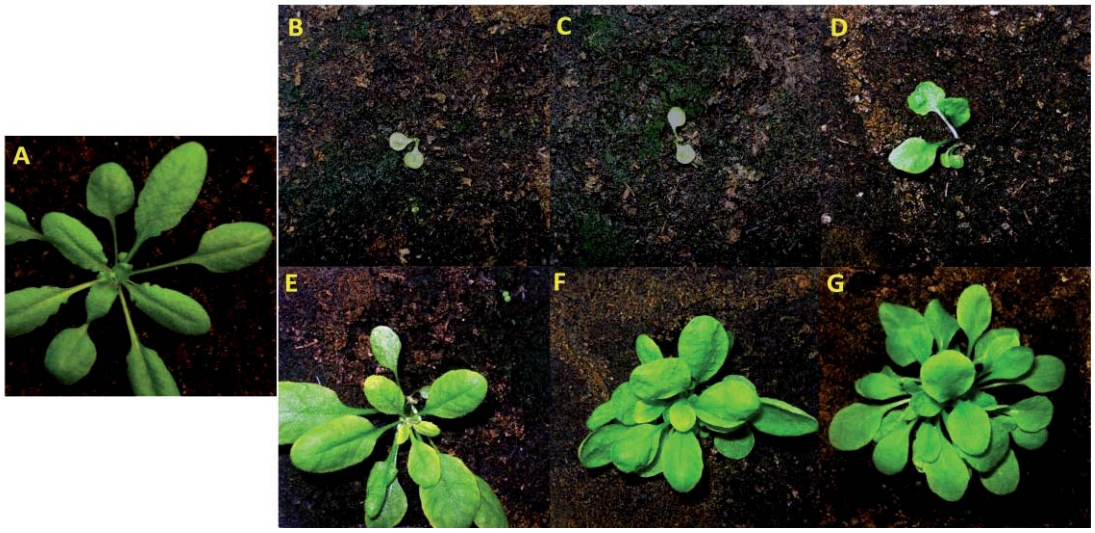

Figure 11. Allelic series of *stm*. Variation of phenotype in 4-week-old plants. Strong *mutants* showed fused cotyledons (*stm4,* B) and completely blocked initiation of SAM development (*stm5,* C). Weak (mild) alleles displayed "stop and go" development (*stm-GK*, *stm6* and stm^{wam1-1}, E, F and G).

3.2 Defective secondary xylem development in *Arabidopsis* hypocotyls *stm* and *knat1* mutants

The successfully isolated mutants of class I and II of *Arabidopsis Knotted1-like homeobox* (*KNOX*) genes were grown under long day condition and the hypocotyls of 6-week-old plants were examined. Hypocotyls of *stm* and *knat1* mutants displayed a strong reduction in diameter compared to the wild type (Figure 12). The reduction was observed for almost all of *stm* and *knat1* alleles. A dramatic reduction in diameter was detected in strong alleles, e.g. *stm 4* and *stm5*, in Ler background, and the double mutants of *stm-GK;knat1*$^{bp-9}$ (Col-0 background), whereas less reduction was observed in *stm-GK* (Col-0 background), *stm6* (Ler background), *stm*$^{wam1-1}$ (C24 background, data not shown)[1], *knat1*$^{bp-9}$ (Col-0 background), and *knat1*$^{bp-1}$(Col-1 background). Hypocotyl morphology of *knat2, knat2-5, knat3, kant4, knat5*, *knat6* and *knat7* (all in Col-0 background) was not different compared to the wild-type.

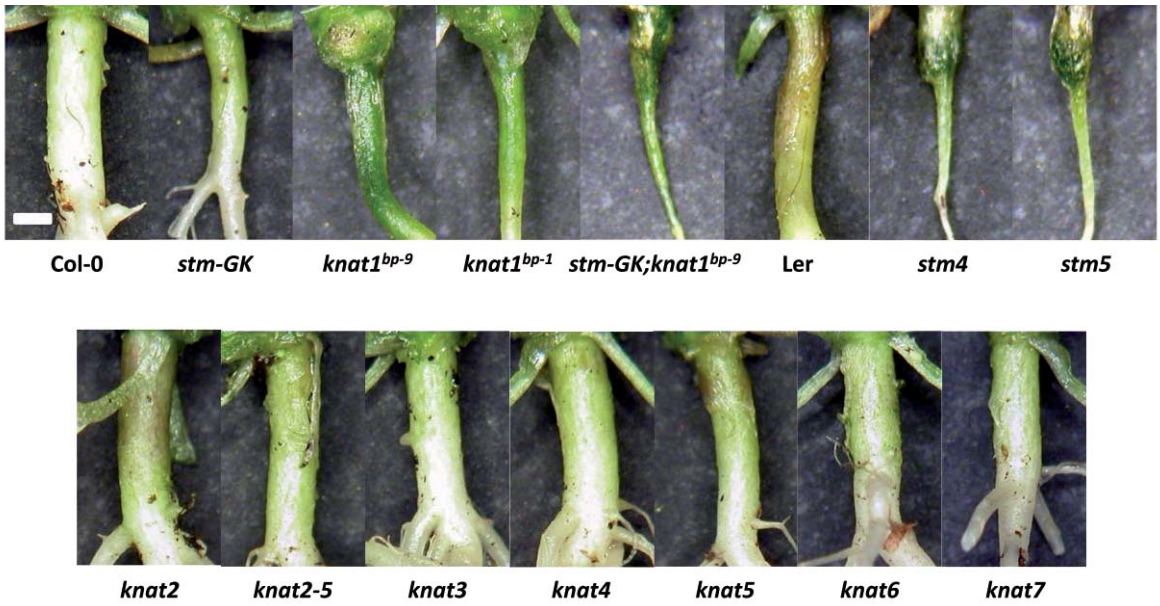

Figure 12. Hypocotyls of *knox* mutants and wild-type. Bar: 1 mm.

To explore the basis of the reduction and to quantify the effects of impaired *KNOX* gene function, hypocotyls were hand-sectioned and stained using phloroglucinol-HCl, which stains lignin. Since lignin is deposited into secondary cell walls, phloroglucionol-HCl is a suitable stain for xylem fibers and vessels during secondary growth. As the observations on the intact hypocotyls already indicated, secondary growth of *stm* and *knat1* mutants was reduced (Figure 13). This was supported by quantitative analyses of the

hypocotyl diameter and area of *stm6*, *stm*$^{wam1-1}$, *knat1*$^{bp-9}$, and *knat1*$^{bp-1}$ (Figure 14A and B). These data suggest that *STM* and *KNAT1* are required for secondary growth of *Arabidopsis* hypocotyls.

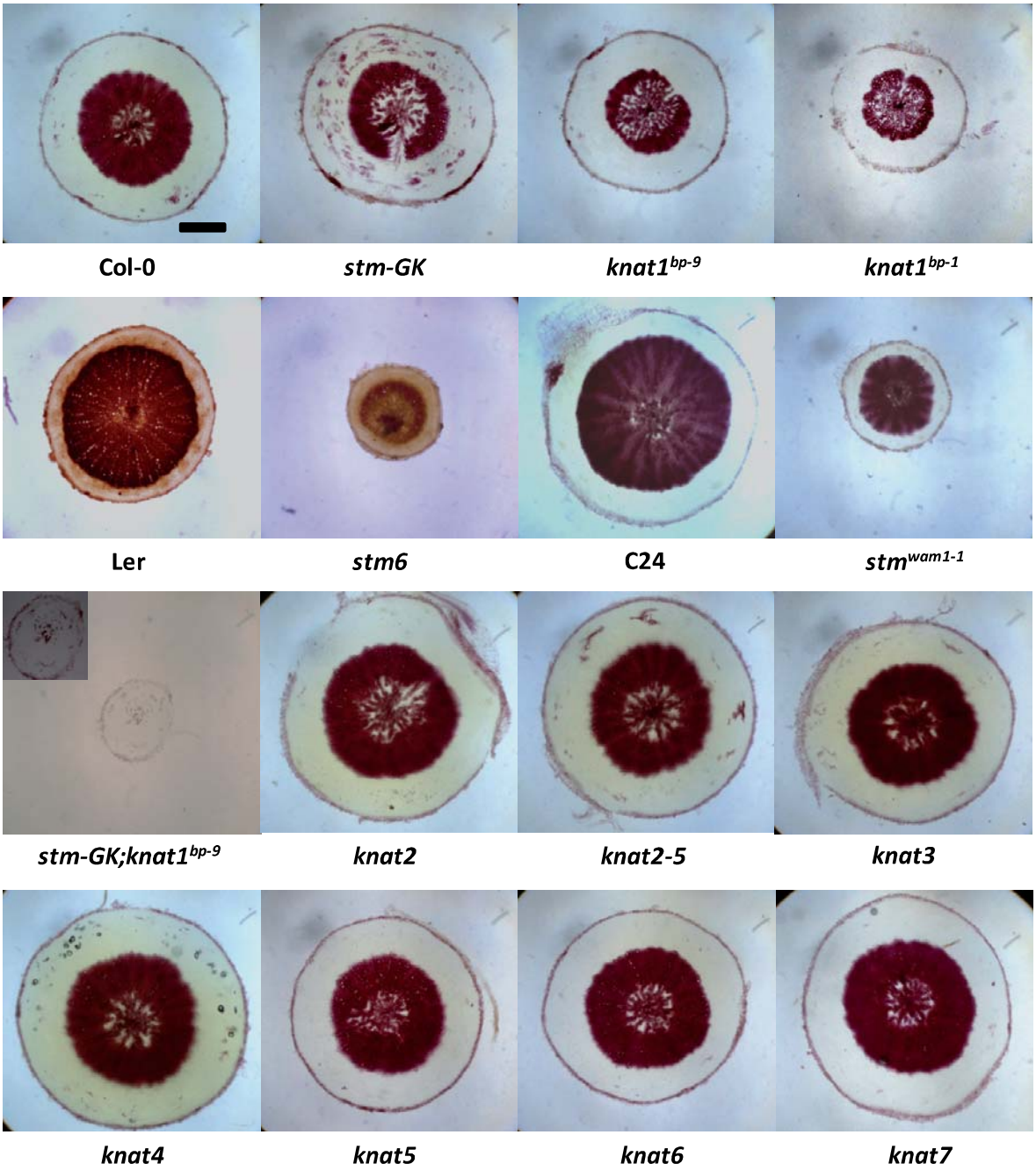

Figure 13. Secondary growth of *knox* hypocotyls compared to the respective wild-types (Col-0, Ler, and C24). Hypocotyls were harvested from 6-week-old plants. The sections were stained using phloroglucinol-HCl. Bar: 200µm.

Secondary xylem development was reduced indicated by a decrease of the ratios of xylem diameter to hypocotyl diameter (later referred to as "xylem diameter ratio") from

0.59 to o.47 and of xylem area to hypocotyl area (later referred to as “xylem area ratio”) from 0.35 to 0.24, in *stm-GK* (Figure 15A, B, Supplemental data 6.1). By contrast, the hypocotyl diameter and area of *stm-GK* were not significantly different to wild-type (Figure 14A, B). Hence, the absolute reduction in xylem formation was compensated by other tissue. In *knat1*$^{bp-9}$, the xylem diameter ratio was decreased from 0.59 to 0.46 and the xylem area ratio was decreased from 0.35 to 0.20. For two other weak alleles, *stm6* and *knat1*$^{bp-1}$, similar results have been obtained as for *stm-GK* and *knat1*$^{bp-9}$ (Figure 15 A and B). The total aerial dry mass of *knat1*$^{bp-9}$ and *stm-GK* were not different from wild-type (Figure 14C) suggesting that the decrease of secondary xylem in those mutants was directly caused by the reduction of *STM* and *KNAT1* not because of indirect effects on plant growth.

Interestingly, hypocotyls of the double mutant of *STM* and *KNAT1* showed a dramatic reduction compared to wild-type (Figure 12 and 13 and 14A, B). The reduction was much stronger than in the single mutants. The xylem development was also significantly reduced indicated by the xylem diameter and area ratio (15A, B). These findings suggest that *STM* and *KNAT1* have a redundant function and act synergistically in xylem development of the *Arabidopsis* hypocotyl.

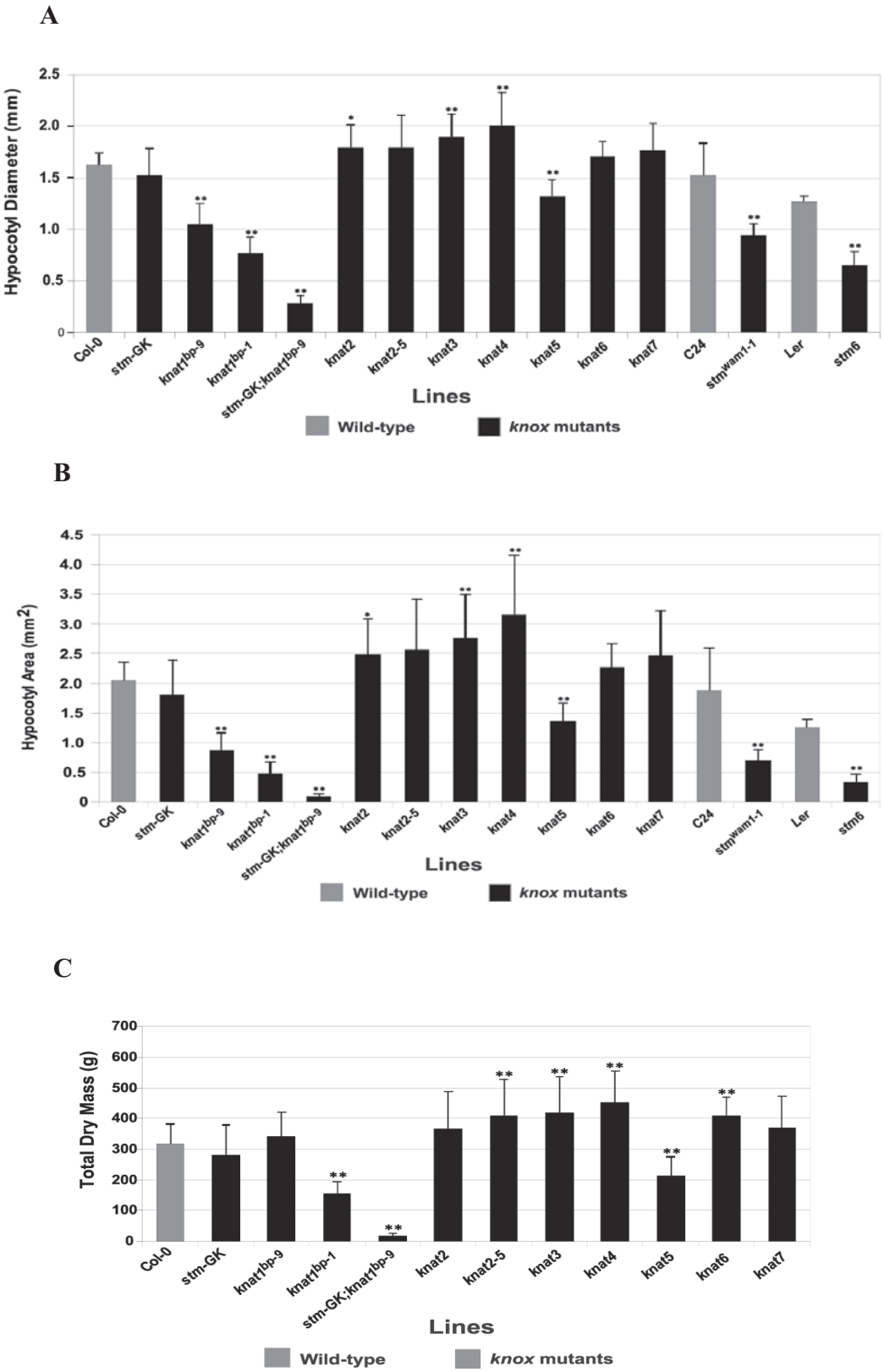

Figure 14. Hypocotyl diameter (A), area (B) and total aerial dry mass (C) of *knox* mutants compared to wild-type. Data was obtained from 3 independent experiments, each with 3 hypocotyls. (**) Significant at $p \leq 0.01$, t-test, compared to wild-type, (*) significant at $0.01 < p \leq 0.05$.

A

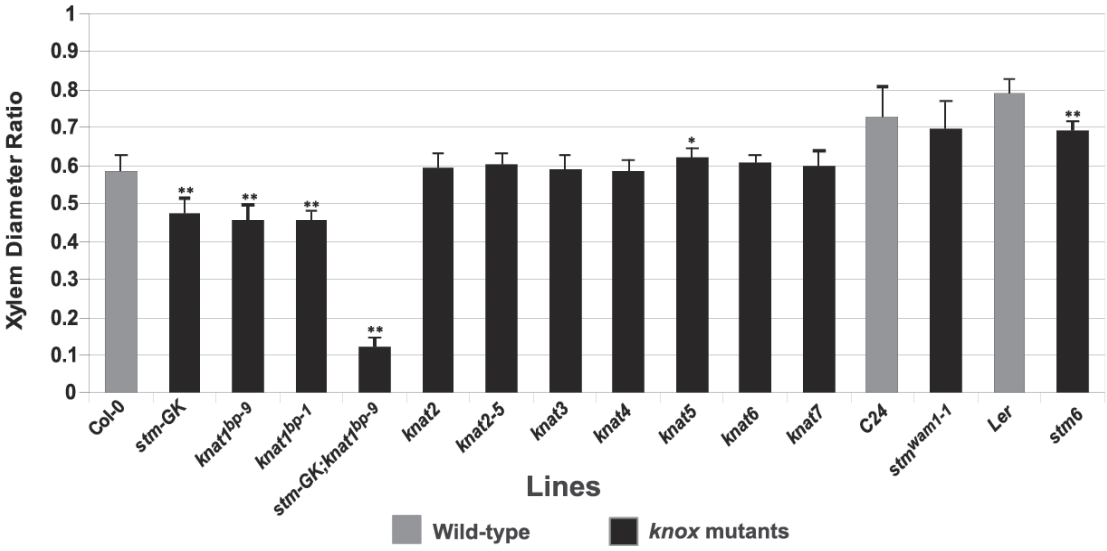

B

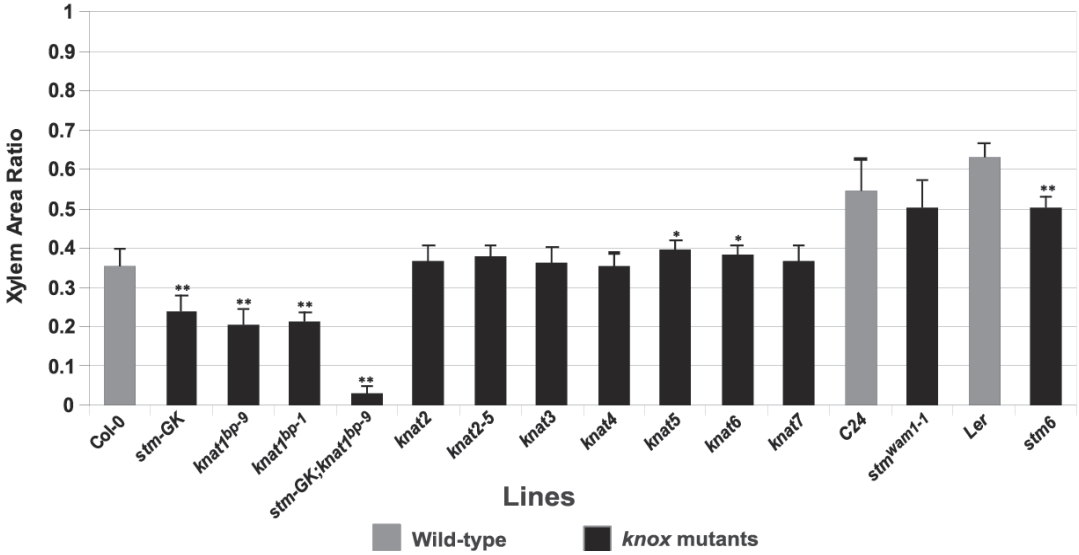

Figure 15. Xylem diameter (A) and area (B) ratio of *knox* mutants compared to wild-type. Data was obtained from 3 independent experiments, each with 3 hypocotyls. (**) Significant $p \leq 0.01$, t-test, compared to wild-type, (*) significant $0.01 < p \leq 0.05$.

No reduction of secondary growth was detected for the other *knox* mutants, *knat2, knat3, knat4, knat5, knat6 and knat7*, showing that *KNAT1* and *STM* are the most important players of secondary xylem formation within the *KNOX* gene family.

3.3 *STM* and *KNAT1* are specifically expressed in the cambial zone of *Arabidopsis* hypocotyls

The observed reduction of xylem formation indicates that *KNAT1* and *STM* are important for cell divisions and cell elongation leading to xylem but not phloem (Supplemental data 6.2). In order to test if *KNAT1* and *STM* are present in cells, which are specified to xylem and undergo subsequent elongation, their expression was monitored by employing *STM::GUS* and *KNAT1::GUS* reporter genes. GUS assays were performed on fresh, 6-week-old hypocotyls of *STM::GUS* and *KNAT1::GUS* transgenic plants. *STM::GUS* and *KNAT1::GUS* expression was specifically detected in the cambial zone located in between secondary xylem and phloem (Figure 16), as well as in the developing xylem. This indicates that *STM* and *KNAT1* are specifically acting on cell division and/or elongation in the cambial cells and the xylem derivates.

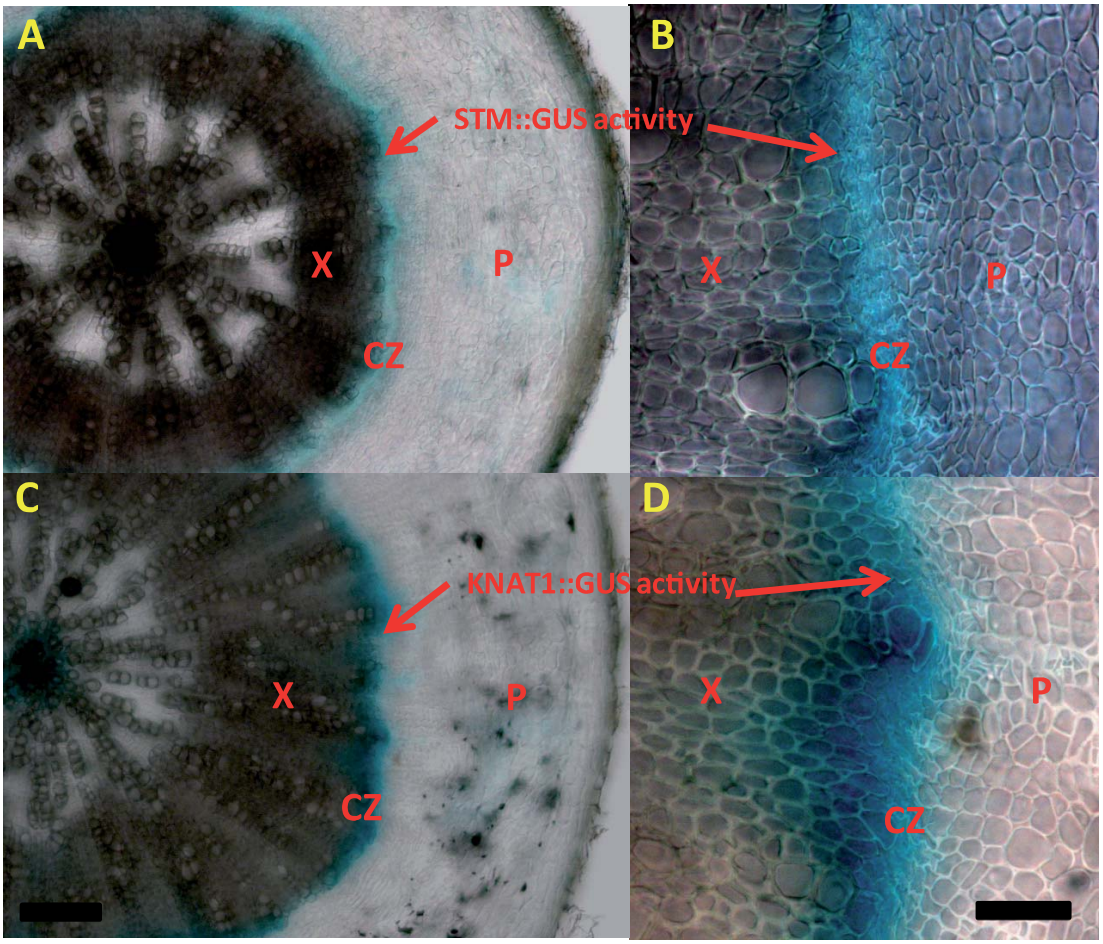

Figure 16. GUS activity in 6-week-old *STM::GUS* (A,B) and *KNAT1::GUS* (C, D) hypocotyls. (CZ) Cambial zone, (X) xylem, and (P) phloem. Bar: 100 µm and 10 µm.

Expression of *STM* and *KNAT1* were determined quantitively by qRT-PCR in different tissues in order to compare expression levels in the hypocotyls with other organs of *Arabidopsis*. *STM* and *KNAT1* were strongly expressed in hypocotyls (Figure 17; Supplemental data 6.6). The highest expression however was detected in young floral apices, containing floral meristems and all floral stages up to pollination. Expression in leaves was very low. By contrast, for the class II *KNOX* gene *KNAT7* the expression was highest in the oldest node inflorescence and low expression was detected in hypocotyls. A similar expression pattern for *STM* and *KNAT1* (Figure 17; Supplemental data 6.6) indicates that these two genes in particular tissues may have redundant function and the relatively high expression in hypocotyls underlines their important role in secondary growth.

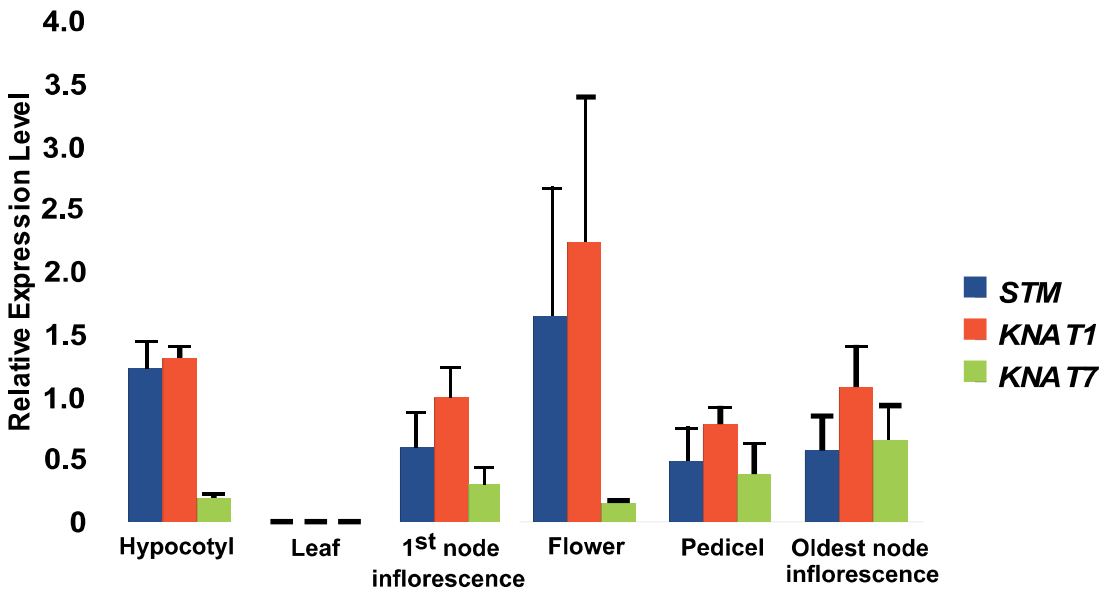

Figure 17. *STM* and *KNAT1* expression in different tissues of *Arabidopsis* plant. Data were analyzed from 3 biological and 3 technical replicates and normalized to the expression of *ACTIN2*.

3.4 The development of secondary xylem is inhibited in *stm* and *knat1* mutants

In order to describe the developmental process during secondary xylem development and to identify differences, hypocotyls from 2, 4, and 6-week-old Col-0, *stm-GK*, *knat1*$^{bp-9}$, and *stm-GK*;*knat1*$^{bp-9}$ grown in long day conditions, were paraffin-embedded and cut in 30 µm thick cross sections and were observed under a light microscope as described under 2.8.

Extensive secondary xylem formation was detected in hypocotyls of plants grown in long days (Figure 18). 2-week-old hypocotyls comprise an epidermal cell layer, (EP) cortex parenchyma (CoP), endodermis (En), and vascular stele (VS) (Figure 18 A and B). At this stage the vascular cambium was not yet initiated. In of 4-week-old hypocotyls the vascular cambium was completely established and the secondary xylem and phloem was visible (Figure 18 C and D). At this stage the xylem consists of xylem vessels and parenchymatic cells, but no xylem fibers. In 6-week-old hypocotyls the newly formed xylem contained besides vessel cells also fibers. Parenchymatic cells were absent. Hence, two distinct phases of xylem formation could be observed, phase I with vessel and parenchymatic cells and phase II with vessels and fibers. This has been observed earlier by Chaffey et al (2002) in *Arabidopsis* hypocotyls grown under short days. The results presented here show that under long days similar secondary growth and phases in xylem development occur as under short days. In short days secondary growth starts after 29 days (Chaffey et al. 2002), while under the conditions presented here already large parts of the phase II xylem were accomplished after 6 weeks.

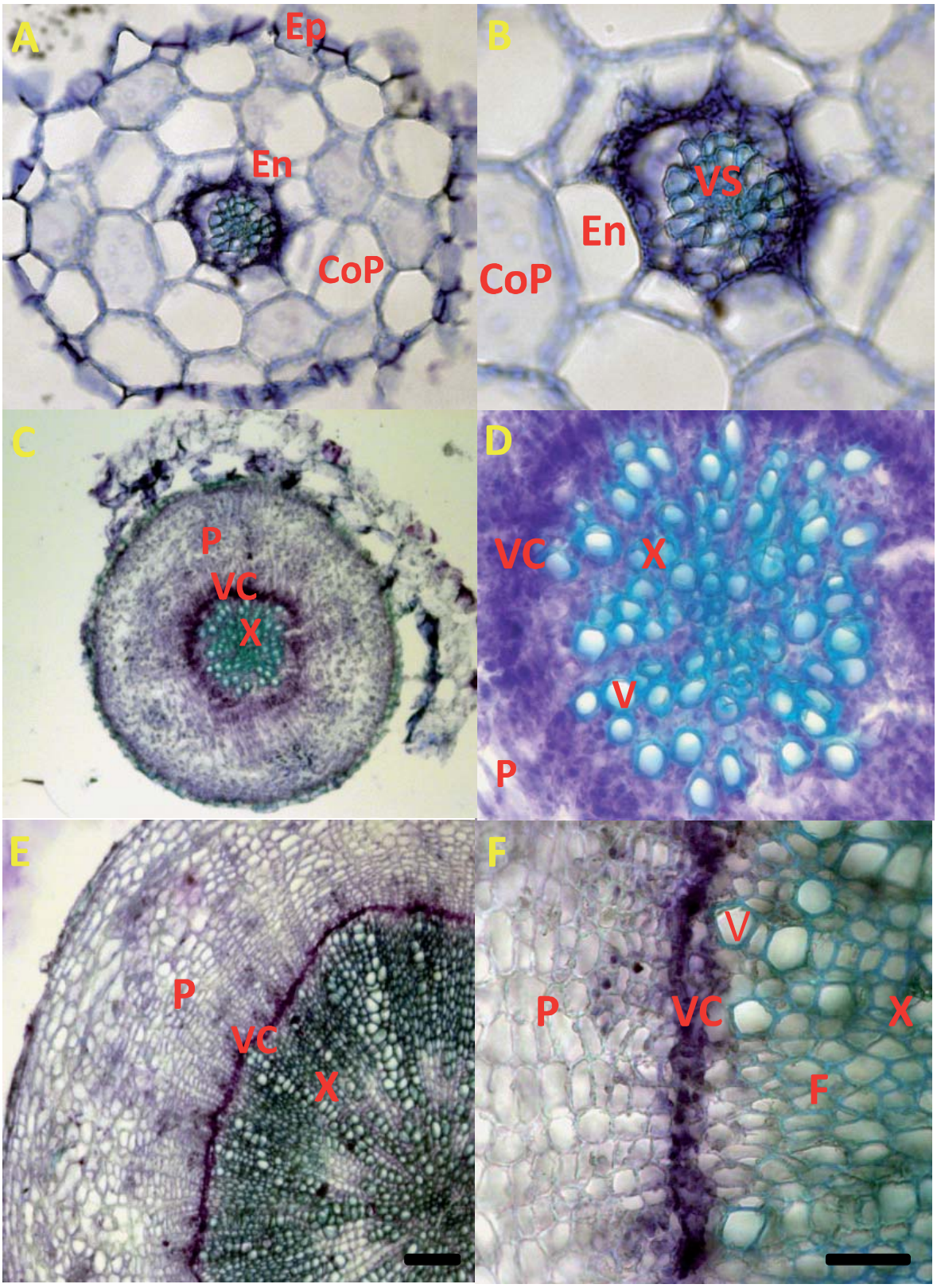

Figure 18. Developmental anatomy of the vascular cambium and secondary growth in *Arabidopsis* grown in long day conditions. (A and B) Sections from 2-week-old plants, (C and D) from 6-week-old plants and (E and F) from 6-week-old plants. (EP) Epidermal cell layer, (CoP) cortex parenchyma, (En) endodermis, (VS) vascular stele, (VC) vascular cambium, (P) phloem, (X) xylem, (F) fiber and (V) vessel element. Stained using toluidine blue. Bar for A, C, E: 100 µm and bar for D, B, F: 10 µm.

Figure 19. Tangential section of an *Arabidopsis* hypocotyl. (V) Vessel elements, (F) fibers, (yellow arrow) perforation plates, (red arrow) secondary cell wall thickenings. Stained with phloroglucinol-HCl. Bar: 10 µm.

Tangential sectioning of hypocotyls from wild-type plants showed water conducting elements, characterized by distinct perforation plates at both ends of vessel cells (Figure 19). Secondary cell wall thickenings were very prominent and fibers appeared as elongated cells filled between vessel elements. These anatomical properties are similar to those known from woody species, except for ray cells, which were missing.

Compared to wild-type development, there were no differences between the single mutants *stm-GK* and *knat1*$^{bp-9}$ in anatomy of hypocotyls harvested 2 weeks after planting (Figure 20A, B, C). Also *stm-GK*;*knat1*$^{bp-9}$ appeared at this time point like wild-type (Figure 20D). After 4 weeks, a narrow band of intensely stained cells encircled the vessel elements of the phase I xylem in the wild-type, marking the cambial zone (Figure 20E). In the single mutants, vessels of phase I xylem were present as well, however their arrangement occurred disordered (Figure 20F, G). Intensely stained cells were not

restricted to the cambial zone but also could be found in between single vessel elements. In the double mutant, large cortex cells surrounded the vascular cylinder, similarly as seen in the wild-type after two weeks, indicating a delay in development (Figure 20H). After 6 weeks, the cambial zone, marked by intensely stained cells, became more distinct in the wild-type and files of cells with vessel or/and fiber cells appeared, characteristic for phase II of xylem development (Figure 20I). While in the single mutants the cambial zone was often intercepted and less fibers occurred (Figure 20J, K), in the double mutant the development was seemingly arrested (Figure 20L)

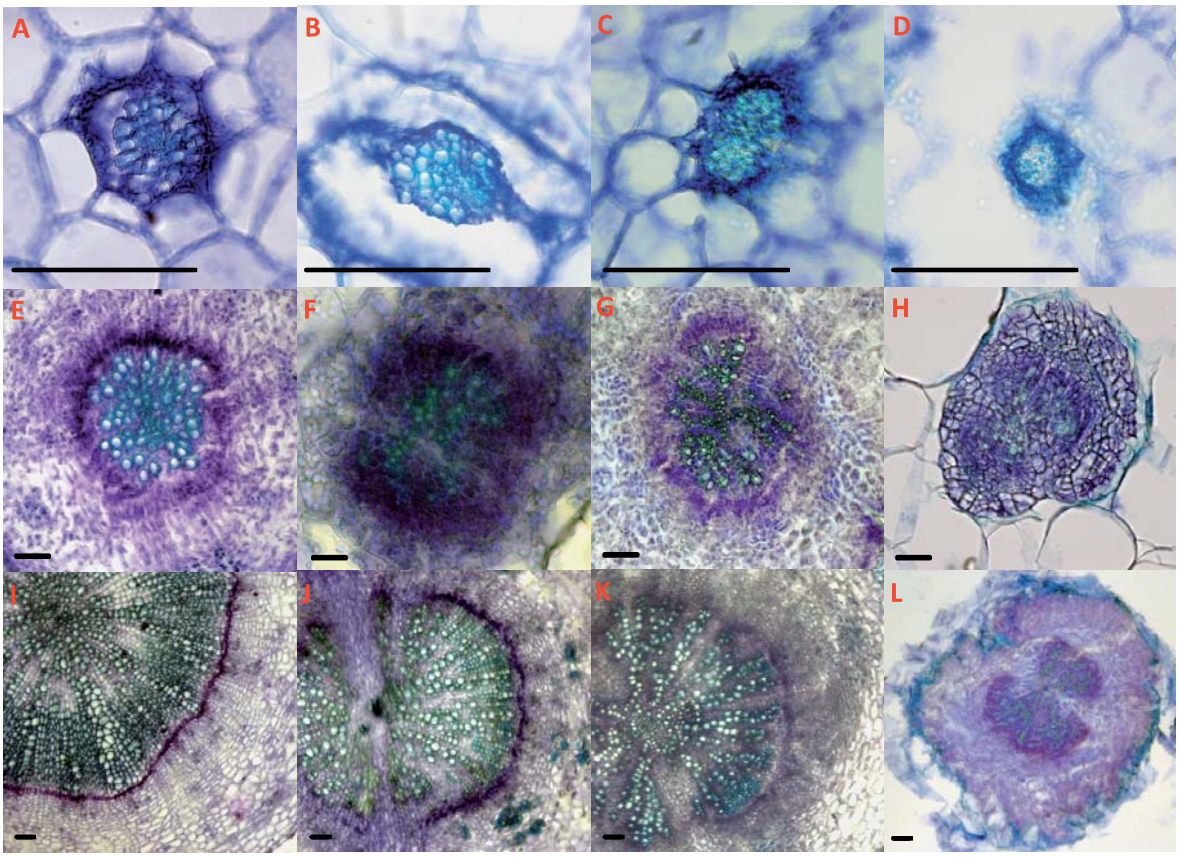

Figure 20. Anatomy of *stm* and *knat1* hypocotyls grown in long day conditions. Hypocotyls were harvested of 2-week-old plants (A, B, C, D), 4 weeks (E, F, G, H) and 6 weeks (I, J, K, L) from wild type/Col-0 (A, E, I), *stm-GK* (B, F, J), *knat1*$^{bp-9}$(C, G, K), and *stm-GK; knat1*$^{bp-9}$ (D, H, L). Bar: 50 µm. Stained using toluidine blue.

The secondary cell wall of vessel elements differentiated immediately adjacent to the cambial zone in the wild-type, as seen by thickening and turquoise staining of the cell wall (Figure 21A). In contrast, fully expanded xylem fibers were subjected to secondary cell wall formation 2-4 cells distal to the cambial zone (Figure 21B). Such behavior of faster maturation of vessel cells compared to fibers has been reported previously by

Chaffey et al (2002). In both single mutants, xylem fibers, symptomatic for phase II xylem, were formed too, but cell files containing parenchymatic cells occurred aside (Figure 21C, D, E and F). While in wild-type the narrow band of intensely stained cells surrounding the xylem was completed, in *knat1*$^{bp-9}$ and in *stm-GK* frequent gaps occurred. Interestingly, such gaps were at the origin of parenchymatic cell files. The dense staining represented supposedly interphase nuclei, indicating active cell division in such cells. In the double mutant, no xylem fibers could be found and xylem vessels were irregularly distributed in the often split xylem cylinder (Figure 21G, H). As in *knat1*$^{bp-9}$, but not in *stm-GK*, cytoplasmatically dense cells appeared throughout the whole xylem but no distinct cambial zone had been formed. In the null alleles *stm4* and *stm5*, neither fibers nor a cambial zone could be observed and undifferentiated, cytoplasmatic cells appeared in the xylem (Figure 21I, J, K, and L). The xylem phenotype in the null alleles appeared to be even more pronounced than in the double mutant between the weak *stm* and *knat1* allele. Taken together these results show that both genes are involved in determination of xylem fiber identity, hence in the formation of phase II xylem, and in the establishment of the cambial zone.

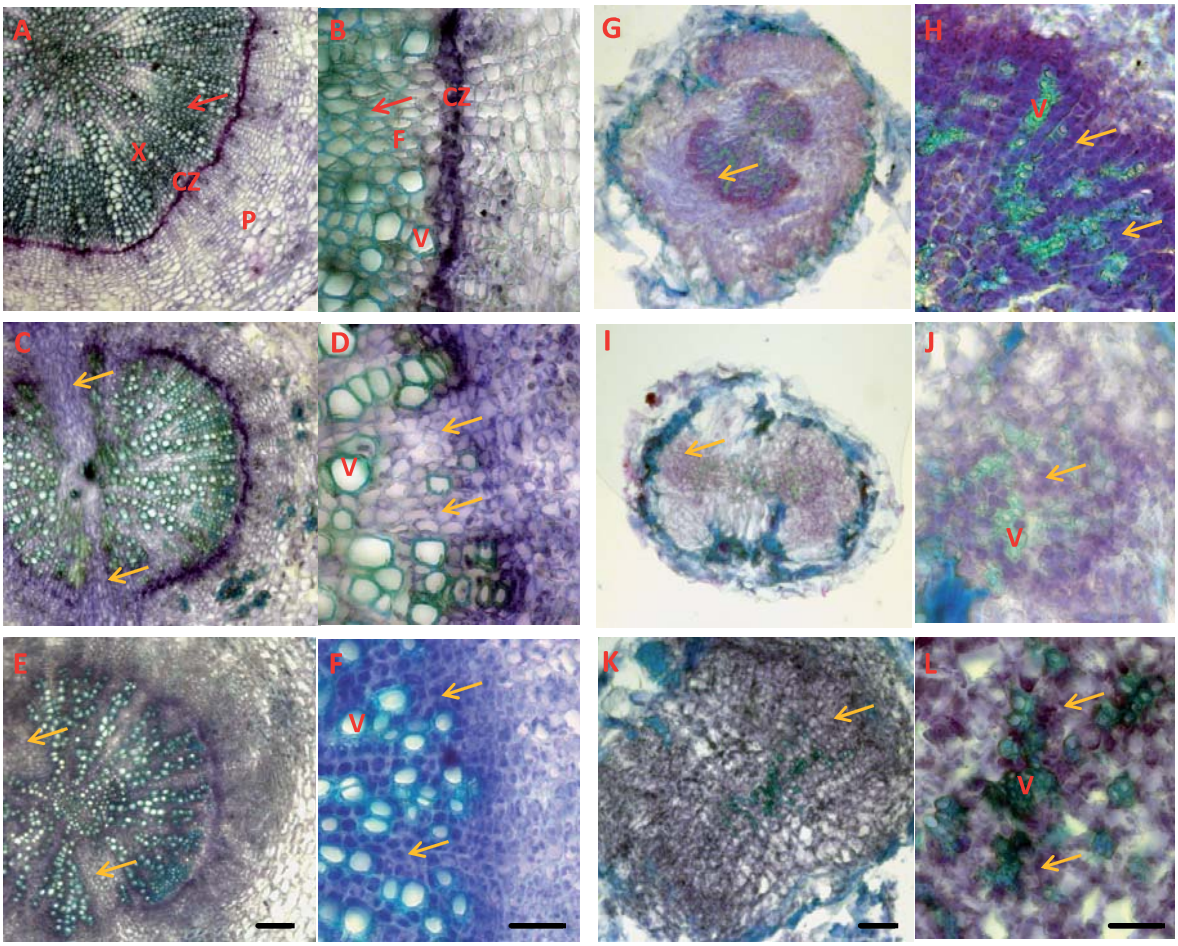

Figure 21. Differentiation of cambial cells into xylem daughter cells in *stm* and *knat1* mutants. Wild-type/Col-0 (A, B), *stm-GK* (C, D), *knat1*$^{bp-9}$ (E, F), *stm-GK;knat1*$^{bp-9}$ (G, H), *stm4* (I, J), *stm5* (K, L). (red arrow) Terminally differentiated cells, characterized by secondary cell wall thickenings, (yellow arrow) undifferentiated cells, (X) xylem, (P) phloem, (CZ) cambial zone, (F) fiber cells, (V) vessel elements. Bar for A, C, E, G, I, K: 100 µm and bar for B, D, F, H, I, L: 10 µm.

3.5 Phase II of secondary xylem development of *Arabidopsis* hypocotyl is inhibited in *stm* and *knat1* mutants

In order to quantify the defect in phase II of xylem development, the ratios of the diameter and area between phase II xylem and total xylem were determined for the previously isolated *knox* mutants. Formation of phase II xylem was significant reduced for *stm-GK* and *stm6*, while the weakest *stm* allele, judged from its shoot phenotype, *stm*$^{wam1-1}$ was not different from wild-type (Figure 22A, B and 23A, B, C, D). *knat1*$^{bp-9}$ and *knat1*$^{bp-1}$ showed an even more dramatic effect compared to the *stm* mutants (Figure 22A, B and 23E, F). In the double mutant phase II xylem was completely absent underlying a synergistic genetic interaction between *STM* and *KNAT1* (Figure 22A, B and 23G, H). For

all the other *knox* mutants no significant failure in phase II xylem formation could be recorded.

A

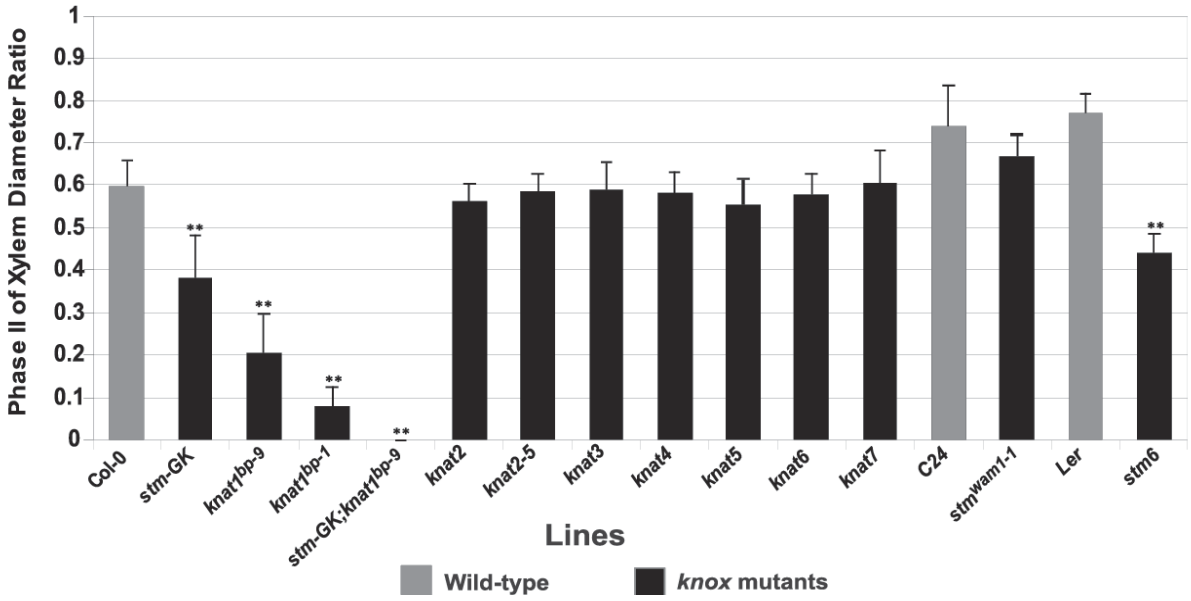

B

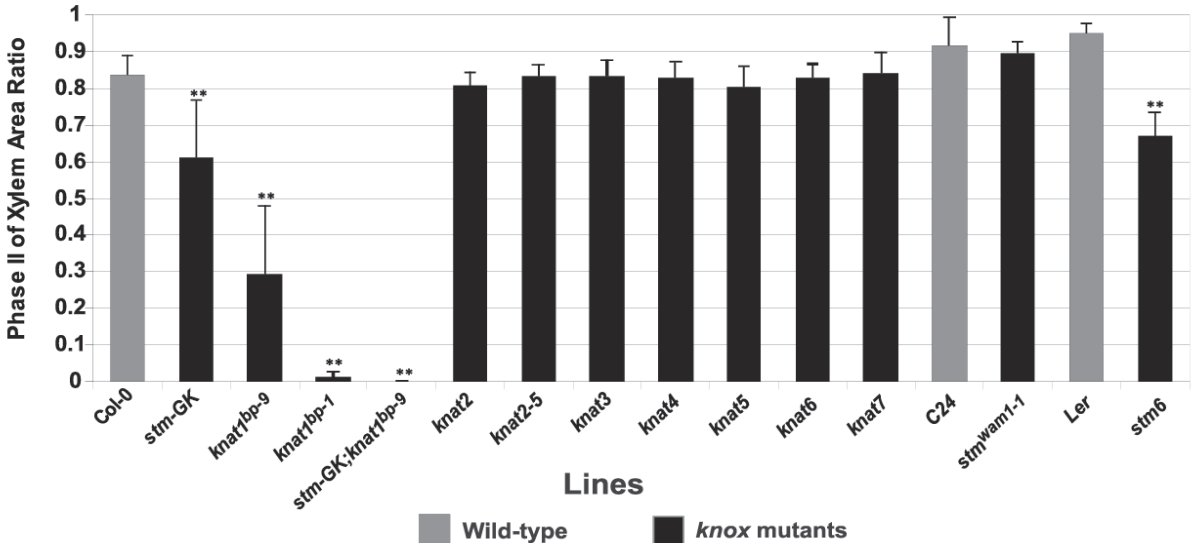

Figure 22. Phase II of secondary xylem development of *knox* mutants compared to wild-type. Ratios are taken between the diameter (A) or area(B) of phase II xylem and total xylem. Data was obtained from 3 independent experiments, each with 3 hypocotlys. (**) Significant at $p \leq 0.01$, t-test, compared to wild-type, (*) significant at $0.01 < p \leq 0.05$.

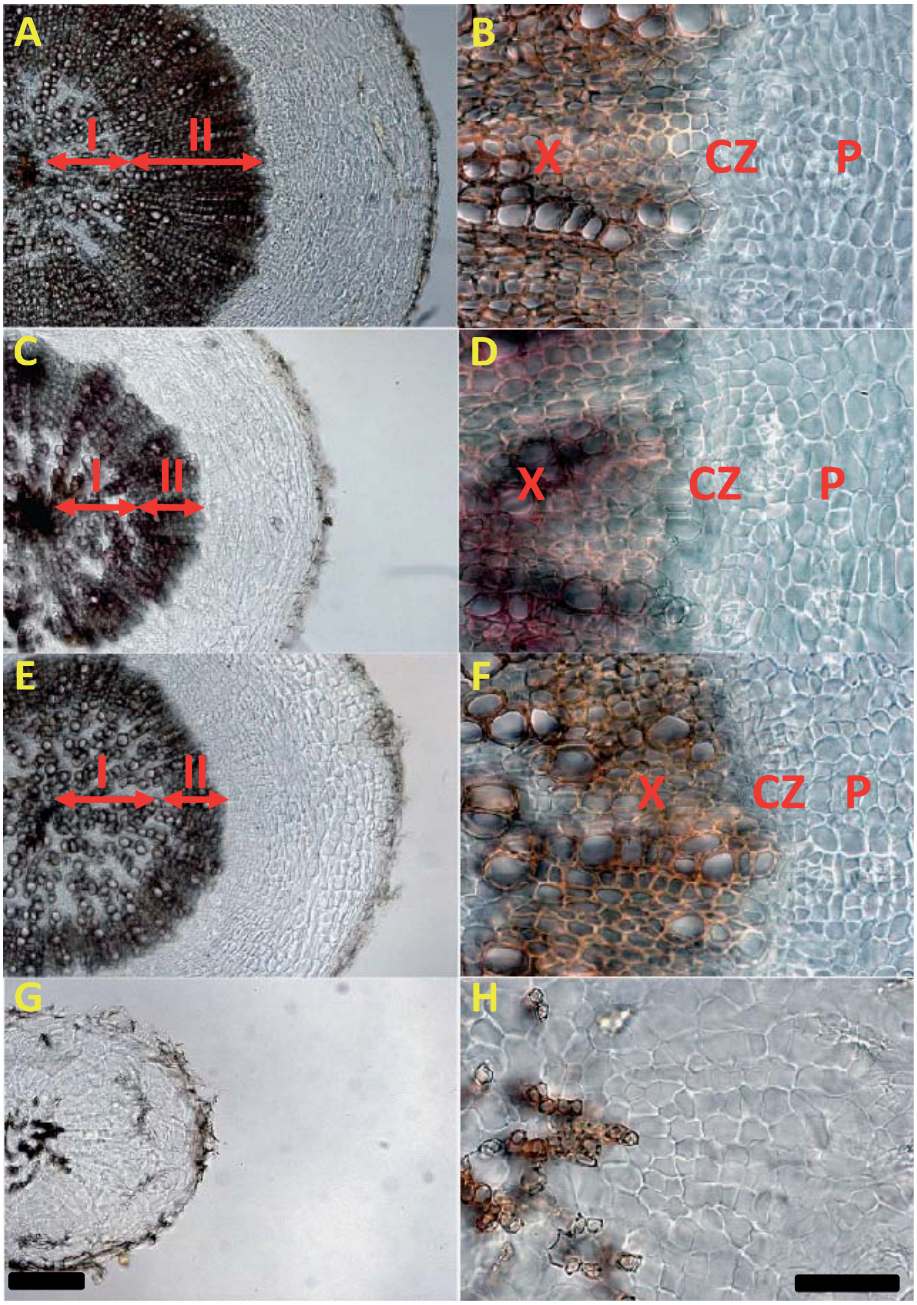

Figure 23. Phase II of secondary xylem development was reduced in *stm* and *knat1* mutants compared to wild-type. Wild-type/Col-0 (A, B), *stm-GK* (C, D), *knat1*$^{bp-9}$ (E, F), and *stm-GK;knat1*$^{bp-9}$ (G, H). Stained using phloroglucinol-HCl. Bar for A, C, E, G: 100 µm and bar for B, D, F, H: 10 µm.

3.6 Non-epistatic interaction between *STM* and *KNAT1* in *Arabidopsis* hypocotyls

In order to further investigate the genetic interaction between *KNOX* genes in secondary growth of the *Arabidopsis* hypocotyl, an expression analysis using qRT-PCR in *stm-GK*, *knat1*$^{bp-9}$, the double mutant *stm-GK*;*knat1*$^{bp-9}$ and *knat7* was performed. The previous data have shown that *STM* and *KNAT1* are required in secondary growth and secondary xylem development (see 3.2 and 3.3) and indicated synergistic interaction between these two genes (Figure 24, Supplemental data 6.7). In addition, *KNAT7* was reported to have an important role in secondary cell wall biosynthesis (Zhong et al. 2008).

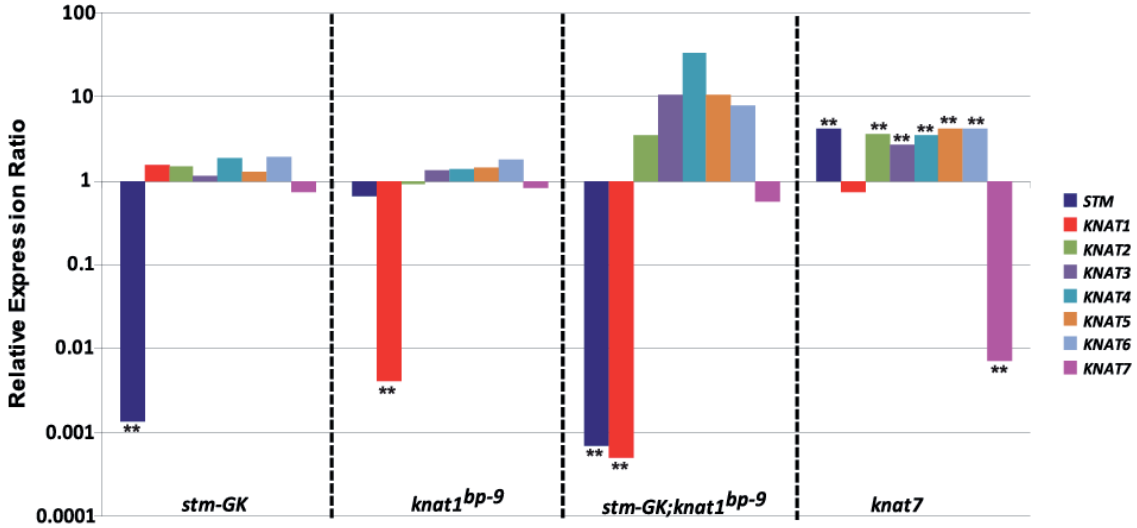

Figure 24. *KNOX* expression in hypocotyls of 6 weeks old *stm-GK*, *knat1*$^{bp-9}$, *stm-GK;knat1*$^{bp-9}$ and *knat7* mutants relative to wild-type. Data were analyzed from 3 biological and 3 technical replicates and normalized to the expression of *ACTIN2*. (**) Significant $p \leq 0.01$, t-test, compared to wild-type.

STM was significantly down-regulated in *stm-GK*, but not reduced in *knat1*$^{bp-9}$ (Figure 24). Similary, *KNAT1* was strongly reduced in the *knat1*$^{bp-9}$, but not significantly different in *stm-GK*. The expression of *STM* and *KNAT1* was dramatically reduced in the double mutants of *stm-GK;knat1*$^{bp-9}$. These results were consistent with the activity of reporter gene constructs in single mutant background (Figure 25). No difference in strength and pattern for either STM::GUS activity in *knat1*$^{bp-9}$ (Figure 25C, D) or KNAT1::GUS activity in *stm-GK* (Figure 25G, H) could be observed. In summary no evidence for an epistatic interaction could be found. This is in line with the interpretation of the anatomical phenotype in the hypocotyl, which supports a synergistic interaction between *STM* and *KNAT1*. In *knat7* hypocotyls, *STM* and *KNAT1* are slightly misregulated.

Interestingly, a trend for derepression of the other *KNOX* genes (*KNAT2*, *KNAT3*, *KNAT4*, *KNAT5* and *KNAT6*) appeared in *knat7* (significantly) as well as in *stm-GK;knat1*$^{bp-9}$. This may indicate overlapping functions for *STM*, *KNAT1* and *KNAT7* in the formation of xylem in the *Arabidopsis* hypocotyl.

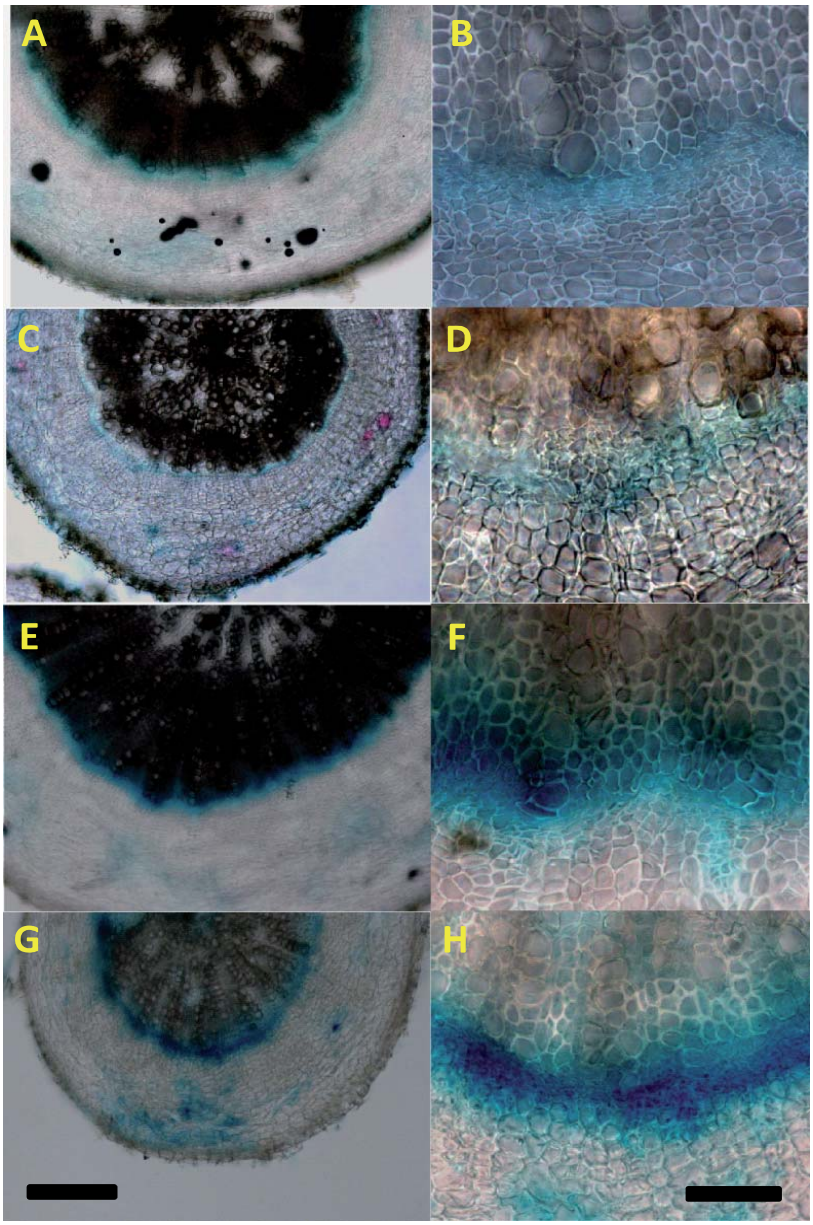

Figure 25. STM::GUS and KNAT1::GUS activity in *knat1*$^{bp-9}$ and *stm-GK*. *STM::GUS* (A, B), *STM::GUS; knat1*$^{bp-9}$ (C, D), *KNAT1::GUS* (E, F), and *stm-GK::KNAT1*::GUS (G, H). Bar for A, C, E, G: 100 and bar for B, D, F, H: 10 µm.

3.7 Secondary growth of *Arabidopsis* hypocotyls was reduced by overexpression of *KNAT1*

Using *35S::KNAT1* in Nossen (No-0) (Chuck et al. 1996) background and a steroid-inducible line of *35::KNAT1-GR* (Hay et al. 2003) in Col-0 ecotype, the effect of *KNAT1* over-expression was examined. 35::KNAT1-GR is a fusion protein between KNAT1 and the glucocorticoid receptor (GR) driven under the control of the constitutive promoter 35S. When glucocorticoids are absent from the medium KNAT1-GR resides in the cytoplasm. Upon binding of a glucocorticoid, e.g. dexamethasone (Dex), to the receptor domain, transport of the fusion protein to the nucleus is allowed and KNAT1-dependent transcription can be induced without translation.

Figure 26. Phenotype and secondary growth of *KNAT1* overexpressors compared to wild-type. No-0 (A, E, I), *35S::KNAT1* (B, F, J), Col-0 (+ Dex, C, G, K), *35S::KNAT1-GR* (+ Dex, D, H, L). Bar for hypocotyl: 1000 µm, and for secondary growth: 200µm. Note that leaves of *35S::KNAT1* (B) appeared more glossy since they formed less trichomes than the wild-type (A).

In *35S::KNAT1*, lobed leaves were initiated beginning with the first true leaves after the emergence of cotyledons, whereas in *35S::KNAT1-GR*, they started following Dex application at very early stage of postembryonic growth. These findings are in line with previously published data (Hay et al. 2003). After 4 weeks, all leaves of both lines were lobed (Figure 26). The diameter and area of *35S::KNAT1* hypocotyls were not different compared to wild-type, conversely, the hypocotyl diameter and area of *35S::KNAT1-GR* were significantly reduced (Figure 27).

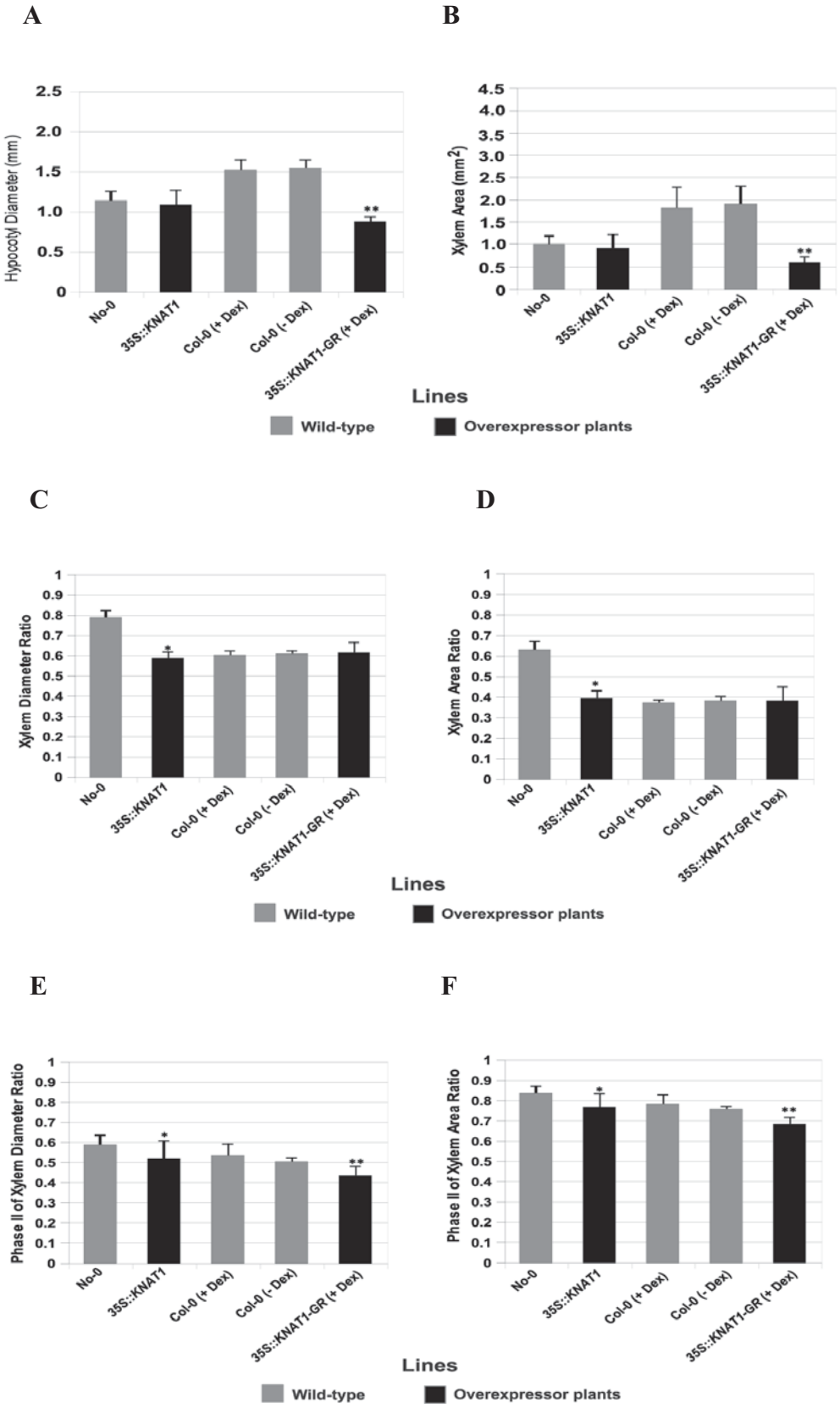

Figure 27. Secondary growth of *KNAT1* overexpressor plants in *Arabidopsis* hypocotyl compared to wild-type. Data were measured from 6 biological replicates. (**) Significant $p \leq 0.01$, t-test, compared to wild-type, (*) significant $0.01 < p \leq 0.05$.

The same indication was observed for the formation of secondary xylem, xylem diameter and area ratio were reduced significantly in *35S::KNAT1*. On the other hand there was no difference in *35S::KNAT1-GR* (Figure 27C, D; Supplemental data 6.3). The phase II of xylem development showed significant reduction in over-expressors compared to wild-type (Figure 27E, F; Supplemental data 6.3). In conclusion, over-expression of *KNAT1* is not sufficient to induce an opposite phenotype observed in the *knat1* mutants.

3.8 Overexpression of *KNAT1* gene did not restore the *stm* phenotype in *stm-GK*

In order to test if *KNAT1* overexpression can restore secondary growth in *stm-GK*, *35S::KNAT1-GR* was introduced into homozygous *stm-GK* background. *stm-GK;35S::KNAT1-GR* plants showing *stm* phenotype were exposed to Dex in order to induce KNAT1 activity. At the same time, Col-0, *35S::KNAT1-GR* and *stm-GK* were also treated with Dex.

Induction of KNAT1-GR activity in *35S::KNAT1-GR* and *stm-GK;35S::KNAT1-GR* resulted in lobed leaves at early stage of growth (Figure 28) indicating that the Dex treatment worked successfully. Hypocotyl diameter and area of Dex treated *35S::KNAT1-GR*, *stm-GK*, and *stm-GK;35S::KNAT1-GR* were significantly reduced compared to Col-0 treated with the Dex (Figure 29 and 30A, B; Suplemental data 6.4). Similarly, phase II of xylem development was reduced in Dex treated *35S::KNAT1-GR*, *stm-GK*, and *stm-GK;35S::KNAT1-GR* (Figure 30E, F; Supplemental data 6.4). The xylem diameter and area ratio of *stm-GK* and the double mutant *stm-GK;35S::KNAT1-GR* were significantly decreased compared to wild-type, on the other hand, there was no difference between *35S::KNAT1-GR* and wild-type (Figure 30C, D). The treatment with Dex did not result in an effect on secondary growth of wild-type. Importantly, the secondary xylem development represented by xylem diameter and area ratio as well as phase II of xylem development of Dex induced *stm-GK;35S::KNAT1-GR* was not different from *stm-GK* (Figure 30 C, D, and 30E, F). This suggests that the overexpression of *KNAT1* does not recover the *stm* phenotype and that the overexpression phenotype of *KNAT1* does not require full STM activity.

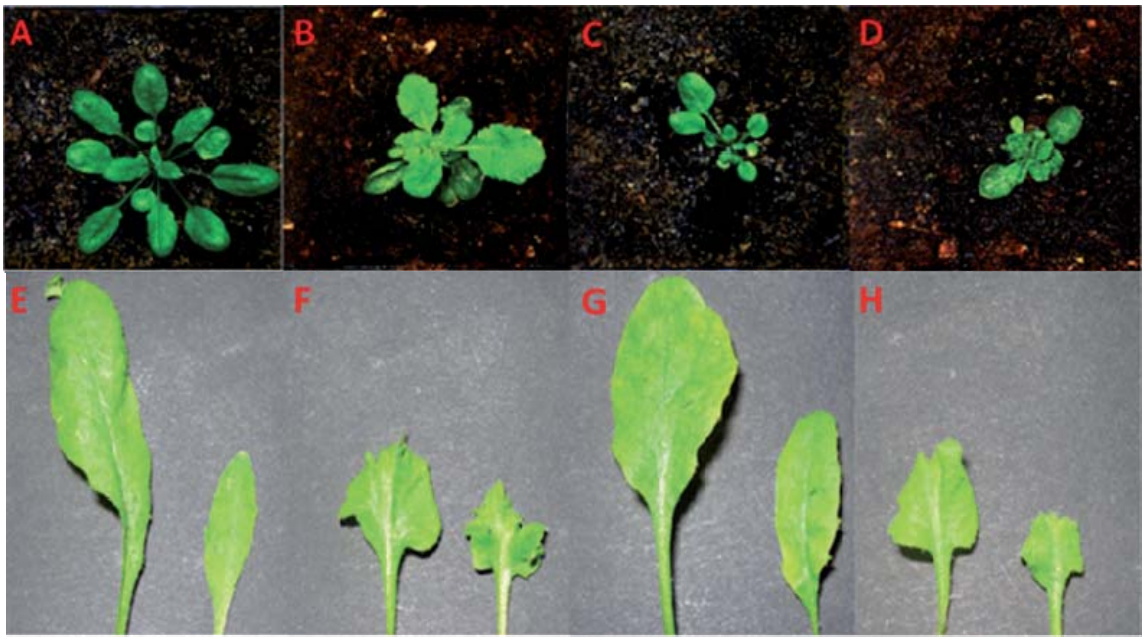

Figure 28. The leaves of *35S::KNAT1-GR* and the *stm-GK;35S::KNAT1-GR* started to lob due to Dex exposure. (A, E) Col-0 + Dex, (B, F) *35S::KNAT1-GR* + Dex, (C, G) *stm-GK* + Dex, (D, H) *stm-GK;35S::KNAT1-GR*.

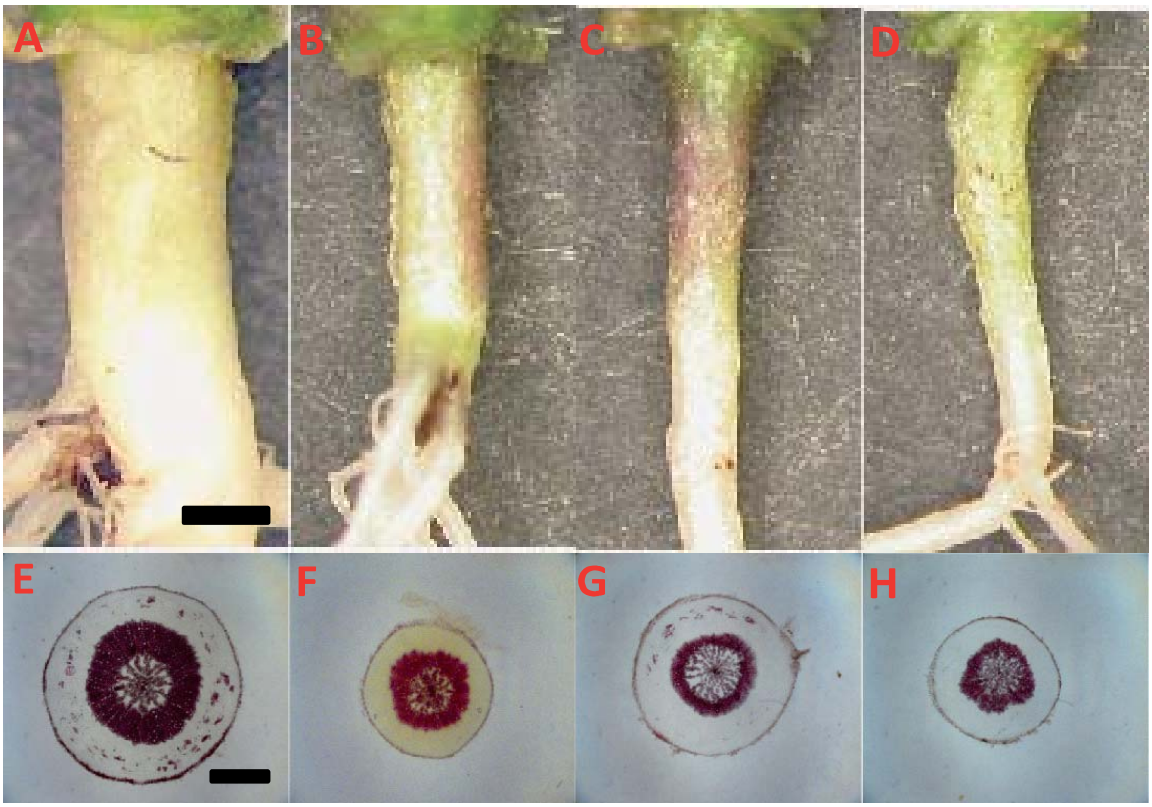

Figure 29. Effect of *KNAT1* overexpression on *stm* phenotype in secondary growth of *Arabidopsis* hypocotyls. (A, E) Col-0 + Dex, (B, F) *35S::KNAT1-GR* + Dex, (C, G) *stm-GK* + Dex, (D, H) *stm-GK;35S::KNAT1::GR* + Dex. Bar for A, B, C, D: 1000 µm and bar for E, F, G, H: 200µm.

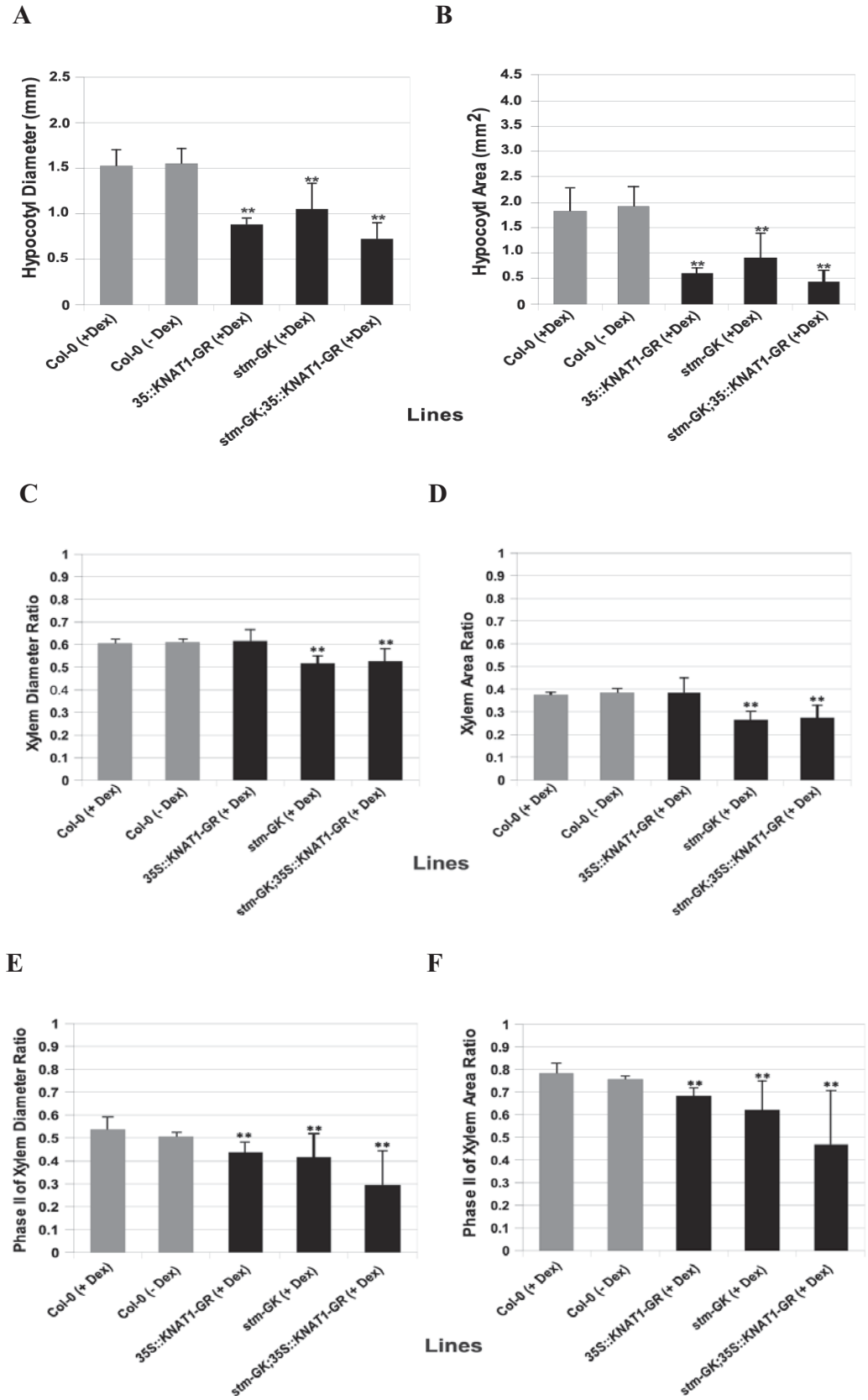

Figure 30. Secondary growth of *KNAT1* overexpression in *stm* background compared to wild-type. Data includes 5 independent replicates. (**) Significant $p \leq 0.01$, t-test, compared to wild-type, (*) significant $0.01 < p \leq 0.05$.

3.9 *STM* and *KNAT1* are required for *ATHB-8::GUS* expression in precursors of xylem fibers

ATHB-8, a member of a small homeodomain-leucine zipper family, is expressed in the procambial cells and cambium during vascular cell differentiation and is considered as an early marker of vascularization (Baima et al. 2001). Its expression pattern during secondary growth in the hypocotyls has not yet been determined. In the hypocotyl *ATHB-8::GUS* was strongly expressed in the cambial zone and the early developing xylem (Figure 31A, B). It was expressed continuously along the cambial zone with strongest expression in cells adjacent to the vessel elements. In *stm-GK* and *knat1*$^{bp-9}$, *ATHB-8::GUS* was still expressed in cells adjacent to vessel elements, but expression in cells at the origin of files of xylem fibers was absent (Figure 31C, D and E, F). Hence, reduced formation of xylem fibers in *stm* and *knat1* mutants could be explained by inhibition of early differentiation steps mediated by *ATHB-8*. Furthermore *KNAT1* and *STM* function are required for *ATHB-8* expression in early xylem fiber derivates.

In order to determine if the reduced formation of xylem fibers is a consequence of reduced cell division activity in the cambial cells giving rise to fibers, the cell division reporter *CyclinB1;1::GUS* (Colon-Carmona et al. 1999) was crossed into *stm* and *knat1* mutant background. *CyclinB1;1::GUS* was specifically expressed in distinct cells outside of the xylem, highlighting cambial cells, which are supposedly the only dividing cells in this position (Figure 31G, H). Although the division rate appeared to be reduced in *stm-GK* and *knat1*$^{bp-9}$, divisions could also be observed at the site where in wild-type fiber cells differentiate (Figure 31I, J and K, L). This was in contrast to xylem vessels, which differentiated also in the mutants just adjacent to the dividing cambial cell. Although the parenchymatic cells, which occurred instead of fiber cells in the mutants, had a dense cytoplasm and no secondary cell wall, no expression of the cell division marker could be observed in these cells. This suggests that those parenchymatic cells are arrested in an early step of differentiation but no longer mitotically active.

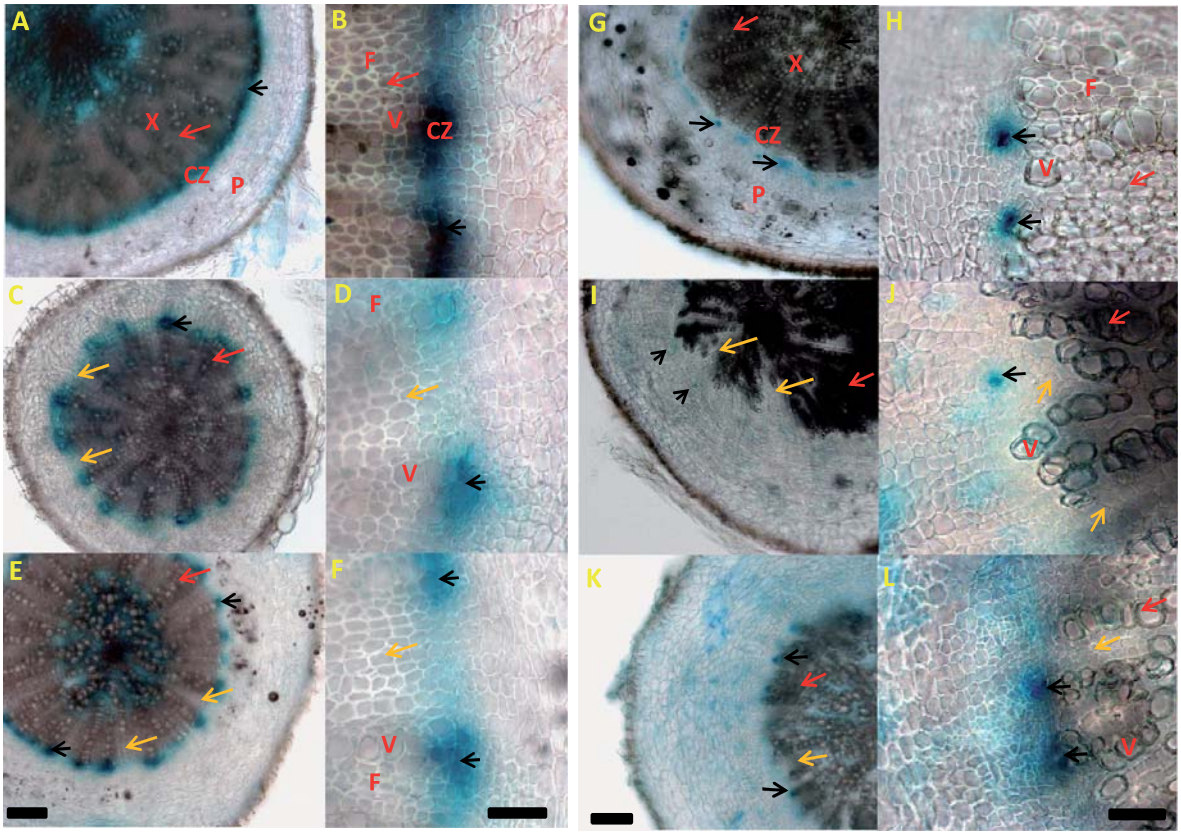

Figure 31. *ATHB8::GUS* and *CyclinB1;1::GUS* expression in wild-type, *stm-GK*, and *knat1*$^{bp-9}$. *ATHB8::GUS* (A, B), *stm-GK*; *ATHB8::GUS* (C, D), *ATHB8::GUS;knat1*$^{bp-9}$ (E, F), *CyclinB1;1::GUS* (G, H), *stm-GK;CyclinB1;1::GUS* (I, J), *CyclinB1;1::GUS;knat1*$^{bp-9}$(K, L). (Black arrow) GUS positive cells, (red arrow) differentiated cells, (yellow arrow) undifferentiated cells. (CZ) Cambial zone, (X) xylem, (P) phloem, (F) fiber cells, (V) vessel elements. Bar for A, C, E, G, I, K: 100 µm and bar for B, D, F, H, J, L: 10 µm.

3.10 *STM*/*KNAT1* are upstream of genes associated with vascular meristem differentiation, fiber development and secondary cell wall formation

If *KNAT1* and *STM* act as transcription factors, the target genes should be coexpressed with them. In order to identify genes which act downstream of *KNAT1* and *STM* co-expression analysis of publicly available microarray data was performed, using *Arabidopsis* Co-expression Tool (ACT; www.arabidopsis.leedsac.uk/ACT). Genes, which are positively regulated by *KNAT1* or *STM* should be co-expressed with both of them, since they have overlapping function in secondary growth. From 100 genes co-expressed with either *STM* or *KNAT1*, 69 genes (69%) were identical (supplemental data 6.11). In other words, those 69 genes are co-expressed with *STM* and also *KNAT1*. This astonishingly high overlap underlines the redundant function of *STM* and *KNAT1*. Of 69 overlapping genes seven genes (Table 3) were selected based on their association with secondary cell wall formation and their ranking of co-expression (Supplemental data 6.11).

Quantitative expression analysis in wild-type, *stm-GK*, *knat1*$^{bp-9}$ and the double mutant was subsequently performed for the selected genes.

Table 3. *STM* and *KNAT1* co-expressed genes selected based on their association with secondary cell wall formation.

No.	**Locus**	**Name of Protein**	**Function (Putative)**
1.	AT3G59010	Pectin methylesterase, PME61	Cell wall modification
2.	AT5g59310	Lipid transfer protein 4, LTP4	Unknown
3.	AT5G3170	Fasciclin-like arabinogalactan 11, FLA11	Unknown
4.	AT4G18780	Cellulose synthase, CesA8 (IRX1)	Cellulose biosynthesis
5.	AT5G17420	Cellulose synthase, CesA7 (IRX3)	Cellulose biosynthesis
6.	AT5G44030	Cellulose synthase, CesA4 (IRX5)	Cellulose biosynthesis
7.	AT5G15630	Cobra like 4 (COBL4), IRX6	Arrangement of cellulose microfibrils

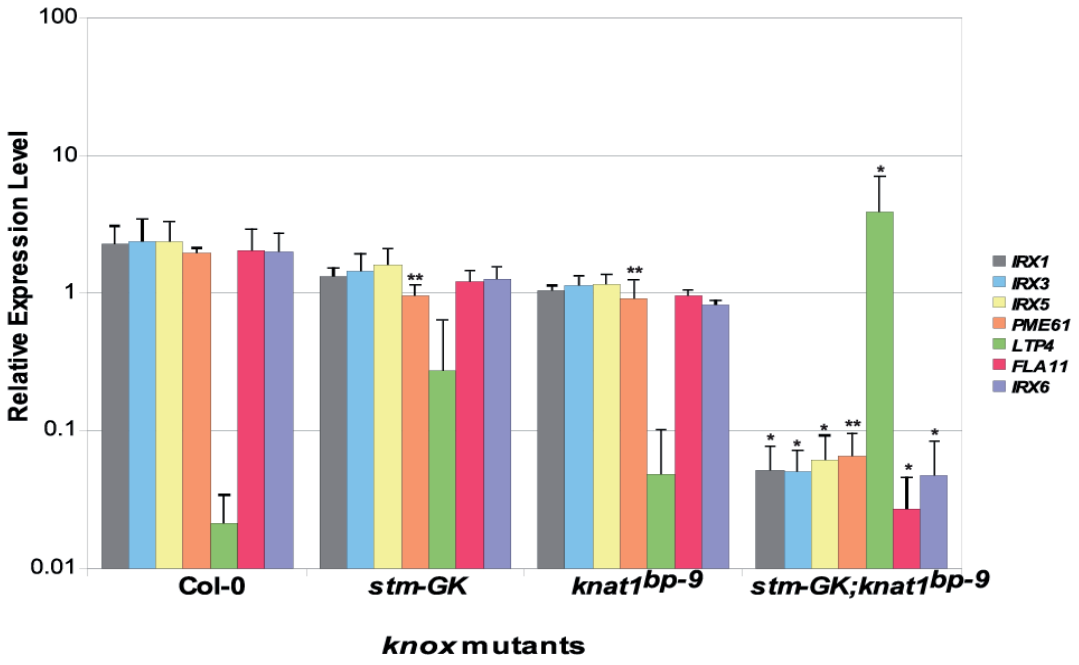

Figure 32. *STM* and *KNAT1* are involved in cellulose biosynthesis. qRT-PCR analysis of co-expressed genes in *stm-GK*, *knat1*$^{bp-9}$ and *stm-GK*;*knat1*$^{bp-9}$. Data were analyzed from 3 biological and 3 technical replicates and normalized to the expression of *ACTIN2*. (**) Significant $p \leq 0.01$, t-test, compared to wild-type, (*) significant $0.01 < p \leq 0.05$.

Down-regulation of *STM* and *KNAT1* was always followed by a not significant trend of down-regulation of cellulose synthases (*IRX1, IRX3* and *IRX5*), *cobra-like 4* (*IXR6*), *pectin methylesterase61 (PME61)*, and *fasciclin-like arabinogalactan 11*(*FLA11*) in the single mutants (Figure 32, Supplemental data 6.9). In the double mutant the down-regulation for all those genes was greater than 10 times and highly significant (Table 5). Only the *lipid transfer protein 4* (*LTP4*) behaved in an opposite manner and was upregulated in the double mutant. Thus, *STM* and *KNAT1* are upstream of *IRX1, IRX3, IXR6*, *PME61* and *FLA11*.

To address the potential involvement of *STM* and *KNAT1* in lignin deposition during secondary cell wall formation, key-genes of lignin biosynthesis previously identified by Mele et al (2003) were tested for their expression in the mutants. Those genes have been shown to be misregulated in *knat1*$^{bp-9}$ five day old seedlings in a microarray experiment employing 2 replicates (Mele et al. 2003).

Table 4. Selected key-genes of lignin biosynthesis as reported by Mele et al (2003). These genes were differentially regulated in two week old *knat1*$^{bp-9}$ seedlings (Mele et al. 2003).

No.	Abreviation	Locus	Name of Protein	Function
1.	At4CL1	AT1G51680	4-Coumarate-CoA ligase1	Lignin biosynthesis
2.	PAL1	AT2G37040	Phenylalanine ammonia-lyase 1	Lignin biosynthesis
3.	CAD1	AT4G39330	Cinnamyl-alcohol dehydrogenase 1	Lignin biosynthesis
4.	PRX	AT3G21770	Peroxidase	Lignin biosynthesis

Interestingly, the expression of *At4CL1, PAL1, CAD1*, and *PRX* in *stm-GK*, *knat1*$^{bp-9}$, and *stm-GK;knat1*$^{bp-9}$ was not different from wild type (Col-0) (Figure 33, Supplemental data 6.10). In contrast to cellulose biosynthesis, this may indicate that *STM* and *KNAT1* are not directly involved in lignin biosynthesis.

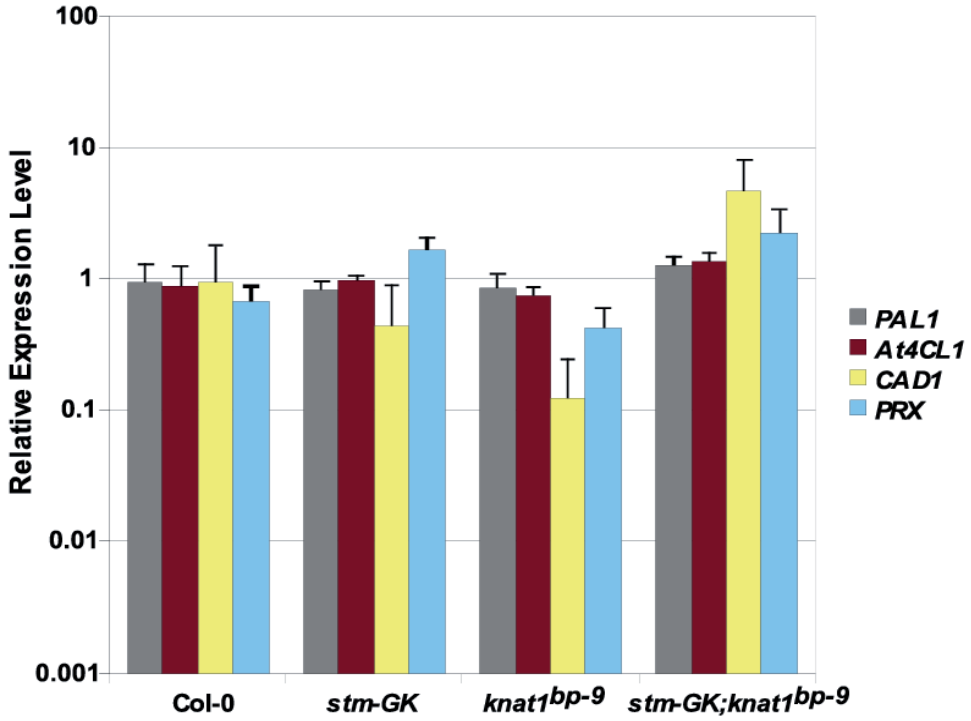

Figure 33. *STM* and *KNAT1* were not required for the expression of key-genes of lignin biosynthesis. Data were analyzed from 3 biological and 3 technical replicates and normalized to the expression of *ACTIN2*. (**) Significant $p \leq 0.01$, t-test, compared to wild-type, (*) significant $0.01 < p \leq 0.05$.

In order to identify more downstream targets of *STM* and *KNAT1*, further candidates of the list of co-expressed genes were tested. Since *STM* and *KNAT1* show genetic redundancy this analysis was restricted to quantitative expression in double mutant hypocotyls compared to wild-type.

Almost all genes selected from listed co-expressed genes by *STM* and *KNAT1* were significantly downregulated in the double mutant compared to the wild-type (Table 5, Supplemental data 6.12) except for *Lipid transferase protein4* (*LTP4*) and *BELL* (*BELLINGER*). The expression of *ATHB-8* which has been previously identified to be involved in vascular meristem differentiation (see part 3.9) was significantly reduced by almost 3 times. This supports the previous findings employing GUS reporter constructs (Figure 31), that *ATHB-8* is a downstream target of *STM*/*KNAT1*. Other genes which have been previously reported to be involved in xylem fiber identity (*SND1* and *NST1*, Zhong et al. 2006; Mitsuda et al. 2007; Zhong et al. 2007) and xylem vessel identity (*SND2*) were also downstream targets of *STM/KNAT1* since their expression was significantly reduced in the double mutant. Besides genes associated with cellulose biosynthesis (*IRX1, IRX3, IRX5, IRX6*) and pectin formation (*PME61*) (Figure 32), also hemicelluloses biosynthesis

seemed to be a target of combined *STM/KNAT1* action, as seen in the down-regulation of the galacturonosyltransferase *IRX8* (Table 5, Supplemental data 6.12). In respect to lignin biosynthesis, the abundance of both the laccase (*IRX12*) and the transcript for the chitinase-like protein *CTL2* were strongly decreased. However, these genes might have opposite functions since a mutation in *CTL2* leads to increased lignification (Hossain et al. 2010). Furthermore, one gene associated with auxin signaling (*IAA27*) was significantly downregulated.

In order to test if induction of *KNAT1* function is sufficient to drive expression of the identified downstream targets, expression analyses were performed with the help of a steroid-inducible (Dexamethasone, Dex) line of *35::KNAT1-GR*. Cycloheximide (Cyc) an inhibitor of protein translation was employed to see if Dex-induced gene expression is a direct effect of KNAT1-GR or if additional protein biosynthesis is required.

Table 5. The expression of coexpressed-downstream target gene candidates in the double mutant *stm-GK;knat1*$^{bp-9}$. Data were analyzed from 4 biological and 2 technical replica and normalized to the expression of *ACTIN2*. Negative ratios correspond to a decrease of expression compared to wild-type (Col-0), positive ratio to an increase. (*) Calculated based on t-test. (N.D) Not detectable, (N.A) not applicable.

No.	Locus	Gene	Relative Expression Ratio	p Value (*)
1.	AT3G59010	*PME61*	- 44 x	0.0212
2.	AT5g59310	*LTP4*	+ 47 x	0.0319
3.	AT5G3170	*FLA11*	- 39 x	0.0243
4.	AT4G18780	*CesA8* (*IRX1*)	- 30 x	0.0009
5.	AT5G17420	*CesA7* (*IRX3*)	- 186 x	0.0317
6.	AT5G44030	*CesA4*(*IRX5*)	- 76 x	0.0296
7.	AT5G15630	*COBL4*(*IRX6*)	- 42 x	0.0248
8.	AT4G32880	*ATHB-8*	- 3 x	0.0150
9.	AT1G32770	*SND1*	N.D.	N.A.
10.	AT4G28500	*SND2*	- 107 x	0.0111
11.	AT2G46770	*NST1*	- 278 x	0.0164
12.	AT5G60450	*ARF4*	- 3 x	0.0507
13.	AT4G29080	*IAA27*	- 57 x	0.0005
14.	AT5G54690	*Galacturonosyltransferase (IRX8)*	- 723 x	0.0009
15.	AT2G38080	*Laccase4* (*IRX12*)	- 404 x	0.0116
16.	AT3G16920	*CTL2 (chitinase like)*	- 100 x	0.0033
17.	AT3G42950	*GH28(polygalacturonase)*	- 2 x	0.0899
18.	AT3G10340	*PAL4*	- 3 x	0.0167
19.	AT5G02030	*BELL*	+ 1 x	0.1011

The expression of almost all of the *STM/KNAT1* downstream target genes in Dex as well as in Dex + Cyc media were not significantly different to the control (+DMSO), although there was a trend to slight over-expression (Table 6). This indicates that *KNAT1* itself is not sufficient to induce the expression of most of the *STM/KNAT1* downstream target genes. In contrast, the expression of *KNAT1, ARF4* and *IAA27* in treatments employing Dex + Cyc were significantly upregulated (Table 6). This suggests that *KNAT1* regulates its own expression and that it directly modifies auxin signaling in hypocotyls.

Table. 6. Expression target genes of *STM* and *KNAT1* in *35S::KNAT1-GR* hypocotyls. Data were analyzed from 4 biological and 2 technical replicates and normalized to the expression of *ACTIN2*. Negative ratio corresponds to a decrease of expression compared to the control (treated with DMSO), positive ratio is to an increase. (*) Calculated based on t-test. (Dex) treated with dexamethasone, (Cyc) treated with cycloheximide.

Gene	Relative Expression Ratio (fold change)					
	Dex	p value(*)	Cyc	p value(*)	Dex+Cyc	p value(*)
KNAT1	+1.54	**0.013**	+1.70	**0.013**	+3.03	**0.014**
ARF4	+1.74	**0.041**	+1.52	0.055	+2.60	**0.016**
IAA27	+1.06	0.380	+1.16	0.290	+2.05	**0.033**
IRX6	+1.94	**0.015**	+1.74	**0.011**	+2.77	0.060
STM	+1.03	0.447	+1.16	0.202	+1.79	0.059
ATHB-8	+1.22	0.176	+1.30	0.160	+1.47	0.186
SND1	+1.05	0.435	+1.05	0.408	+1.91	0.134
SND2	+1.24	0.270	+1.26	0.285	+1.99	0.087
NST1	+1.28	0.083	+1.32	0.134	+2.57	0.058
IRX1	-1.07	0.378	-1.19	0.195	+1.10	0.353
IRX1 (in seedling)	-1.12	0.428	-2.27	0.073	-1.86	0.089
IRX5 (in seedling)	+1.06	0.457	-2.52	0.044	-1.24	0.212

Intriguingly, many of the *STM/KNAT1* downstream genes were identified previously in screens for collapsed xylem vessels in the *Arabidopsis* inflorescences (Turner and Somerville, 1997) and are known as "**ir**regular **x**ylem" *irx* mutants. Collapsed or irregularly shaped vessels were attributed to changes in the secondary cell wall formation. Therefore, the vessel phenotype was examined more closely in *stm-GK*, *knat1*$^{bp-9}$ and the double mutant (Figure 34). In wild-type, *stm-GK* and *knat1*$^{bp-9}$ the vessel elements appeared to be almost round, while in the double mutant vessel diameter was markedly reduced and the cells had a more angular shape, reminiscent to various *irx* mutants. Additionally, the staining of the secondary cell walls in vessel elements appeared to be

fainter. These results suggest that *STM* and *KNAT1* are a limiting factor for cell wall biosynthesis in vessels, which is in line with the function of their down-stream targets.

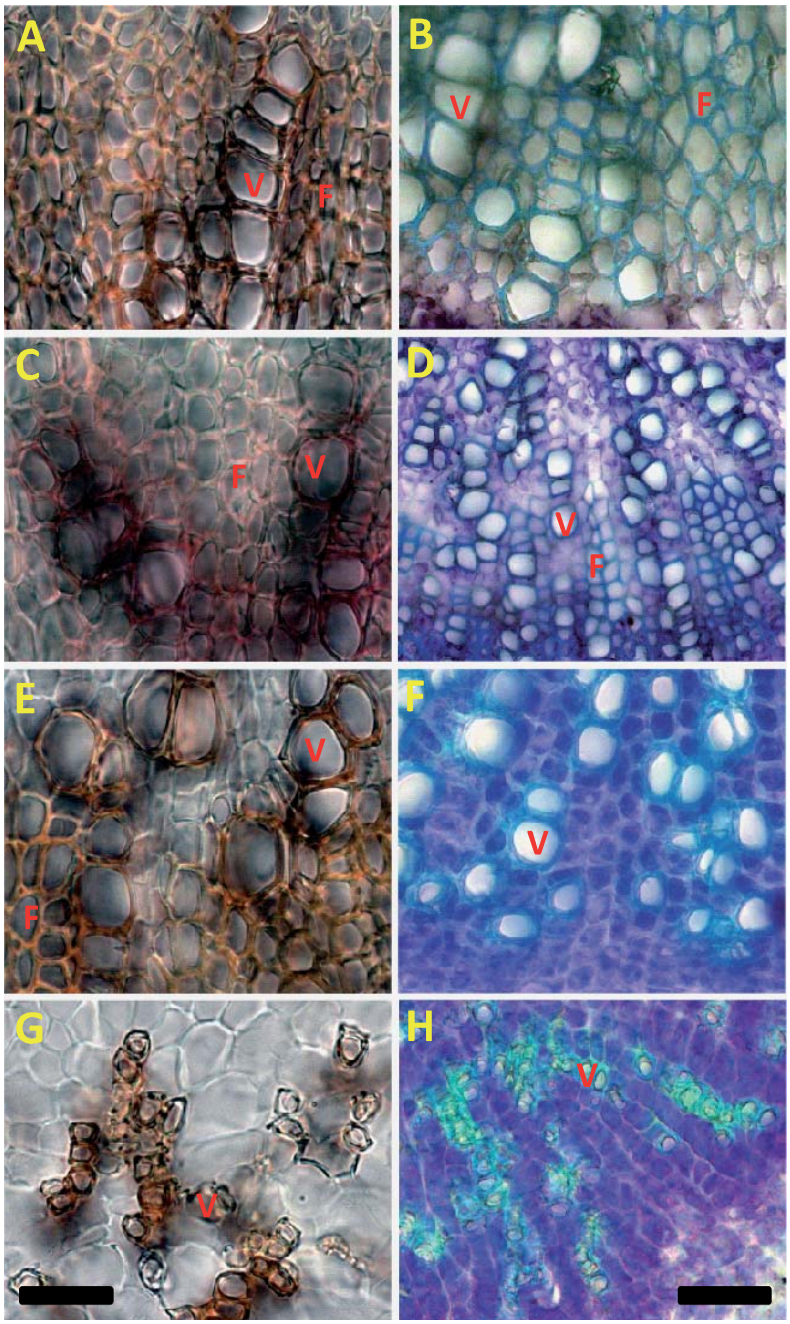

Figure 34. Vessel element structures of *Arabidopsis* hypocotyl in Col-0 (A, B), *stm-GK* (C, D), *knat1*^{bp9} (E, F) and *stm-GK;knat1*$^{bp-9}$ (G, H). (A, C, E, G) Stained using phloroglucinol-HCl, (B, D, F, H) stained using toluidine blue. Bar: 10µm.

Since the phenotypes observed in the single mutants of *knat1* are in sharp contrast to published data for the inflorescence of *knat1* mutants (Mele et al. 2003), inflorescences of all *knox* mutants were harvested and subjected to a qualitative analyses of lignification (Figure 35). s*tm-GK* developed inflorescences without functional flowers and the *knat1*

mutants had downward pointing siliques, while the other mutants were not different from wild-type (Figure 35A). As noted by Mele et al (2003) some fasicular bundles in *knat1* mutants were not lignified and appeared still green (Figure 35B). In the other mutants a similar defect in differentiation was not observed. In contrast to Mele et al (2003), neither ectopic nor increased lignifications were observed in the most basal internode of *knat1* inflorescences (Figure 35)

A

B

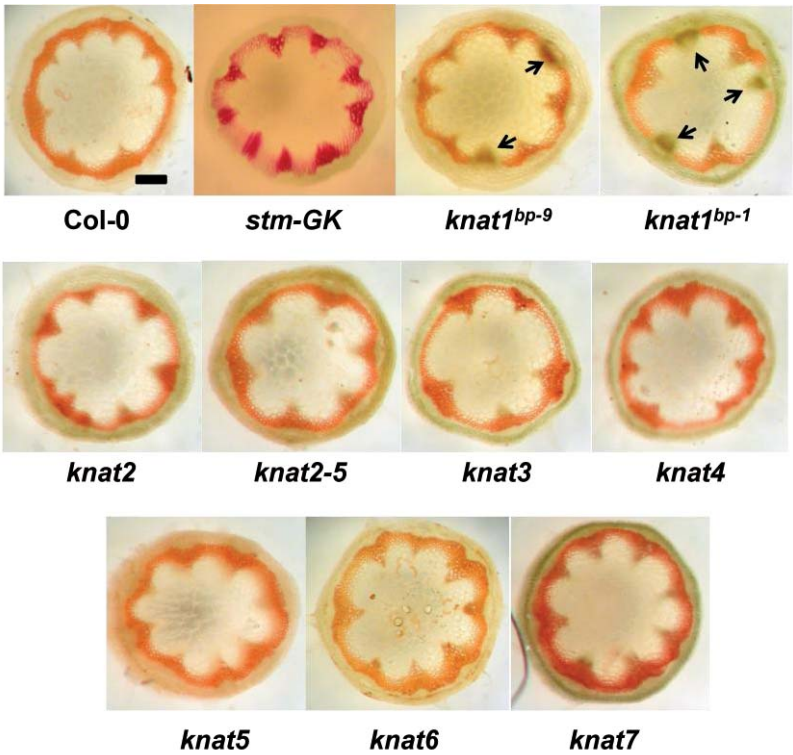

Figure 35. Inflorescences (A) and lignification (B) of *knox* mutants compared to wild-type. Note the green fasicular bundles in *knat1* mutants (B). (Black arrows) Unlignified fasicular budles. Bar: 200µm.

4 Discussion

4.1 Insertional mutagenesis

This work describes the successful isolation of insertional mutants for all known *Arabidopsis KNOTTED1*-like homeobox (*KNOX*) genes. Gene expression analysis using 6-week-old hypocotyls showed that the tagged *KNOX* genes were dramatically downregulated in *stm-GK*, *knat1*$^{bp-9}$, *knat2*, *knat3*, *knat6* and *knat7*, respectively (Table 1). However, the magnitude of the reduction varied for the different mutants. All the analyzed insertions are located in introns, which may interfere for example with splicing or RNA stability. Exon insertions for *KNOX* genes have so far not been described, with the exception of *knat2-5*. Since T-DNA does not integrate preferentially into introns (Kim et al. 2007), this may indicate that exon insertions in *KNOX* genes interfere strongly with embryo or seedling viability. Alternatively, gene structure of *KNOX* genes may hinder integration of T-DNA. Other means to disrupt gene function are the use of chemical mutagens as well as RNAi (RNA-interference). While chemical mutagenesis is not applicable for species with long generation time, RNAi has been proven to be a powerful technology in various plant species, e.g. poplar. RNAi allows to isolate transgenic lines with a broad range of suppression although target gene suppression greater than 90% is rare (Li et al. 2008). In the case of *stm-GK* a suppression of more than 99.8 % was measured (Table 1), however the mutant phenotype in the hypocotyl of *stm-GK* was still very mild compared to the null alleles (Figure 11). Hence, such a phenotype could possibly not have been observed by using RNAi, since the degree of downregulation is generally too low.

Previous work uncovered a complex network of genetic interaction of *KNOX* and closely related genes in the floral architecture of *Arabidopsis* (Ragni et al. 2008). Here, genetic interaction between *STM* and *KNAT1* could be shown. In both studies insertional mutants were employed. Likely, by RNAi such genetic interactions between *KNOX* genes could not have been found, since RNAi constructs usually target several similar sequences in a genome, so called off-targets (Filichkin et al. 2007).

Insertional mutagenesis often leads to the expression of truncated proteins, e.g. 5' flanking sequence of the insertion. Such truncated proteins may still be fully or partially functional or even produce dominant effects. For none of the mutants a dominant phenotype could be observed in crossing experiments. Albeit, the expression of the 5'

flanking sequence in *stm-GK* was slightly but significantly overexpressed. Since the insertion in *stm-GK* is in the first intron, overexpression of the 5' flanking sequence is unlikely to have an effect.

The genome of *Arabidopsis* has relatively small introns and little intergenic material (Krysan et al. 1999). This makes insertional mutagenesis efficient. In the last decade countless insertional lines have been made available to the *Arabidopsis* community (Alonso et al. 2003). Without this effort the functional analysis and the study of genetic interactions within small gene families, as it is reported here, would have been strongly impeded. For other species however a similar initiative to create insertional stocks seems not to be feasible. Regeneration of transgenics from tissue culture, long generation time, short period of seed viability are only few of the hurdles, which would be faced in other model species as poplar.

4.2 Secondary growth in *Arabidopsis* hypocotyls *versus* inflorescence stems

For reasons outlined above, trees are genetically poorly accessible in comparison with *Arabidopsi*s. Although secondary growth of trees is economically relevant, *Arabidopsis* has become increasingly important in the study of secondary growth and secondary cell wall formation. Especially, the *Arabidopsis* root and hypocotyl (Dolan et al. 1993; Dolan and Roberts. 1995) which have a vascular cambium (Busse and Evert. 1999) are reminiscent to woody structures in trees. In inflorescence stems secondary vasculature is formed by the fasicular cambium, which derives from the traces of lateral organs. The interfascicular cambium fills the gaps between the traces with extensively lignified xylem fibers (Dharmawardhana et al. 1992). Research on the *Arabidopsis* inflorescence contributed valuable data in regards of xylem fiber and vessel specification as well as secondary cell wall formation. Since vessels only occur within the fasicular bundles and fibers are restricted to interfasicular regions, the resemblance of secondary growth to woody structures is only limited. In contrast to the inflorescence, *Arabidopsis* hypocotyls show separation of elongation and radial growth and no apical-basal developmental gradient (Sibout et al. 2008). Furthermore, the secondary growth of *Arabidopsis* hypocotyls shows no seasonal regulation, which facilitates genetic studies of secondary growth. In *Arabidopsis* hypocotyls, the xylem comprise vessel elements, xylem parenchyma and fibers but lack rays. However, under certain growing conditions rays can be detected (Busse and Evert, 1999). Apparently, they are not commonly required for

Arabidopsis development. On one hand the reduction to only three cell types in the secondary *Arabidopsis* xylem is an advantage which facilitates its study; on the other hand *Arabidopsis* "wood" is lacking one cell type typical for wood.

While Chaffey et al (2002) claimed that growth under short days favors excessive radial expansion, Sibout et al (2008) convincingly showed that induction of flowering correlates with induction of radial expansion. It seems that the extended growth period after bolting led to the observation of Chaffey et al (2002) under short day. Since Sibout et al (2008) did not comment on the day-length used for their experiments it remained unclear if under long days secondary growth will take place. In both winter-annual or rapid cycling *Arabidopsis,* flowering occurs faster if plants are exposed to long days (16 hours of light; 8 hours of darkness) rather than to short days (8 hours of light; 16 hours of darkness) (Kim et al. 2008). The experiments shown here prove that long day conditions are sufficient to induce secondary growth. This facilitates experiments since growth cycles will not exceed six weeks and since laborious short-day growth conditions can be avoided.

4.3 Pleiotropic effects of reduced *STM* and *KNAT1* gene function on secondary growth

STM is required for the establishment and maintenance of the shoot apical meristem. Null-alleles lead to a complete developmental arrest during late embryogenesis. In such mutants potential postembryonic functions of *STM* cannot be studied. A way of overcoming this dilemma is the construction of inducible mutants or the examination of weak *stm* alleles. As shown here, the weak *stm* alleles *stm-GK*, *stm6*, stm^{wam1-1} allow to study postembryonic development even though they are sterile. It should be kept in mind that late developmental defects in weak *stm* mutants might be a consequence of earlier developmental failures rather than direct effects. By the generation of inducible mutants, e.g. a heatshock promoter controlled *STM*-RNAi construct, such problems could be circumvented. However, such approaches will most likely lead to the formation of genetic mosaic plants (Heidstra et al. 2004), whose analysis might be complex. In respect of *STM* and *KNAT1* function in the *Arabidopsis* hypocotyl, direct effects however are likely, since both of the genes are expressed specifically in the cambial zone (Figure 16).

Among various functions, hypocotyls connect roots and shoots. In other words, nutrients, photoassimilates and other molecules transported from roots to shoots or *vice versa* have to pass the hypocotyl. In this respect, secondary growth is necessary to provide

enough transport capacity for the distribution of solutes within the plant. Interestingly, although the size of hypocotyls of various weak *stm* and *knat1* mutants was significantly decreased (Figure 12, 13, and 14A, B), the shoot dry mass was not different for *stm-GK* and *knat1*$^{bp-9}$ (Figure 14C). This suggests that a decrease of secondary xylem in the range of those mutants does not decrease the transport capacity substantially and the mutants are still supported sufficiently with the required minerals and water. Although not shown, no limitation for redistribution through the phloem would be expected, since no reduction of phloem formation was observed in *stm-GK* and *knat1*$^{bp-9}$. In contrast, in the double mutants *stm-GK;knat1*$^{bp-9}$, the drastically reduced area of xylem and phloem might result in limiting transport capacity and hence contribute to the dwarf shoot. This is supported by the occurrence of smaller and collapsed vessel elements in *stm-GK;knat1*$^{bp-9}$ (Figure 23 and 34). Further experiments would be required to clarify the role of secondary growth and hypocotyl diameter on the growth capacity. Observation of senescence, grafting experiments, determination of shoot to root ratio in those mutants could contribute to a better understanding. It is interesting, to note that the weak *stm* mutants were all strongly delayed in senescence (data not shown). This is most likely due to their failure in flowering, however a blockage of redistribution could contribute to the late senescence phenotype as well.

Xylem development was inhibited in the *stm* and *knat1* mutants in 4-week-old and 6-week-old plants but not in the 2-week-old seedlings (Figure 20). This shows that *STM* and *KNAT1* are required for secondary growth, which is initiated after 4 weeks. On the other hand the primary growth of the hypocotyl was not affected by this amount of reduction of *KNAT1* or *STM* activity. This finding supports the idea of direct and specific effects of *STM* and *KNAT1* on secondary growth, rather than an indirect effect on developmental processes during primary growth.

Of the distinct zones seen in cross sections of hypocotyls, the phase II secondary xylem was most drastically reduced in the *stm* and *knat1* mutants. In the double mutants, the reduction was significantly stronger or phase II xylem was even completely absent (Figure 22 and 23). Since phase II xylem contains xylem fibers a reduction of physical strength could be expected. In a rosette plant like *Arabidopsis* however, the supportive role of the hypocotyl is of minor importance compared to a stem, the homologues structure in trees. The rosette usually supports itself since some leaves are in direct contact with the soil. The lack of importance of physical support by xylem fibers in *Arabidopsis* hypocotyls

should lead to a low selective pressure for such traits. Hence, screening the countless *Arabidopsis* ecotypes (Koorneef et al, 2004) for variation in xylem fiber properties can be expected to be valuable.

The observed reduction of xylem area could be due to a reduced rate of cambial cell division and/or cell expansion of xylem derivates. In the double mutant obviously both processes were affected (Figure 21), since xylem vessel cell had a reduced diameter and less cells were formed. In the single mutants of *stm-GK* and *knat1*$^{bp-9}$ however, cell sizes appeared to be normal. Consequently, cell division must be reduced in the single mutants. In other words, cambial cell division seems to be more sensitive to a reduction of *STM/KNAT1* function than cell expansion. This conclusion was supported by the observation of the cell cycle marker *CyclinB1;1::GUS* in the single mutant background (Figure 31). *CyclinB1;1* is an *Arabidopsis* mitotic cyclin expressed only in the G2/M transition stage, when the cell is ready to divide into two daughter cells (Doerner et al. 1996; Shaul et al. 1996). In the cell cycle reporter construct *CyclinB1;1::GUS*, GUS was destabilized by including a PEST-box (Doerner et al. 1996). Therefore, *CyclinB1;1::GUS* is an excellent reporter to identify dividing cells in rapidly growing tissue. In the *stm-GK* and *knat1*$^{bp-9}$, *CyclinB1;1::GUS* was expressed in a few single cells in the cambial zone (Figure 31) although the number seemed to be lower than in wild-type. Only occasionally, GUS activity could be detected in cambial cells giving rise to fibers. Lower cambial activity at places, which give rise to xylem fibers could explain the reduction in phase II xylem formation. More extensive quantitative microscopic analysis will be required in future to conclusively distinguish between effects on cell expansion or division in the different mutants.

While there is no distinct histologic feature, which differentiates a cambial cell from its early derivates (Evert, 2006), the common hallmark of a cambial cell is its division activity. In the absence of molecular markers for cambial cells, the longstanding controversy if the cambium forms a layer of single-celled sheath or if there are several cells, organized in radial files, which are capable of cell division, is unresolved (Evert, 2006). The results shown here identify *CyclinB1;1::GUS* as a useful tool to answer this question. During this study only single and separated cells and more rarely two adjacent cells with *CyclinB1;1::GUS* activity have been observed. This favors the theory of a sheath of single dividing cells. However, since the cell division activity in 6-week-old hypocotyls was rather low, more observation or more actively dividing cambial cells

would be required to draw a final conclusion. In support of a single-celled sheath cambium are previous findings stemming from the analysis of clonal sectors, extending form the cambial zone into the xylem and phloem (Spokevicius, 2006). A common single cambial cell at the origin of the xylem and phloem portion of such a sector is the most likely explanation for this phenomenon.

If the cambium consists of a single sheath of cells, the cell pools of phloem and xylem are in direct completion. If a cambial cell divides it will give rise to a cambial cell and to a daughter cell which will either differentiate into xylem or phloem. If both daughter cells differentiated, maintenance of the cambial cell pool would be given up and there would be cessation of cell division activity. Loss of cambial maintenance leads to discontinuation of cell files, a phenomenon which can be rarely observed in wood (Evert, 2006). In *stm-GK* and *knat1*$^{bp-9}$ the xylem area was significantly decreased (Figure 15), while the dimension of outer tissue was not altered. This indicates that specification of xylem is more sensitive to reduction of *STM* and *KNAT1* activity than the specification of phloem cells. In the single mutants, relatively more cambial daughter cells differentiate into phloem cells on the expenses of differentiation into xylem cells. Alternatively, if more cells in a cell file are able to divide, as depicted in the model of Figure 36, *STM* and *KNAT1* could be suggested to act on the activity of the so called xylem mother cell. This model is based on the assumption that the cambial initial, which itself is dividing relatively slowly, gives rise to rapidly dividing xylem and phloem mother cells, which in contrast to the initial have a shorter period of cell division activity. This latter model resembles more to the situation known of the shoot apical meristem, where the initial cells (stem cells), in the very center of the apical dome, are dividing less frequently, as the cells replaced to the flanks (Baurle and Laux, 2003). In contrast, if assuming a single-celled sheath of dividing cells, the cambium would be more closely related to the root apical meristem, where the bulk of cell divisions are made by stem cells in direct contact with the quiescent center (Sarkar et al. 2007). Intriguingly both *STM* and *KNAT1* play an important role in the shoot apical meristem (Barton and Poethig, 1993; Long et al. 1996; Hake et al, 2004; Byrne et al. 2002), for none of them a function in the root apical meristem has been assigned (Truernit et al. 2006).

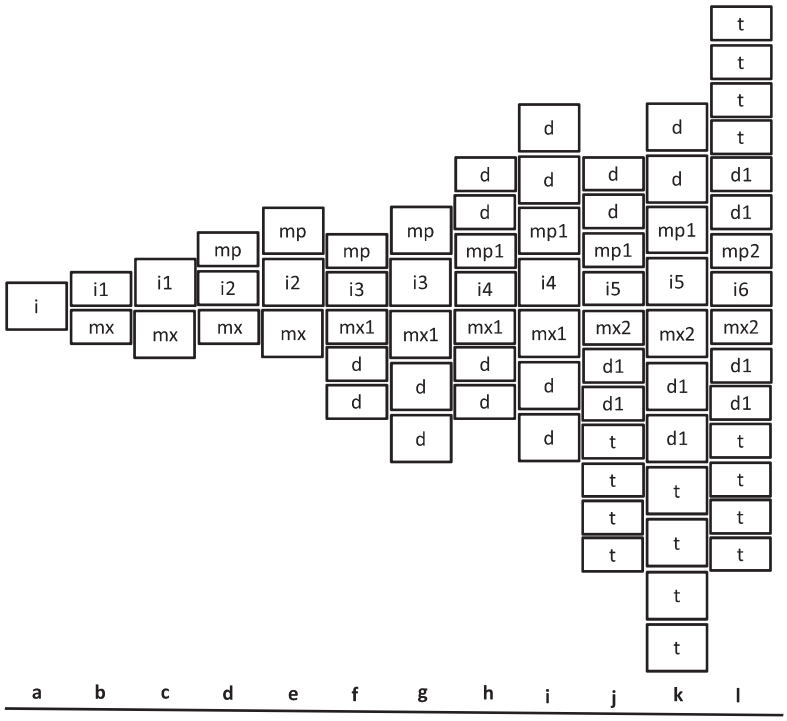

Figure 36. The cambial cell and its derivates. Formation of secondary xylem and phloem in a theoretical scheme; redrawn and modified from Evert (2006). (i) Initials, (mx) mother cells of xylem, (mp) mother cells of phloem, (d) daughter cells, (t) tissue cells derived from daughter cells. (a-l) time events.

4.4 Genetic interaction between *KNAT1* and *STM*

Here, overlapping function for *STM* and *KNAT1* in secondary xylem development of *Arabidopsis* hypocotyl could be shown (Figure 24 and 25). The phenotype in secondary xylem development was much stronger in the double mutant *stm-GK;knat1*$^{bp-9}$ than in the single mutants. This suggests that *STM* and *KNAT1* have redundant functions and work synergistically. This non-epistatic interaction is further substantiated by the fact that the downregulation of *STM* in the *stm-GK* did not repress the expression of *KNAT1* and *vice versa* (Figure 24 and 25). Based on phylogenetic analysis of nucleotide and amino-acid sequences, *STM* and *KNAT1* are closely related (Scofield and Murray, 2006) and they were proposed to have evolved after an ancient gene duplication event (Bharathan et al. 1999). In the development of shoot meristems *STM* and *KNAT1* were reported to have overlapping functions too (Scofield and Murray, 2006) and when ectopically expressed,

KNAT1 can replace the function of *STM* to activate meristem formation (Byrne et al. 2000). Based on the analysis of expression patterns from microarrays, a close interaction of these genes is obvious (Sunaryo and Fischer, 2009), and 69 % of the genes positively co-expressed with *STM* are also co-expressed with *KNAT1* (supplemental data 6.11). This high number of overlapping genes is further evidence that *STM* and *KNAT1* not only have redundant function in secondary growth of the *Arabidopsis* hypotcotyl but also in many other different processes.

Besides genetic interaction between *STM* and *KNAT1* other interacting partners within the *KNOX* genes have previously been reported or suggested. *STM* together with *KNAT1, KNAT2 and KNAT6* have been suggested to be required for the maintenance of a functional shoot apical meristem (Barton and Poethig, 1993; Long et al. 1996). Belles-Boix et al (2006) reported that *KNAT6* together *STM* contribute to SAM maintenance and boundary establishment in the embryo. *KNAT1*, *KNAT2*, *KNAT6* and another homeodomain transcription factor *PENNYWISE* interact in the patterning of floral architecture in *Arabidopsis* (Ragni et al. 2008). The synergistic phenotype of *stm-GK;knat1*$^{bp-9}$ double mutant indicates very close interaction. If the proteins physically interact, as other homeodomain transcription factors (Cole et al. 2006), was beyond the scope of this thesis. The recently developed method of split YFP has been implemented to plants (Ohad et al. 2007) and therefore such an undertaking becomes approachable.

4.5 Downstream factors

The degree of shared co-expressed genes between *STM* and *KNAT1* was surprisingly high. Many of the overlapping genes are related to cellulose biosynthesis and indeed the regulation involved in this process is very similar (Persson et al. 2005). Together with the requirement of *STM* and *KNAT1* for the expression of some of these genes, the fact of co-expression indicates that *STM* and *KNAT1* are true regulators.

The downregulation of *STM* and *KNAT1* repressed the expression of the *Cellulose Synthases* (*CesA*) *IRX1*, *IRX3*, *IRX5* (Figure 32, Supplemental data 6.9). This repression is synergistically controlled by *STM* and *KNAT1*. Doblin et al (2002) and Brown et al (2005) reported that the down-regulation of *IRX1* (*CesA8*), *IRX3* (*CesA7*), and *IRX5* (*CesA4*) resulted in collapsed cell walls of secondary of xylem in the inflorescence. The same indication has been reported by Turner and Somerville for *IRX1* (*CesA8*) (1997), *IRX3* (*CesA7*), and *IRX5* (*CesA4*) encode catalytic sub-units of cellulose synthases required for

cellulose biosynthesis. Intriguingly, these cellulose synthases are active during the secondary cell wall formation, while another subset of CesAs are specific for primary cell wall biosynthesis (Brown et al. 2005). In addition, these three genes are co-expressed in the same cells indicating that they work together to constitute cellulose synthase complexes (Doblin et al. 2002; Tailor et al. 2003). According to Brown et al (2005) a *Phytochelatin Synthethase* (*IRX6*) is associated with secondary cell wall biosynthesis, as evidenced by the weak and fragile inflorescence stem of the mutant. Chemical analysis of cellulose content in *irx6* showed a dramatic reduction, which was much higher than in any other of the *irx* mutants (Brown et al. 2005). Defective secondary cell wall in xylem vessels represented by collapsed and smaller vessel elements, was also found the double mutants of *stm-GK;knat1*$^{bp-9}$ (Figure 21 and 34), even though this phenotype could not be observed in the single mutants. The high correlation for co-expression of *STM* and *KNAT1* with cellulose biosynthesis genes, and the requirement of *STM* and *KNAT1* for their expression indicates that *STM* and *KNAT1* regulate cellulose biosynthesis during secondary growth of the hypocotyl.

On the other hand, downregulation of *STM* and *KNAT1* did not correlate with the expression of most of the key-genes of lignin biosynthesis represented by the unaltered gene expression of *PAL1*, *AtCL1*, *CAD1*, and *PRX* in the double mutant (Figure 33, Supplemental data 6.10). The fact that *STM* and *KNAT1* are strongly correlated with cellulose biosynthesis but not with lignin formation is consistent with evidence previously reported by Turner and Somerville (1997); downregulation of *IRX1*, *IRX2* and *IRX3* did not have an influence on lignin content. Furthermore, lignin biosynthesis is considered to occur after cellulose deposition into the secondary cell wall (Boerjan et al. 2003). In conclusion, *STM* and *KNAT1* regulate early process in secondary cell wall formation but not late ones, as lignin formation. In addition, *STM* and *KNAT1* might be involved in the regulation of hemicellulose (via *IRX8*) and pectin (*PME61*).

If *STM* and *KNAT1* directly bind to the promoters of those biosynthetic genes is not yet clear. Other downstream targets of *STM* and *KNAT1* are the transcription factors *SND1*, *SND2*, *NST1* and *ATHB-8*, which could be the direct activators of e.g. cellulose biosynthesis genes. These genes were previously shown to be involved in vascular meristem and fiber differentiation (*ATHB-8*, see part 3.9), xylem fiber identity (*SND1* and *NST1*, Zhong et al. 2006; Mitsuda et al. 2007; Zhong et al. 2007) and xylem vessel identity (*SND2*). All of these downstream targets provide further evidence that *STM* and *KNAT1*

are involved in early decisions of secondary wall formation. *ATHB-8* is a member of a small homeodomain-leucine zipper gene family and is expressed in the procambial cells and cambium during vascular cell regeneration (Baima et al. 1995; Baima et al. 2001). It has been suggested to play an important role in cell proliferation and differentiation during vascularization (Baima et al. 2001). Sessa et al (1998) identified other homologues genes, *ATHB-9* and *ATHB-14*, characterized by a HD-Zip motif at the N-terminus of the protein. *In situ* hybridization of *ZeHB-10*, *ZeHB-11, ZeHB-12*, *ATHB*-homologs in *Zinnia elegans,* showed that the mRNAs accumulated preferentially in the procambium and in immature xylem cells (Ohashi-ito, 2002). The strong expression of *ATHB-8::GUS* in cambial zone of the hypocotyls (Figure 31) is in line with these results and shows that *ATHB-8::GUS* can be used as a marker to locate and identify cambial cells and their early derivates.

In contrast to the expression in the wild type, the expression of the *ATHB-8::GUS* in *stm-GK* and $knat1^{bp-9}$ could only be detected in cells close to developing vessel elements, but not in cells giving rise to xylem fiber cells (Figure 31). The lacking expression of *ATHB-8::GUS* at the place of fiber derivates indicates that these cells do neither have cambial activity nor undergo early differentiation; underlining the results of the toluidine blue staining which showed in the mutants densely stained and undifferentiated cells at the place, where normally fiber cells occur (Figure 21).

4.6 Overexpression controversy

Both, constitutive and induced overexpression of *KNAT1* led unexpectedly to no or a similar phenotype concerning hypocotyl and xylem diameter as seen in the single *knat1* and weak *stm* mutants (Figure 26 and 27, Supplemental data 6.3). As reported by Lincoln et al (1994) the overexpression of *KNAT1* in *Arabidopsis* induced highly abnormal leaf morphology, including severely lobed leaves. The severity of lobed leaf morphology is depending on the dosage of *KNAT1* (Hay et al. 2003). A similar phenotype was observed for *35S::KNAT1-GR* (+Dex) (Figure 26), which proves that the Dex induction worked. The decrease of number of leaves and area in *KNAT1* overexpressors could result in a limitation of photoassimilates, which can be allocated for secondary growth. Another possible explanation for the reduction is RNA silencing, which can be induced if a certain gene-specific threshold of expression is surpassed, as reported by Lindbo et al (1993) and Schubert et al (2004). This possibility however is unlikely since the typical overexpressor

phenotype has been observed in leaves. However, one could propose tissue specific silencing in the hypocotyl.

Although *STM* and *KNAT1* have overlapping functions, overexpression of *KNAT1* did not recover the secondary growth phenotype of *stm-GK* (Figure 29 and 30C, D, E, F, Supplemental data 6.4). The failure of *KNAT1* overexpression to restore the *stm* phenotype could be explained if STM and KNAT1 form heterodimers with each other to be functional in secondary growth. This underlines the importance of investigating the physical interaction between STM and KNAT1 as already previously stated (part. 4.4). Additionally it would be interesting to see if simultaneous overexpression of *STM* and *KNAT1* have an promoting effect on secondary growth.

4.7 Conflict with previously published data

The data presented here support a role for *STM* and *KNAT1* in cambial activity leading to xylem derivates as well as in the induction of their early differentiation, e.g. cellulose biosynthesis for the secondary cell wall. This is in sharp contrast of the proposed role of *KNAT1* in the inflorescences stem. Mele at al (2003) have previously reported that in *knat1* mutants premature and ectopic lignification occurs. In contrast, overexpression of *KNAT1* led to decreased lignification in the inflorescence. Furthermore, their interpretation of *KNAT1* as an inhibitor of differentiation and though lignification is supported by the misregulation of lignin biosynthesis genes in the mutant and in opposite pattern in the overexpressor. In summary, Mele et al (2003) interpret the role of *KNAT1* as an inhibitor of differentiation, whereas in this work *KNAT1* is thought to trigger early differentiation. Although it cannot be excluded that *KNAT1* plays different roles in different tissues or that different growth conditions led to a different outcome, these explanations are not satisfactory. The interpretation of Mele et al (2003) is based on what they call ectopic lignin depositions, which in reality are phloem fibers. As shown in Figure 35, there was not larger area of lignified xylem in *knat1*. However, some fasicular bundles were only partly developed and still green. This phenotype was described by Mele et al (2003) too, but was not taken into consideration for their interpretation. Expression data presented here is based on qRT-PCR of at least 3 experimental replicates from isolated hypocotyls of 6-week-old plants grown under long day conditions. In contrast, Mele et al (2003) employed two experimental replicates of whole 2-week-old seedlings grown under short days. However, Chaffey et al (2002) reported that in 15 days old hypocotyls grown under short

days, secondary growth and xylem development were just initiated. Therefore the relevance of this expression data is questionable. The interpretation of *KNAT1* as an inhibitor of differentiation is largely supported by Groover et al (2006) and Du et al. (2009), who performed analysis of poplar homologs. But as shown by Sunaryo and Fischer (2009), a group of *KNAT1* homologs is specifically upregulated in the zone of secondary cell wall formation, which may indicate complex interactions between various *KNOX* genes in the poplar cambium.

The outlined difference in the role of *KNAT1* shows the difficulty in the interpretation of pleiotropic developmental phenotypes. While here most of the data derives from 6-week-old seedlings, Mele et al (2003) put more emphasis on the documentation of the phenotype at different developmental stages. Indeed such an approach can help to identify early phenotypes, which are more likely to be direct effects of a mutant allele. Therefore concepts presented here should be subjected to higher temporal resolution, in future.

4.8 A Working model of action of *STM* and *KNAT1* during secondary xylem development

Secondary growth in the hypocotyls of *Arabidopsis* has been shown to be a valid model system for secondary growth of Angiosperm trees (Chaffey et al. 2002). Therefore, it can be used as a model for wood formation (Chaffey et al. 2001, Nieminen et al. 2004). The secondary xylem development of *Arabidopsis* hypocotyls involves a cascade of developmental processes similar as in wood, including cambial cell division, cell specification, differentiation and maturation, regulation of cell expansion, deposition of secondary cell wall, and programmed cell death (Nieminen et al. 2004).

A working model is presented in Figure 37. A series of experiments has been outlined in this discussion, which will allow to test this model.

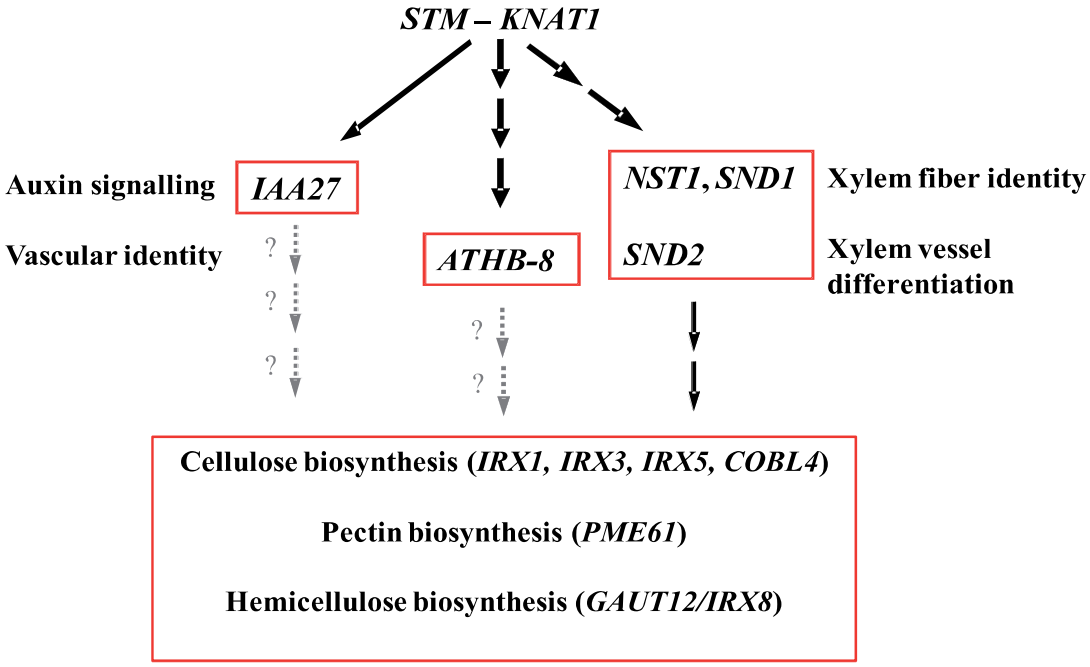

Figure 37. A hypothetical model of *STM* and *KNAT1* functions in secondary xylem development. (One arrow) Direct interaction, (several arrows) indirect interaction, (black arrows) interaction shown in this work, (grey arrows) hypothetic interaction.

5 References

Alonso JM, Stepanova AN, Leisse TJ, Kim CJ, Chen H, Shinn P, Stevenson DK, Zimmerman J, Barajas P, Cheuk R, Gadrinab C, Heller C, Jeske A, Koesema E, Meyers CC, Parker H, Prednis L, Ansari Y, Choy N, Deen H, Geralt M, Hazari N, Hom E, Karnes M, Mulholland C, Ndubaku R, Schmidt I, Guzman P, Aguilar-Henonin L, Schmid M, Weigel D, Carter DE, Marchand T, Risseeuw E, Brogden D, Zeko A, Crosby WL, Berry CC, Ecker JR (2003). Genome-wide insertional mutagenesis of *Arabidopsis thaliana*. Science, 301:653-657.

Andersson-Gunnerås S, Mellerowicz EJ, Love J, Segerman B, Ohmiya Y, Coutinho PM, Nilsson P, Henrissat B, Moritz T and Sundberg B (2006). Making cellulose enriched tension wood in *Populus*: global analysis of transcripts and metabolites identifies biochemical and developmental regulators in secondary wall biosynthesis. The Plant Journal, 45:144–165.

Baima S, Nobili F, Sessa G, Lucchetti S, Ruberti I and Morelli G (1995). The expression of the *Athb-8* homeobox gene is restricted to provascular cells in *Arabidopsis thaliana*. Development, 121:4171-4182.

Baima S, Possenti M, Matteucci A, Wisman E, Altamura MM, Ruberti I and Morelli G (2001). The *Arabidopsis* ATHB-8 HD-Zip protein acts as a differentiation-promoting transcription factor of the vascular meristems. Plant Physiology, 126:643–655.

Barton MK and Poethig SR (1993). Formation of the shoot apical meristem in *Arabidopsis thaliana*: an analysis of development in the wild type and in the *shoot meristemless* mutant. Development, 119: 823-831.

Bäurle I, Laux T (2003). Apical meristems: the plant's fountain of youth. Bioessays, 25:961-970.

Belles-Boix E, Hamant O, Witiak, SM, Morin H, Traas J and Pautot V (2006). *KNAT6*: An *Arabidopsis* homeobox gene involved in meristem activity and organ separation. The Plant Cell, 18:1900–1907.

Bharathan G, Janssen BJ, Kellogg EA and Sinha N (1999). Phylogenetic relationships and evolution of the KNOTTED class of plant homeodomain proteins. Molecular Biology and Evolotion, 16:553–563.

Boerjan W, Ralph J, Baucher M (2003). Lignin biosynthesis. Annual Review of Plant Biology, 54:519-546.

Brown DM, Zeef LA., Ellis J, Goodacre R and Turner SR (2005). Identification of novel genes in *Arabidopsis* involved in secondary cell wall formation using expression profiling and reverse genetics. The Plant Cell, 17:2281–2295.

Busse JS and Evert RF (1999). Vascular differentiation and transition in the seedling of *Arabidopsis thaliana* (Brassicaceae). International Journal of Plant Sciences, 160: 241–251.

Byrne, ME, Barley R, Curtis M, Arroyo JM, Dunham M, Hudson A and Martienssen RA (2000). *Asymmetric leaves1* mediates leaf patterning and stem cell function in *Arabidopsis*. Nature, 408:967–971.

Byrne ME, Simorowski J and Martienssen RA (2002). *ASYMMETRIC LEAVES1* reveals knox gene redundancy. Development, 129:195-1965.

Chaffey N, Cholewa E, Regan S and Sundberg B (2002). Secondary xylem development in *Arabidopsis*: a model for wood formation. Physiologia Plantarum, 114:594-600.

Chuck G, Lincoln C and Hake S (1996). *KNAT1* lnduces lobed leaves with ectopic meristems when overexpressed in *Arabidopsis*. The Plant Cell, 8:1277-1289.

Cole M, Nolte C and Werr W (2006). Nuclear import of the transcription factor SHOOT MERISTEMLESS depends on heterodimerization with BLH proteins expressed in discrete sub-domains of the shoot apical meristem of *Arabidopsis thaliana*. Nucleic Acids Research, 34:1281–1292.

Colon-Carmona A, You R, Haimovitch-Gal T and Doerner P (1999). Spatio temporal analysis of mitotic activity with a labile cyclin-GUS fusion protein. The Plant Journal, 20:503-508.

Dharmawardhana DP, Ellis BE and Carlson JE (1992). Characterization of vascular lignification in *Arabidopsis thaliana*. Canadian Journal of Botany, 70: 2238–2244.

Doblin MS, Kurek I, Jacob-Wilk D and Delmer DP (2002). Cellulose biosynthesis in plants: from genes to rosettes. Plant Cell Physiology, 43:1407–1420.

Doerner P, Jorgensen JE, You R, Steppuhn J and Lamb C (1996). Control of root growth and development by cyclin expression. Nature, 380:520-523.

Dolan L, Janmaat K, Willemsen V, Linstead P, Poethig S, Roberts K and Scheres B (1993). Cellular organization of the *Arabidopsis thaliana* root. Development, 119: 71–84.

Dolan L and Roberts K (1995). Secondary thickening in roots of *Arabidopsis thaliana*: anatomy and cell surface changes. New Phytologist, 131: 121–128.

Du J, Mansfield SD and Groover AT (2009). The Populus homeobox gene *ARBORKNOX2* regulates cell differentiation during secondary growth. The Plant Journal, 60:1000–1014.

Edwards K, Jonstone C and Thomson C (1991). A simple and rapid method for the preparation of plant genomic DNA for PCR analysis. Nucleic Acid Research, 19:1349-1350.

Evert RF (2006). Esau's plant anatomy. Third edition:323-355. John Wiley & Sons, Inc, UK.

Filichkin SA, DiFazio SP, Brunner AM, Davis JM, Yang ZK, Kalluri UC, Arias RS, Etherington E, Tuskan GA, Strauss SH (2007). Efficiency of gene silencing in *Arabidopsis*: direct inverted repeats vs. transitive RNAi vectors. Plant Biotechnology Journal, 5:615-626.

Gehring WJ (1987). Homeo boxes in the study of development. Science, 236: 1245–1252.

Groover AT, Mansfield SD, DiFazio SP, Dupper G, Fontana JR, Millar R and Wang Y (2006). The *Populus* homeobox gene *ARBORKNOX1* reveals overlapping mechanisms regulating the shoot apical meristem and the vascular cambium. Plant Molecular Biology, 61:917-932.

Haecker A, Gross-Hardt R, Geiges B, Sarkar A, Breuninger H, Herrmann M and Laux T (2004). Expression dynamics of *WOX* genes mark cell fate decisions during early embryonic patterning in *Arabidopsis thaliana*. Development, 131: 657–668.

Hake S, Smith HMS, Holtan H, Magnani E, Mele G and Ramirez J (2004). The role of *KNOX* genes in plant development. Annual Review of Cell and Developmental Biology, 20:125–51.

Hay A, Jackson D, Ori N and Hake S (2003). Analysis of the competence to respond to *KNOTTED1* activity in *Arabidopsis* leaves using a steroid induction system. Plant Physiology, 131:1671–1680.

Heidstra R, Welch D, Scheres B (2004). Mosaic analyses using marked activation and deletion clones dissect *Arabidopsis* SCARECROW action in asymmetric cell division. Genes and Development, 8:1964-1969.

Hertzberg M, Aspeborg H, Schrader J, Andersson A, Erlandsson R, Blomqvist K, Bhalerao R, Uhlen M, Teeri TT, Lundeberg J, Sundberg B, Nilsson P and Sandberg G (2001). A transcriptional roadmap to wood formation. Proceedings of the National Academy of Sciences of the United States of America, 98:14732-14737.

Hossain MA, Noh HN, Kim KI, Koh EJ, Wi SG, Bae HJ, Lee H, Hong SW (2010). Mutation of the chitinase-like protein-encoding AtCTL2 gene enhances lignin accumulation in dark-grown *Arabidopsis* seedlings. Journal of Plant Physiology, 167:650–658.

Kim SI, Veena and Gelvin SB (2007). Genome-wide analysis of Agrobacterium T-DNA integration sites in the *Arabidopsis* genome generated under non-selective conditions. Plant Journal, 51:779-791.

Kim SY, Yu X and Michaels SD (2008). Regulation of *CONSTANS* and *FLOWERING LOCUS T* expression in response to changing light quality. Plant Physiology, 148: 269–279.

Ko JH and Han KH (2004). *Arabidopsis* whole-transcriptome profiling defines the features of coordinated regulations that occur during secondary growth. Plant Molecular Biology, 55:433–53.

Koornneef M, Alonso-Blanco C, Vreugdenhil D (2004). Naturally occurring genetic variation in *Arabidopsis thaliana*. Annual Review of Plant Biology, 55:141-172.

Krysan PJ, Young JC and Sussman MR (1999). T-DNA as an insertional mutagen in *Arabidopsis.* The Plant Cell, 11: 2283–2290.

Lenhard M, Jurgens G and Laux T (2002). The *WUSCHEL* and *SHOOTMERISTEMLESS* genes fulfil complementary roles in *Arabidopsis* shoot meristem regulation. Development, 129: 3195-3206.

Li J, Brunner AM, Shevchenko O, Meilan R, Ma C, Skinner JS, Strauss SH (2008). Efficient and stable transgene suppression via RNAi in field-grown poplars. Transgenic Research,17:679-694.

Lincoln C, Long J, Yamaguchi J, Serikawa K and Hake S (1994). A knottedl-like homeobox gene in *Arabidopsis* is expressed in the vegetative meristem and dramatically alters leaf morphology when overexpressed in transgenic plants. The Plant Cell, 6:1859-1876.

Lindbo JA, Silva-Rosales L, Proebsting WM and Dougherty WG (1993). Induction of a highly specific antiviral state in transgenic plants: Implications for regulation of gene expression and virus resistance. The Plant Cell, 5:1749–1759.

Long JA, Moan EI, Medford JI and Barton MK (1996). A member of the *KNOTTED* class of homeodomain proteins encoded by the *STM* gene of *Arabidopsis*. Nature, 379:66-69.

Manfield LW, Jen CH, Pinney JW, Michalopoulos L, Bradford JR, Gilmartin PM and Westhead DR (2006). *Arabidopsis* Co-expression Tool (ACT): web server tools for microarray-based gene expression analysis. Nucleic Acids Research, 34:504-509.

McDougall GJ, Morrison IM, Stewart D, Weyers JDB and Hillman JR (1993). Plant fibres: botany, chemistry and processing for industrial use. Journal of the Science of Food Agriculture, 62:1–20.

Mele G, Ori N, Sato Y and Hake S (2003). The knotted1-like homeobox gene *BREVIPEDICELLUS* regulates cell differentiation by modulating metabolic pathways. Genes & Development, 19:412-412.

Mitsuda N, Iwase A, Yamamoto H, Yoshida M, Seki M, Shinozaki K and Ohme-Takagi M (2007). NAC transcription factors, NST1 and NST3, are key regulators of the formation of secondary walls in woody tissues of *Arabidopsis*. The Plant Cell, 19:270-280.

Nieminen KM, Kauppinen L and Helariutta Y (2004). A weed for wood? *Arabidopsis* as a genetic model for xylem development. Plant Physiology, 135:653–659.

Ohad N, Shichrur K, Yalovsky S (2007). The analysis of protein-protein interactions in plants by bimolecular fluorescence complementation. Plant Physiology, 145:1090-1099.

Ohashi-Ito K, Demura T and Fukuda H (2002). Promotion of transcript accumulation of novel Zinnia immature xylem-specific HD-Zip III homeobox genes by Brassinosteroids. Plant Cell Physiology, 43:1146–1153.

Persson S, Wei H, Milne J, Page GP, Somerville CR (2005). Identification of genes required for cellulose synthesis by regression analysis of public microarray data sets. Proceedings of the National Academy Sciences of the United States of America, 102:8633-8.

Ragni L, Belles-Boix E, Günl M and Pautot V (2008). Interaction of *KNAT6* and *KNAT2* with *BREVIPEDICELLUS* and *PENNYWISE* in *Arabidopsis* inflorescences. The Plant Cell, 20:888-900.

Raven P, Evert RF and Eichhorn (1999). Biology of plants: Secondary growth in stems (sixth edition). Freeman Worth, New-York, USA.

Reiser L, Modrusan Z, Margossian L, Samach A, Ohad N, Haughn GW and Fischer RL (1995). The *BELL1* gene encodes a homeodomain protein involved in pattern formation in the *Arabidopsis* ovule primordium. Cell, 83:735–742.

Roberts K and McCann MC (2000). Xylogenesis: the birth of a corpse. Current Opinion in Plant Biology, 3:517-522.

Sarkar AK, Luijten M, Miyashima S, Lenhard M, Hashimoto T, Nakajima K, Scheres B, Heidstra R, Laux T (2007). Conserved factors regulate signalling in *Arabidopsis thaliana* shoot and root stem cell organizers. Nature, 446:811-814.

Schrader J, Nilsson J, Mellerowicz E, Berglund A, Nilsson P, Hertzberg M and Sandberg G (2004). A high-resolution transcript profile across the wood-forming meristem of poplar identifies potential regulators of cambial stem cell identity. The Plant Cell, 16:2278-2292.

Schubert D, Lechtenberg B, Forsbach A, Gils A, Bahadur S and Schmidt R (2004). Silencing in *Arabidopsis* T-DNA transformants: the predominant role of a gene-specific RNA sensing mechanism versus position effects. The Plant Cell, 16:2561–2572.

Scofield S and Murray JAH (2006). *KNOX* gene function in plant stem cell niches. Plant Molecular Biology, 60:929–946.

Sessa G, Morelli G and Ruberti I (1993). The ATHB-1 and -2 HD-ZIP domains homodimerize forming complexes of different DNA binding specificities. The EMBO Journal, 12: 3507-3517.

Sessa G, Steindler C, Morelli G and Ruberti I (1998). The *Arabidopsis ATHB-8*, *-9* and *-14* genes are members of a small gene family coding for highly related HD-ZIP proteins. Plant Molecular Biology, 38:609-22.

Shani E, Yanai O, and Ori N (2006). The role of hormones in shoot apical meristem function. Current Opinion in Plant Biology, 9: 484-489.

Shaul O, Mironov V, Burssens S, van Montagu M and Inzé D (1996). Two *Arabidopsis* promoters mediate distinctive transcriptional oscillation in synchronized tobacco BY-2 cells. Proceedings of the National Academy Sciences of the United States of America, 93:4868-4872.

Sibout R, Plantegenet S, Hardtke CS (2008). Flowering as a condition for xylem expansion in *Arabidopsis* hypocotyl and root. Current Biology, 18:458–463.

Sinha NR, Williams RE and Hake S (1993). Overexpression of the maize homeobox gene, *KNOTTED-1*, causes a switch from determinate to indeterminate cell fates. Gene and Development, 7:787–795.

Sjödin A, Bylesjo M, Skogström O, Eriksson D, Nilsson P, Ryden P, Jansson S and Karlsson J (2006). UPSC-BASE–*Populus* transcriptomics online. The Plant Journal, 48: 806–817.

Smith LG, Greene B, Veit B and Hake S (1992). A dominant mutation in the maize homeobox gene, *Knotted-1*, causes its ectopic expression in leaf cells with altered fates. Development, 116: 21–30.

Spokevicius AV (2006). The use of induced somatic sectors for the elucidation of gene function and developmental patterns in xylogenic tissue. PhD thesis, School of Forest and Ecosystem Science, The University of Melbourne, Australia.

Sunaryo W and Fischer U (2009). *In silico* expression analysis of the *Arabidopsis KNAT1* gene and its homologs in poplar. Review of forests, wood products and wood biotechnology of Iran and Germany - Part III (Ali Reza Kharazipour, Christian Schöpper, Cora Müller and Markus Euring, Eds.). Universitätsdrucke Göttingen, p: 293-302.

Tailor NG, Howells RM, Huttly AK, Vickers K and Turner SR (2003). Interactions among three distinct CesA proteins essential for cellulose synthesis. Proceedings of the National Academy Sciences of the United States of America, 100: 1450–1455.

Timell TE (1969). The chemical composition of tension wood. Svensk Papperstidning, 72: 173–181.

Truernit E, Siemering KR, Hodge S, Grbic V and Haseloff J (2006). A Map of *KNAT* gene expression in the *Arabidopsis* root. Plant Molecular Biology, 60:1–20.

Turner SR and Somerville CR (1997). Collapsed xylem phenotype of *Arabidopsis* identifies mutants deficient in cellulose deposition in the secondary cell wall. The Plant Cell, 9:689–701.

Turner S, Gallois P and Brown D (2008). Tracheary element differentiation. Annual Review of Plant Biology, 58:407–33.

Tuskan GA, DiFazio S, Jansson S, Bohlmann J and Grigoriev I (2006). The genome of black cottonwood, *Populus trichocarpa* (Torr & Gray ex. Brayshaw). Science, 313:1596–1604.

Venglat SP, Dumonceaux T, Rozwadowski K, Parnell L, Babic V, Keller W, Martienssen R, Selvaraj G and Datla R (2002). The homeobox gene *BREVIPEDICELLUS is* a key regulator of inflorescence architecture in *Arabidopsis.* Proceedings of the National Academy Sciences of the United States of America, 99:74730–4735.

Vollbrecht E, Veit B, Sinha N and Hake S (1991). The developmental gene *Knotted-1* is a member of a maize homeobox gene family. Nature, 350: 241–243.

Zhao CS, Craig JC, Petzold HE, Dickerman AW and Beers EP (2005). The xylem and phloem transcriptomes from secondary tissues of the *Arabidopsis* root-hypocotyl. Plant Physiology, 138:803–18.

Zhong R and Demura T, Ye Z-H (2006). SND1, a NAC domain transcription factor, is a key regulator of secondary cell wall synthesis in fibers of *Arabidopsis*. The Plant Cell, 18:3158-3170.

Zhong R, Richardson EA and Ye Z-H (2007). Two NAC domain transcription factors, SND1 and NST1, function redundantly in regulation of secondary wall synthesis in fibers of *Arabidopsis*. Planta, 225:1603-1611.

Zhong R and Ye ZH (2007). Regulation of cell wall biosynthesis. Current Opinion in Plant Biology, 10:564–572.

Zhong R, Lee C, Zhou J, McCharthy and Ye ZH (2008). A battery of transcription factors involved in the regulation of secondary cell wall biosynthesis in *Arabidopsis*. The Plant Cell, 20: 2763-2782.

Zhou J, Lee C, Zhong R and Ye ZH (2009). MYB58 and MYB63 are transcriptional activators of the lignin biosynthetic pathway during secondary cell wall formation in *Arabidopsis*. The Plant Cell, 21: 248–266.

6 Supplemental Data

6.1 Secondary growth of *knox* mutants and wild-type

Lines		HD (µm)	XD (µm)	XDR	PIXD (µm)	PIIXD (µm)	PIIXDR	HA (μm^2)	XA (μm^2)	XAR	PIXA (μm^2)	PIIXA (μm^2)	PIIXAR	PH (cm)	DM (g)
Col-0	**X**	1622.42	950.93	0.59	376.39	574.54	0.60	2047483.00	727089.91	0.35	111735.05	615354.86	0.84	56.33	319.44
	N	9	9	9	9	9	9	9	9	9	9	9	9	9	9
	SD	116.24	104.75	0.04	34.42	112.39	0.06	308421.31	154861.23	0.04	23213.24	160698.99	0.05	1.03	63.17
	p														
stm-GK	**X**	1525.16	725.83	0.47	437.15	288.69	0.38	1800341.86	441377.09	0.24	152434.76	288942.32	0.61	27.23	283.00
	N	9	9	9	9	9	9	9	9	9	9	9	9	9	9
	SD	258.97	153.69	0.04	56.25	121.26	0.10	588479.49	189212.28	0.04	38215.71	173911.13	0.16	4.46	96.57
	p	0.1596	0.0011	0.0000	0.0069	0.0000	0.0000	0.1405	0.0015	0.0000	0.0074	0.0004	0.0004	0.0000	0.0534
knat1^{bp-9}	**X**	1051.43	481.70	0.46	375.67	106.04	0.21	857143.08	182512.21	0.20	116599.53	65912.68	0.29	44.00	342.56
	N	8	8	8	8	8	8	8	8	8	8	8	8	8	8
	SD	197.28	108.08	0.03	56.75	60.63	0.09	300634.31	88358.12	0.04	34233.14	57601.06	0.19	6.20	77.57
	p	0.0000	0.0000	0.0000	0.4874	0.0000	0.0000	0.0000	0.0000	0.0000	0.3669	0.0000	0.0000	0.0004	0.1177
knat1^{bp-1}	**X**	768.29	353.18	0.46	326.55	26.64	0.08	471439.39	102123.34	0.21	101154.60	968.75	0.01	24.05	156.62
	N	6	6	6	6	6	6	6	6	6	6	6	6	6	6
	SD	153.29	81.26	0.02	82.21	12.48	0.05	201711.88	47291.31	0.02	47532.84	700.30	0.01	2.50	37.69
	p	0.0000	0.0000	0.0000	0.0626	0.0000	0.0000	0.0000	0.0000	0.0000	0.2861	0.0000	0.0000	0.0000	0.0000
stm-GK;knat1^{bp-9}	**X**	285.24	35.83	0.12	35.83	0.00	0.00	77235.22	2820.94	0.03	2820.94	0.00	0.00	0.48	18.97
	N	6	6	6	6	6	6	6	6	6	6	6	6	6	6
	SD	75.42	17.34	0.04	17.34	0.00	0.00	53748.89	3935.63	0.02	3935.63	0.00	0.00	0.20	6.51
	p	0.0000	0.0000	0.0000	0.0000	0.0000	0.0000	0.0000	0.0000	0.0000	0.0000	0.0000	0.0000	0.0000	0.0000

Continued

Lines		HD (µm)	XD (µm)	XDR	PIXD (µm)	PIIXD (µm)	PIIXDR	HA (μm^2)	XA (μm^2)	XAR	PIXA (μm^2)	PIIXA (μm^2)	PIIXAR	PH (cm)	DM (g)
knat2	**X**	1799.39	1070.40	0.59	463.46	606.94	0.56	2488187.57	920368.06	0.37	167278.29	753089.77	0.81	52.50	368.37
	N	9	9	9	9	9	9	9	9	9	9	9	9	9	9
	SD	214.52	165.36	0.03	51.53	130.04	0.04	599849.50	276899.61	0.04	29285.75	255069.54	0.03	5.24	119.39
	p	0.0224	0.0429	0.3152	0.0003	0.2898	0.0722	0.0338	0.0432	0.2823	0.0002	0.0947	0.0986	0.0547	0.0327
knat2-5	**X**	1797.68	1085.69	0.60	443.85	641.84	0.59	2561500.77	964465.23	0.38	154731.09	809734.14	0.83	53.00	410.30
	N	9	9	9	9	9	9	9	9	9	9	9	9	9	9
	SD	311.59	191.58	0.02	58.08	146.01	0.04	871468.34	327292.09	0.03	42736.48	295801.55	0.03	7.32	117.66
	p	0.0667	0.0413	0.1035	0.0043	0.1447	0.2933	0.0574	0.0334	0.0997	0.0087	0.0512	0.3833	0.1477	0.0004
knat3	**X**	1894.96	1118.96	0.59	451.21	667.75	0.59	2776081.44	1020702.53	0.36	158290.01	862412.52	0.83	52.67	420.67
	N	9	9	9	9	9	9	9	9	9	9	9	9	9	9
	SD	224.80	175.69	0.04	48.53	172.15	0.06	730654.58	326675.90	0.04	26463.61	317987.64	0.05	4.13	115.97
	p	0.0026	0.0127	0.4225	0.0008	0.0963	0.3619	0.0070	0.0134	0.3067	0.0006	0.0270	0.4059	0.0306	0.0001
knat4	**X**	2003.46	1165.44	0.58	480.27	685.18	0.58	3156597.10	1113245.30	0.35	178973.73	934271.57	0.83	62.00	452.15
	N	9	9	9	9	9	9	9	9	9	9	9	9	9	9
	SD	326.41	175.06	0.03	46.41	153.50	0.05	1015498.45	343601.28	0.03	38404.74	326903.92	0.04	1.41	102.93
	p	0.0023	0.0031	0.4499	0.0000	0.0501	0.2575	0.0032	0.0036	0.4764	0.0002	0.0092	0.3567	0.0000	0.0000
knat5	**X**	1313.74	818.91	0.62	359.50	459.41	0.56	1354545.21	539730.28	0.40	100651.92	439078.36	0.80	50.33	215.67
	N	9	9	9	9	9	9	9	9	9	9	9	9	9	9
	SD	164.27	109.06	0.02	32.91	101.87	0.06	310667.09	131310.95	0.02	14529.51	130322.12	0.06	2.66	59.72
	p	0.0001	0.0087	0.0089	0.1499	0.0169	0.0598	0.0001	0.0066	0.0132	0.1178	0.0102	0.0866	0.0002	0.0000
knat6	**X**	1704.61	1035.92	0.61	432.47	603.45	0.58	2261328.22	872131.81	0.39	143334.62	728797.19	0.83	61.33	408.78
	N	9	9	9	9	9	9	9	9	9	9	9	9	9	9
	SD	144.58	102.95	0.02	26.74	106.68	0.05	398541.46	168069.58	0.02	19234.82	166347.68	0.04	3.67	60.92
	p	0.1012	0.0509	0.0612	0.0007	0.2917	0.2117	0.1106	0.0375	0.0373	0.0031	0.0803	0.3556	0.0046	0.0000

Continued

Lines		HD (µm)	XD (µm)	XDR	PIXD (µm)	PIIXD (µm)	PIIXDR	HA (μm^2)	XA (μm^2)	XAR	PIXA (μm^2)	PIIXA (μm^2)	PIIXAR	PH (cm)	DM (g)
knat7	**X**	1761.77	1058.85	0.60	406.06	652.79	0.61	2479307.39	919989.04	0.37	130491.20	789497.84	0.84	49.17	371.44
	N	9	9	9	9	9	9	9	9	9	9	9	9	9	9
	SD	264.80	184.78	0.03	26.73	182.97	0.08	746223.95	317346.20	0.04	22456.44	310194.15	0.06	3.19	101.42
	p	0.0838	0.0735	0.1884	0.0290	0.1452	0.4269	0.0641	0.0604	0.2644	0.0503	0.0771	0.4317	0.0002	0.0140
C24	**X**	1529.30	1109.36	0.73	278.36	831.00	0.74	1878979.70	1013981.89	0.55	67081.08	946900.81	0.92	34.00	600.67
	N	7	7	7	7	7	7	7	7	7	7	7	7	7	7
	SD	305.40	204.72	0.05	61.81	221.25	0.10	719559.59	348196.50	0.08	29758.15	354465.38	0.08	2.76	61.08
	p														
stm^{wam1-1}	**X**	942.54	658.58	0.70	215.03	443.55	0.67	696254.00	348527.48	0.50	34227.37	314300.11	0.90		174.42
	N	6	6	6	6	6	6	6	6	6	6	6	6		6
	SD	111.75	93.49	0.04	16.50	95.48	0.05	177899.73	103458.94	0.07	5346.41	103464.50	0.03		82.83
	p	0.0005	0.0002	0.1492	0.0169	0.0011	0.0733	0.0012	0.0005	0.1580	0.0113	0.0007	0.2678		0.0000
Ler	**X**	1265.61	1002.36	0.79	226.82	775.55	0.77	1260331.17	794448.74	0.63	36800.61	757648.13	0.95	17.71	
	N	4	4	4	4	4	4	4	4	4	4	4	4	4	
	SD	54.55	64.13	0.02	37.30	83.22	0.04	134261.90	108530.84	0.04	18733.44	115954.89	0.03	3.41	
	p														
stm6	**X**	648.40	447.83	0.69	251.99	195.84	0.44	331228.56	165210.98	0.50	56148.37	109062.61	0.67		
	N	4	4	4	4	4	4	4	4	4	4	4	4		
	SD	139.39	92.46	0.01	70.62	21.84	0.04	127537.75	55383.33	0.03	28644.08	26739.26	0.06		
	p	0.0005	0.0004	0.0015	0.2882	0.0004	0.0005	0.0006	0.0009	0.0069	0.1801	0.0009	0.0006		

Note: (HD) Hypocotyl diameter, (XD) xylem diameter, (XDR) xylem diameter ratio, (PIXD) phase I of xylem diameter, (PIIXD) phase II of xylem diameter, (PIIXDR) phase II of xylem diameter ratio, (HA) hypocotyl area, (XA) xylem area, (XAR) xylem area ratio, (PIXA) phase I of xylem area, (PIIXA) phase II of xylem area, (PIIXAR) phase II of xylem area ratio, (PH) plant height, (DM) dry mass, (X) mean value, (N) number of observation, (SD) standard deviation, (p) p value of statistic analysis using t-test compared to wild-type (Col-0).

6.2 Phloem diameter and area of *knox* mutants and wild-type

Lines	N	Phloem Diameter (µm)			Phloem Area (µm^2)		
		HD-XD	SD	p	HA-XA	SD	p
Col-0	9	671.49	57.78		1320393.10	199102.05	
stm-GK	8	799.33	129.3	0.0101	1358964.78	422474.28	0.4044
knat1^{bp-9}	9	569.73	95.90	0.0120	674630.87	220267.84	0.0000
knat1^{bp-1}	6	415.11	73.94	0.0000	369316.05	155450.20	0.0000
stm-GK;knat1^{bp-9}	6	249.42	64.92	0.0000	74414.28	50546.26	0.0000
knat2	9	728.99	72.37	0.0410	1567819.52	347943.53	0.0437
knat2-5	9	712.00	129.66	0.2051	1597035.54	553828.90	0.0944
knat3	9	776.01	87.31	0.0049	1755378.91	428154.85	0.0090
knat4	9	838.02	163.79	0.0083	2043351.80	685492.06	0.0067
knat5	9	494.83	60.97	0.0000	814814.93	172294.68	0.0000
knat6	9	668.69	55.86	0.4590	1389196.41	243788.28	0.2608
knat7	9	702.92	94.84	0.2055	1559318.35	451025.37	0.0870
C24	7	419.95	135.12		864997.81	413920.42	
stm^{wam1-1}	6	283.96	48.07	0.0000	347726.52	95881.90	0.0000
Ler	4	263.25	19.69		465882.43	55259.42	
stm6	2	200.57	46.93	0.0095	166017.58	72154.42	0.0109

Note: (HD) Hypocotyl diameter, (XD) xylem diameter, (HA) hypocotyl area, (XA) xylem area, (N) number of observation, (SD) standard deviation, (p) p value of statistic analysis using t-test compared to wild-type. Phloem diameter and area were calculated by subtracting the hypocotyl diameter and area value with the xylem diameter and area value.

6.3 Secondary growth of *KNAT1* overexpressor plants and wild-type

Lines		HD (µm)	XD (µm)	XDR	PIXD (µm)	PIIXD (µm)	PIIXDR	HA (μm^2)	XA (μm^2)	XAR	PIXA (μm^2)	PIIXA (μm^2)	PIIXAR	PH (cm)	DM (g)
Nossen (No-0)	**X**	1143.66	899.52	0.79	366.81	532.71	0.59	1013111.19	639331.10	0.63	100266.15	539064.96	0.84	36.43	
	N	4	4	4	4	4	4	4	4	4	4	4	4	4	
	SD	110.64	72.86	0.04	21.29	83.14	0.05	180908.79	114446.81	0.04	8390.24	117095.97	0.03	8.59	
	p														
35S::KNAT1	**X**	1094.17	646.01	0.59	301.10	344.90	0.52	920841.83	365783.30	0.39	78167.19	287616.11	0.77	47.50	185.19
	N	9	9	9	9	9	9	9	9	9	9	9	9	9	9
	SD	181.57	122.16	0.03	28.66	123.73	0.09	308763.94	139883.59	0.04	14497.50	133320.02	0.07	5.61	73.78
	p	0.3140	0.4184	0.0112	0.3602	0.0006	0.0097	0.0034	0.1718	0.0292	0.3009	0.0000	0.0534	0.0050	
Col-0	**X**	1528.96	927.04	0.61	424.15	502.89	0.54	1835596.14	691004.91	0.37	142815.88	548189.04	0.79		
(+Dex)	**N**	5	5	5	5	5	5	5	5	5	5	5	5		
	SD	181.37	124.01	0.02	55.87	103.74	0.05	449506.87	190494.4	0.01	27880.82	173988.65	0.04		
	p														
Col-0	**X**	1558.46	954.79	0.61	471.79	483	0.51	1914355.11	733155.18	0.38	178040.62	555114.56	0.76		
(-Dex)	**N**	5	5	5	5	5	5	5	5	5	5	5	5		
	SD	164.54	93.2	0.01	54.21	43.91	0.02	401050.74	137272.44	0.02	39854.54	98245.46	0.01		
	p	0.3930	0.3452	0.2040	0.0937	0.3502	0.1134	0.3842	0.3450	0.1529	0.0593	0.4695	0.0905		
35S::KNAT1::GR	**X**	878.18	541.19	0.62	303.99	237.19	0.43	612726.21	233924.08	0.38	72989.34	160934.74	0.68		
(+Dex)	**N**	4	4	4	4	4	4	4	4	4	4	4	4		
	SD	73.75	60.62	0.05	21.69	46.78	0.05	107698.79	51954.24	0.06	13065.62	40254.07	0.03		
	p	0.0001	0.0002	0.3065	0.0019	0.0007	0.0067	0.0004	0.0009	0.3627	0.0009	0.0013	0.0019		

Note: (HD) Hypocotyl diameter, (XD) xylem diameter, (XDR) xylem diameter ratio, (PIXD) phase I of xylem diameter, (PIIXD) phase II of xylem diameter, (PIIXDR) phase II of xylem diameter ratio, (HA) hypocotyl area, (XA) xylem area, (XAR) xylem area ratio, (PIXA) phase I of xylem area, (PIIXA) phase II of xylem area, (PIIXAR) phase II of xylem area ratio, (PH) plant height, (DM) dry mass, (X) mean value, (N) number of observation, (SD) standard deviation, (p) p value of statistic analysis using t-test compared to wild-type (Col-0).

6.4 Secondary growth of *stm-GK;35S::KNAT1-GR* treated with dexamethasone (Dex) compared to the *KNAT1* overexpressors and wild-type plants

Lines		HD (µm)	XD (µm)	XDR	PIXD (µm)	PIIXD (µm)	PIIXDR	HA (μm^2)	XA (μm^2)	XAR	PIXA (μm^2)	PIIXA (μm^2)	PIIXAR
Col-0	**X**	1528.96	927.04	0.61	424.15	502.89	0.54	1835596.14	691004.91	0.37	142815.88	548189.04	0.79
(+Dex)	**N**	5	5	5	5	5	5	5	5	5	5	5	5
	SD	181.37	124.01	0.02	55.87	103.74	0.05	449506.87	190494.4	0.01	27880.82	173988.65	0.04
	p												
Col-0	**X**	1558.46	954.79	0.61	471.79	483	0.51	1914355.11	733155.18	0.38	178040.62	555114.56	0.76
(-Dex)	**N**	5	5	5	5	5	5	5	5	5	5	5	5
	SD	164.54	93.2	0.01	54.21	43.91	0.02	401050.74	137272.44	0.02	39854.54	98245.46	0.01
	p	0.3930	0.3452	0.2040	0.0937	0.3502	0.1134	0.3842	0.3450	0.1529	0.0593	0.4695	0.0905
35S::KNAT1::GR	**X**	878.18	541.19	0.62	303.99	237.19	0.43	612726.21	233924.08	0.38	72989.34	160934.74	0.68
(+Dex)	**N**	4	4	4	4	4	4	4	4	4	4	4	4
	SD	73.75	60.62	0.05	21.69	46.78	0.05	107698.79	51954.24	0.06	13065.62	40254.07	0.03
	p	0.0001	0.0002	0.3065	0.0019	0.0007	0.0067	0.0004	0.0009	0.3627	0.0009	0.0013	0.0019
stm-GK	**X**	1053.84	548.84	0.51	309.79	239.05	0.42	912777.61	252915.17	0.26	84225.63	168689.55	0.62
(+Dex)	**N**	5	5	5	5	5	5	5	5	5	5	5	5
	SD	286.42	183.65	0.04	80.94	126.65	0.1	482634.39	166803.88	0.04	44997.57	132870.68	0.13
	p	0.0042	0.0014	0.0002	0.0109	0.0021	0.0149	0.0048	0.0015	0.0000	0.0132	0.0016	0.0081
stm-GK;35S::KNAT1::GR	**X**	727.49	386.14	0.53	264.86	121.28	0.29	442550.91	126584.22	0.28	59632.88	66951.34	0.47
(+Dex)	**N**	5	5	5	5	5	5	5	5	5	5	5	5
	SD	177.3	114.86	0.05	59.43	82.32	0.15	216065.03	77481.55	0.05	26650.68	59478.39	0.24
	p	0.0000	0.0000	0.0037	0.0004	0.0000	0.0019	0.0000	0.0000	0.0007	0.0002	0.0000	0.0049

Note: (HD) Hypocotyl diameter, (XD) xylem diameter, (XDR) xylem diameter ratio, (PIXD) phase I of xylem diameter, (PIIXD) phase II of xylem diameter, (PIIXDR) phase II of xylem diameter ratio, (HA) hypocotyl area, (XA) xylem area, (XAR) xylem area ratio, (PIXA) phase I of xylem area, (PIIXA) phase II of xylem area, (PIIXAR) phase II of xylem area ratio, (PH) plant height, (DM) dry mass, (X) mean value, (N) number of observation, (SD) standard deviation, (p) p value of statistic analysis using t-test compared to wild-type (Col-0).

6.5 Standard curves for quantification of qRT-PCR results from various primer pairs

Genes	Efficiency	Slope	Y
Actin2.1	1.860	-3.71	16.45
STM.1(downstream)	1.887	-3.628	21.74
KNAT1	1.945	-3.462	17.03
KNAT2	1.985	-3.359	23.51
KNAT3	1.998	-3.327	21.42
KNAT4	1.936	-3.486	21.36
KNAT5	1.933	-3.494	21.65
KNAT6	1.883	-3.639	13.75
KNAT7	1.931	-3.498	18.26
STM.2(upstream)	1.994	-3.336	17.24
Actin2.2	1.974	-3.386	21.34
IRX1	1.921	-3.526	23.12
IRX3	1.930	-3.503	23.64
IRX5	1.893	-3.607	23.64
Pecest	1.978	-3.377	23.99
LTP4	1.895	-3.602	25.95
FLA11	1.950	-3.447	21.70
IRX6	1.979	-3.374	22.91
PAL1	1.981	-3.368	20.79
At4CL1	1.957	-3.429	20.57
CAD1	1.876	-3.660	28.30
PRX	1.869	-3.682	23.53
ATHB-8	1.901	-3.585	26.46
SND1	1.915	-3.543	26.40
SND2	1.972	-3.390	24.04
NST1	2.038	-3.038	24.75
ARF4	1.964	-3.411	22.41
IAA27	1.951	-3.446	19.77
IRX8	1.953	-3.441	23.22
IRX12	1.979	-3.374	22.89
GH19	1.935	-3.487	20.80
BELL	1.987	-3.208	22.72

6.6 Relative expression level* of *STM, KNAT1* and *KNAT7* in different tissues

Tissues	*STM*			*KNAT1*			*KNAT7*		
	X	SD	p	X	SD	p	X	SD	p
Hypocotyl	1.2303	0.2129		1.3069	0.0915		0.1866	0.0315	
Leaf	0.0002	0.0002	0.0049	0.0005	0.0003	0.0008	0.0030	0.0013	0.0048
1st node inflorescence	0.5991	0.2756	0.0190	0.9841	0.2489	0.0711	0.3064	0.1220	0.1133
Flower	1.6386	1.0336	0.2835	2.2401	1.1544	0.2657	0.1482	0.0207	0.0819
Pedicel	0.4776	0.2735	0.0110	0.7872	0.1356	0.0039	0.3894	0.2320	0.1340
Oldest node inflorescence	0.5731	0.2735	0.0166	1.0833	0.3230	0.1769	0.6609	0.2675	0.0448

Note: **(**X) Mean value, (SD) standard deviation, (p) p value of statistic analysis using t-test compared to hypocotyl (as a control). (*) Values were normalized to the *Actin2* expression. All data were calculated from 3 biological and 3 technical replicates.

6.7 Relative expression levels* and fold changes** of *KNOX* gene expression in *stm-GK*, *knat1*$^{bp-9}$, *stm-GK;knat1*$^{bp-9}$ compared to the wild-type (Col-0)

Lines	X	SD	p	Fold Changes (times)	Expression
STM					
Col-0	3.4507	0.3456			
stm-GK	0.0046	0.0078	0.0017	-745.70	Downregulated
knat1^{bp-9}	2.2576	0.2015	0.0059	-1.53	Downregulated
stm-GK;knat1^{bp-9}	0.0024	0.0037	0.0017	-1425.49	Downregulated
knat7	14.2251	0.9993	0.0006	+4.12	Upregulated
KNAT1					
Col-0	1.3069	0.0915			
stm-GK	1.9664	0.3979	0.0481	+1.50	Upregulated
knat1^{bp-9}	0.0054	0.0032	0.0008	-242.84	Downregulated
stm-GK;knat1^{bp-9}	0.0007	0.0005	0.0008	-2007.85	Downregulated
knat7	0.9496	0.0157	0.0094	-1.38	Downregulated
KNAT2					
Col-0	2.2320	0.3455			
stm-GK	3.2588	0.3866	0.0135	+1.46	Upregulated
knat1^{bp-9}	2.0057	0.4421	0.2627	-1.11	Downregulated
stm-GK;knat1^{bp-9}	7.6452	4.7374	0.0929	+3.43	Upregulated
knat7	7.9767	0.2630	0.0000	+3.57	Upregulated
KNAT3					
Col-0	0.0940	0.0211			
Stm-GK	0.1067	0.0112	0.2125	+1.13	Upregulated
knat1^{bp-9}	0.1232	0.0548	0.2310	+1.31	Upregulated
stm-GK;knat1^{bp-9}	0.9746	0.7555	0.0904	+10.36	Upregulated
knat7	0.2537	0.0131	0.0005	+2.70	Upregulated

Continued

Lines	X	SD	p	Fold Changes (times)	Expression
KNAT4					
Col-0	0.2234	0.0589			
stm-GK	0.4102	0.0590	0.0089	+1.84	Upregulated
knat1^{bp-9}	0.3115	0.0189	0.0557	+1.39	Upregulated
stm-GK;knat1^{bp-9}	7.4177	4.2334	0.0493	+33.20	Upregulated
knat7	0.7637	0.0350	0.0003	+3.42	Upregulated
KNAT5					
Col-0	1.0151	0.2136			
stm-GK	1.2794	0.3057	0.1471	+1.26	Upregulated
knat1^{bp-9}	1.4302	0.2708	0.0546	+1.41	Upregulated
stm-GK;knat1^{bp-9}	10.6770	5.2079	0.0422	+10.52	Upregulated
knat7	4.2369	0.1208	0.0001	+4.17	Upregulated
KNAT6					
Col-0	0.0134	0.0031			
stm-GK	0.0257	0.0046	0.0114	+1.92	Upregulated
knat1^{bp-9}	0.0239	0.0071	0.0537	+1.78	Upregulated
stm-GK;knat1^{bp-9}	0.1067	0.0801	0.0906	+7.96	Upregulated
knat7	0.0557	0.0009	0.0004	+4.15	Upregulated
KNAT7					
Col-0	0.1866	0.0315			
stm-GK	0.1385	0.0226	0.0527	-1.35	Downregulated
knat1^{bp-9}	0.1520	0.0165	0.0949	-1.23	Downregulated
stm-GK;knat1^{bp-9}	0.1036	0.0597	0.0611	-1.80	Downregulated
knat7	0.0013	0.0002	0.0047	-139.93	Downregulated

Note: (X) Mean value, (SD) standard deviation, (p) p value of statistic analysis using t-test compared to the wild-type (Col). (*) The relative concentration values were normalized to the *ACTIN2* expression. (**) calculated by dividing the mean of relative concentration values of *knox* mutants by the value for the wild-type (downregulated or upregulated). All data were calculated from 3 biological and 3 technical replicates.

6.8 Relative expression level* and ratio fold change of *KNOX* gene expression in the respective mutants compared to the wild-type (Col-0)**

Lines	X	SD	p	Fold Changes (times)	Expression
STM					
Col-0	3.4507	0.3456			
stm-GK	0.0046	0.0078	0.0017	-745.70	Downregulated
KNAT1					
Col-0	1.3069	0.0915			
knat1^{bp-9}	0.0054	0.0032	0.0008	-242.84	Downregulated
KNAT2					
Col-0	2.2320	0.3455			
knat2	0.0070	0.0056	0.0040	-317.72	Downregulated
KNAT3					
Col-0	0.0940	0.0211			
knat3	0.0022	0.0005	0.0085	-42.42	Downregulated
KNAT4					
Col-0	0.2234	0.0589			
knat4	0.2233	0.0394	0.4989	-1.00	Downregulated
KNAT5					
Col-0	1.0151	0.2136			
knat5	17.1493	0.6770	0.0001	+16.89	Upregulated
KNAT6					
Col-0	0.0134	0.0031			
knat6	0.0000	0.0000	0.0088	-1967.07	Downregulated
KNAT7					
Col-0	0.1866	0.0315			
knat7	0.0013	0.0002	0.0047	-139.92	Downregulated

Note: (X) Mean value, (SD) standard deviation, (p) p value of statistic analysis using t-test compared to the wild-type (Col). (*) The relative concentration values were normalized to the *ACTIN2* expression. (**) calculated by dividing the mean of relative concentration values of *knox* mutants by the value for the wild-type (downregulated or upregulated). All data were calculated from 3 biological and 3 technical replicates.

6.9 Relative expression level* and fold change of genes associated with secondary cell wall formation in *stm* and *knat1* mutants compared to the wild-type (Col-0)**

Lines	X	SD	p	Fold Changes (times)	Expression
IRX1					
Col-0	2.2627	0.8163			
stm-GK	1.3313	0.2015	0.0905	-1.70	Downregulated
knat1^{bp-9}	1.0342	0.1058	0.0594	-2.19	Downregulated
stm-GK;knat1^{bp-9}	0.0515	0.0256	0.0212	-43.96	Downregulated
IRX3					
Col-0	2.3778	1.0700			
stm-GK	1.4558	0.4849	0.1367	-1.63	Downregulated
knat1^{bp-9}	1.1346	0.2002	0.0891	-2.10	Downregulated
stm-GK;knat1^{bp-9}	0.0503	0.0220	0.0319	-47.30	Downregulated
IRX5					
Col-0	2.3953	0.9263			
stm-GK	1.6189	0.4723	0.1436	-1.48	Downregulated
knat1^{bp-9}	1.1560	0.2049	0.0703	-2.07	Downregulated
stm-GK;knat1^{bp-9}	0.0608	0.0316	0.0243	-39.39	Downregulated
PME61					
Col-0	1.9679	0.1657			
stm-GK	0.9506	0.2053	0.0015	-2.07	Downregulated
knat1^{bp-9}	0.9131	0.3339	0.0086	-2.16	Downregulated
stm-GK;knat1^{bp-9}	0.0648	0.0316	0.0009	-30.39	Downregulated
LTP4					
Col-0	1.9819	0.7769			
stm-GK	1.2689	0.2789	0.1242	+1.56	Upregulated
knat1^{bp-9}	0.8198	0.0729	0.0605	+2.42	Upregulated
stm-GK;knat1^{bp-9}	0.0477	0.0355	0.0248	+41.58	Upregulated
FLA11					
Col-0	2.0334	0.8863			
stm-GK	1.2114	0.2397	0.1228	-1.68	Downregulated
knat1^{bp-9}	0.9589	0.1052	0.0844	-2.12	Downregulated
stm-GK;knat1^{bp-9}	0.0267	0.0191	0.0296	-76.03	Downregulated
IRX6					
Col-0	1.9819	0.7769			
stm-GK	1.2689	0.2789	0.1242	-1.56	Downregulated
knat1^{bp-9}	0.8198	0.0729	0.0605	-2.42	Downregulated
stm-GK;knat1^{bp-9}	0.0477	0.0355	0.0248	-41.58	Downregulated

Note: (X) Mean value, (SD) standard deviation, (p) p value of statistic analysis using t-test compared to the wild-type (Col). (*) The relative concentration values were normalized to the *ACTIN2* expression. (**) calculated by dividing the mean of relative concentration values of *knox* mutants by the value for the wild-type (downregulated or upregulated). All data were calculated from 3 biological and 3 technical replicates.

6.10 Relative expression level* and fold change of genes associated with lignin biosynthesis in *stm* and *knat1* mutants compared to the wild-type (Col-0)**

Lines	X	SD	p	Fold Changes (times)	Expression
PAL1					
Col-0	0.9369	0.3685			
stm-GK	0.8249	0.1280	0.3298	-1.14	Downregulated
knat1^{bp-9}	0.8536	0.2264	0.3793	-1.10	Downregulated
stm-GK;knat1^{bp-9}	1.2801	0.2112	0.1256	+1.37	Upregulated
At4CL1					
Col-0	0.8945	0.3551			
stm-GK	0.9891	0.0697	0.3461	+1.11	Upregulated
knat1^{bp-9}	0.7495	0.1169	0.2801	-1.19	Downregulated
stm-GK;knat1^{bp-9}	1.3503	0.2475	0.0754	+1.51	Upregulated
CAD1					
Col-0	0.9408	0.8426			
stm-GK	0.4418	0.4553	0.2159	-2.13	Downregulated
knat1^{bp-9}	0.1252	0.1211	0.1170	-7.51	Downregulated
stm-GK;knat1^{bp-9}	4.6305	3.5209	0.1033	+4.92	Upregulated
PRX					
Col-0	0.6769	0.2049			
stm-GK	1.6735	0.4062	0.0165	+2.47	Upregulated
knat1^{bp-9}	0.4220	0.1720	0.0882	-1.60	Downregulated
stm-GK;knat1^{bp-9}	2.2281	1.1289	0.0681	+3.29	Upregulated

Note: (X) Mean value, (SD) standard deviation, (p) p value of statistic analysis using t-test compared to the wild-type (Col). (*) The relative concentration values were normalized to the *ACTIN2* expression. (**) calculated by dividing the mean of relative concentration values of *knox* mutants by the value for the wild-type (downregulated or upregulated). All data were calculated from 3 biological and 3 technical replicates.

6.11 Overlapping co-expressed genes of *STM* and *KNAT1*

Rangking*	R (*STM*)	R (*KNAT1*)	Name of Protein	Locus
1	0.830398	0.848306	NADP-dependent oxidoreductase	AT3G59845
2	0.771591	1.000000	Homeobox protein knotted-1 like 1 (KNAT1)	AT4G08150
3	0.769957	0.787758	Anion exchange protein 1	AT2G47160
4	1.000000	0.771591	Homeobox protein SHOOT MERISTEMLESS (STM)	AT1G62360
5	0.803150	0.782979	Lipid transfer protein 4 (LTP4)	AT5G59310
6	0.837180	0.760413	Homeodomain protein (BELLRINGER)	AT5G02030
7	0.722529	0.787459	Serine carboxypeptidase S10 family protein	AT1G11080
8	0.807422	0.757034	Pectin methylesterase, PMEG61	AT3G59010
9	0.723318	0.778510	Amino acid transporter family protein	AT5G23810
10	0.684741	0.786575	Expressed protein	AT4G27435
11	0.663340	0.797743	Cellulose synthase, catalytic subunit (IRX5)	AT5G44030
12	0.661570	0.821013	Expressed protein	AT1G12320
13	0.674707	0.783798	DNAJ heat shock N-terminal domain-containing protein	AT5G03160
14	0.738768	0.797743	Expressed protein	AT5G44040
15	0.674707	0.783798	Fascilin-like arabinogalactan-protein, FLA11	AT5G03170
16	0.858060	0.791504	WRKY family transcription factor	AT2G44745
17	0.644696	0.726621	Auxin-responsive AUX/IAA family protein, IAA27	AT4G29080
18	0.669736	0.778111	Laccase, IRX12	AT2G38080
19	0.633619	0.791895	Myosin family protein	AT2G31900
20	0.659573	0.759542	Glycoside hydrolase family 28 protein, GH28	AT3G42950
21	0.751533	0.750481	Auxin-responsive factor , ARF4	AT5G60450
22	0.641742	0.712594	COBRA like 4, CBL4 (IRX6)	AT5G15630
23	0.644635	0.735496	Glycoside hydrolase family 19 protein, GH19	AT3G16920
24	0.638346	0.734020	myb family transcription factor, MYB98	AT4G18770
25	0.638346	0.734020	Cellulose synthase, catalytic subunit, IRX1	AT4G18780
26	0.615672	0.775703	Fasciclin-like arabinogalactan-protein, FLA12	AT5G60490
27	0.622656]	0.742277	Tubulin family protein	AT5G17410
28	0.622656	0.742277	Cellulose synthase, catalytic subunit, IRX3	AT5G17420
29	0.629832	0.731802	Glycosyl transferase family 43 protein, IRX9	AT2G37090
30	0.625595	0.733544	Germin-like protein, GLP10	AT3G62020
31	0.671441	0.694079	Expressed protein	AT5G58930
32	0.602988	0.753471	Rhomboid family protein	AT1G63120
33	0.603586	0.750179	Laccase	AT2G29130
34	0.620991	0.732999	Glycogenin glucosyltransferase (glycogenin)-related	AT3G18660
35	0.607986	0.741992	Expressed protein	AT5G60720
36	0.630823	0.711383	Ras-related GTP-binding family protein	AT5G03530

Continued

Rangking*	R (*STM*)	R (*KNAT1*)	Name of Protein	Locus
37	0.615373	0.728941	Laccase	AT5G60020
38	0.600719	0.738009	Calmodulin-binding family protein	AT1G14380
39	0.630345	0.707202	Plastocyanin-like domain-containing protein	AT1G22480
40	0.612921	0.728823	Glycosyl transferase family 8 protein, IRX8	AT5G54690
41	0.615033	0.727821	Expressed protein	AT3G21190
42	0.678251	0.655950	ABC transporter family protein	AT3G25620
43	0.694041	0.645826	Expressed protein	AT1G47485
44	0.598610	0.727543	Expressed protein	AT3G21550
45	0.629641	0.681256	Armadillo/beta-catenin repeat family protein	AT1G12430
46	0.589888	0.725787	Exostosin family protein	AT1G27440
47	0.585410	0.715621	Protein kinase family protein	AT2G40120
48	0.601470	0.697441	O-acetyltransferase-related	AT5G46340
49	0.621571	0.678199	No apical meristem (NAM) family protein, SND2	AT4G28500
50	0.585410	0.715621	Protein kinase family protein	AT4G03175
51	0.600390	0.688569	Homeodomain transcription factor, KNAT7, IRX11	AT1G62990
52	0.634448	0.633443	Leucine-rich repeat family protein	AT4G30520
53	0.584520	0.697867	Transport protein-related	AT2G23360
54	0.578828	0.701564	Calmodulin-binding family protein	AT3G15050
55	0.604933	0.670272	Expressed protein	AT1G09610
56	0.593062	0.679724	Phenylalanine ammonia-lyase, PAL4	AT3G10340
57	0.626814	0.641541	Polygalacturonase	AT1G80170
58	0.568083	0.711085	Plastocyanin-like domain-containing protein	AT1G72230
59	0.592359	0.674258	No apical meristem (NAM) family protein, SND1	AT1G32770
60	0.584939	0.681841	Disease resistance protein (TIR-NBS-LRR class)	AT4G16920
61	0.578743	0.687797	No apical meristem (NAM) family protein, NST1	AT2G46770
62	0.586202	0.673428	Expressed protein	AT2G41610
63	0.585078	0.675697	p21-rho-binding domain-containing protein	AT1G27380
64	0.586402	0.664381	Expressed protein	AT2G31930
65	0.572342	0.683543	Microtubule associated protein (MAP65/ASE1) family protein	AT1G2792
66	0.600248	0.652613	Major intrinsic family protein / MIP family protein, NIP6.1	AT1G80760
67	0.572628	0.662757	Mutase family protein	AT1G21440
68	0.586519	0.637963	Zinc finger (C2H2 type) family protein (ZFP2)	AT5G57520
69	0.568078	0.633628	Expressed protein	AT1G29240

Note: (*) The ranking was determined by adding the value of the rank from the list of co-expressed genes for *STM* and for *KNAT1*. (R) Coefficient correlation value.

6.12 Relative expression level* and fold change of downstream target genes of *STM/KNAT1* in the double mutant of *stm-GK;knat1*$^{bp-9}$.**

Lines	X	SD	p	Fold changes (times)	Expression
ATHB-8					
Col-0	2.30	0.78			
stm-GK;knat1^{bp-9}	0.85	0.20	0.02	- 2.70	Downregulated
SND1					
Col-0	1.99	1.04			
stm-GK;knat1^{bp-9}	N.D.	N.D.	N.A.	N.A	Downregulated
SND2					
Col-0	2.09	0.95			
stm-GK;knat1^{bp-9}	0.02	0.02	0.01	- 106.68	Downregulated
NST1					
Col-0	2.12	1.12			
stm-GK;knat1^{bp-9}	0.01	0.01	0.02	- 277.64	Downregulated
ARF4					
Col-0	2.38	1.12			
stm-GK;knat1^{bp-9}	0.77	0.01	0.05	- 3.09	Downregulated
IAA27					
Col-0	2.83	0.44			
stm-GK;knat1^{bp-9}	0.05	0.04	0.00	- 57.00	Downregulated
IRX8					
Col-0	2.84	0.54			
stm-GK;knat1^{bp-9}	0.00	0.00	0.00	- 722.77	Downregulated
IRX12					
Col-0	2.76	1.28			
stm-GK;knat1^{bp-9}	0.01	0.00	0.01	- 404.47	Downregulated
GH19					
Col-0	2.41	0.7			
stm-GK;knat1^{bp-9}	0.02	0.02	0.00	- 99.54	Downregulated
GH28					
Col-0	1.91	0.97			
stm-GK;knat1^{bp-9}	1.06	0.17	0.09	- 1.80	Downregulated

Continued

Lines	X	SD	p	Fold changes (times)	Expression
PAL4					
Col-0	2.12	0.79			
stm-GK;knat1^{bp-9}	0.78	0.41	0.02	- 2.71	Downregulated
BELL					
Col-0	1.02	0.42			
stm-GK;knat1^{bp-9}	1.46	0.44	0.10	+ 1.43	Upregulated

Note: (X) Mean value, (SD) Standard deviation, (p) p value of statistic analysis using t-test compared to the wild-type (Col). (*) The relative concentration values were normalized to the *ACTIN2* expression. (**) calculated by dividing the mean of relative concentration values of *knox* mutants by the value for the wild-type (downregulated or upregulated). All data were calculated from 4 biological and 2 technical replicates. (N.D) Not detectable and (N:A.) not applicable.

7.13 Relative expression level* and fold change of the *STM/KNAT1* downstream target genes in *35S::KNAT1-GR* under dexamethazone (Dex) and cycliheximide (Cyc) exposes**

Treatments	X	SD	p	Fold Changes (times)	Expression
ATHB					
DMSO	0.91	0.32			
Dex	1.12	0.23	0.18	+ 1.22	Upregulated
Cyc	1.19	0.38	0.16	+ 1.30	Upregulated
Dex+Cyc	1.34	0.78	0.19	+ 1.47	Upregulated
SND1					
DMSO	4.97	1.70			
Dex	5.20	2.02	0.43	+ 1.05	Upregulated
Cyc	5.20	0.82	0.41	+ 1.05	Upregulated
Dex+Cyc	9.51	6.63	0.13	+ 1.91	Upregulated
SND2					
DMSO	2.43	1.58			
Dex	3.02	0.75	0.27	+ 1.24	Upregulated
Cyc	3.07	1.39	0.28	+ 1.26	Upregulated
Dex+Cyc	4.85	2.61	0.09	+ 1.99	Upregulated

Continued

Treatments	X	SD	p	Fold changes (times)	Expression
NST1					
DMSO	0.70	0.12			
Dex	0.90	0.21	0.08	+ 1.28	Upregulated
Cyc	0.92	0.33	0.13	+ 1.32	Upregulated
Dex+Cyc	1.80	1.01	0.06	+ 2.57	Upregulated
STM					
DMSO	2.00	0.63			
Dex	2.05	0.37	0.45	+ 1.03	Upregulated
Cyc	2.32	0.30	0.20	+ 1.16	Upregulated
Dex+Cyc	3.57	1.47	0.06	+ 1.79	Upregulated
KNAT1					
DMSO	0.01	0.00			
Dex	0.02	0.00	0.01	+ 1.54	Upregulated
Cyc	0.02	0.00	0.01	+ 1.70	Upregulated
Dex+Cyc	0.04	0.01	0.01	+ 3.03	Upregulated
ARF4					
DMSO	0.23	0.10			
Dex	0.39	0.12	0.04	+ 1.74	Upregulated
Cyc	0.34	0.08	0.05	+ 1.52	Upregulated
Dex+Cyc	0.58	0.21	0.02	+ 2.60	Upregulated
IAA27					
DMSO	1.69	0.57			
Dex	1.78	0.15	0.38	+ 1.06	Upregulated
Cyc	1.95	0.72	0.29	+ 1.16	Upregulated
Dex+Cyc	3.46	1.31	0.03	+ 2.05	Upregulated
IRX6					
DMSO	1.73	0.66			
Dex	3.35	0.90	0.02	+ 1.94	Upregulated
Cyc	3.01	0.44	0.01	+ 1.74	Upregulated
Dex+Cyc	4.80	2.87	0.06	+ 2.77	Upregulated
IRX1					
DMSO	3.61	0.89			
Dex	3.38	0.84	0.38	- 1.07	Downregulated
Cyc	3.04	0.43	0.19	- 1.19	Downregulated
Dex+Cyc	3.97	1.25	0.35	+ 1.10	Upregulated

Continued

Treatments	X	SD	p	Fold changes (times)	Expression
IRX1 (in seedling)					
DMSO	0.05	0.01			
Dex	0.04	0.04	0.43	- 1.12	Downregulated
Cyc	0.02	0.02	0.07	- 2.27	Downregulated
Dex+Cyc	0.03	0.02	0.09	- 1.86	Downregulated
IRX5 (in seedling)					
DMSO	0.05	0.01			
Dex	0.05	0.04	0.46	+ 1.06	Upregulated
Cyc	0.02	0.01	0.04	- 2.52	Downregulated
Dex+Cyc	0.04	0.01	0.21	- 1.24	Downregulated

Note: (X) Mean value, (SD) Standard deviation, (p) p value of statistic analysis using t-test compared to the wild-type (Col). (*) The relative concentration values were normalized to the *ACTIN2* expression. (**) calculated by dividing the mean of relative concentration values of *knox* mutants by the value for the wild-type (downregulated or upregulated). All data were calculated from 4 biological and 2 technical replicates.

7 Appendixes

7.1 Plant material (seeds) used in the experiment

NASC Stock Number / Sources	Name of lines /mutants	Insertion/Mutation	Ecotype
1. N3161	*knat1*$^{bp-1}$	X rays mutagen	Col-1
2. N409575	*stm-GK*	T-DNA, 1st intron	Col-0
3. N609159	*knat2*	T-DNA, 3rd intron	Col-0
4. N599837	*knat2-5*	T-DNA, 1st exon	Col-0
5. N636464	*knat3*	T-DNA, 1st intron	Col-0
6. N520216	*knat4*	T-DNA, 1st intron	Col-0
7. N616798	*knat5*	T-DNA, 1st intron	Col-0
8. N617904	*knat6*	T-DNA, 3rd intron	Col-0
9. N610899	*knat7*	T-DNA, 2nd intron	Col-0
10. N295	*stm*$^{wam1-1}$	Unknown	C24
11. N12	*stm4*	EMS mutagen	Ler
12. N13	*stm5*	EMS mutagen	Ler
13. N14	*stm6*	EMS mutagen	Ler
14. N3821	*35S::KNAT1*	-	No-0
15. N6141	*KNAT1::GUS*	-	Col-0
16. N296	*ATHB-8::GUS*	-	Col-0
17. N28166	Columbia-0 (Col-0)	-	-
18. N3081	Nossen (No-0)	-	-
19. N28445	Lansberg erecta (Ler)	-	-
20. N28126	C24	-	-
21. Peter Doerner, Edinburgh University	*CylinB1;1::GUS*	-	Col-0
22. Dr. Angela Hey, Oxford University	*knat1*$^{bp-9}$	*dSpm* transposon, 1st intron	Col-0
23. Dr. Angela Hey, Oxford University	*35S::KNAT1-GR*	-	Col-0
24. Prof. R. Sablowski John Innes Centre, UK	*35S::STM-GR*	-	Col-0
25. Prof. Wolfgang Werr, University of Cologne	*STM::GUS*	-	Col-0

7.2 Composition of Murishage and Skoog (MS) medium.

7.2.1 Medium MS + MES.

Composition	Concentrations
1. Macros-MS [10]	50 ml/l
2. Micros-MS [1000]	0.5 ml/l
3. Vitamin-MS [1000]	1 ml/l
4. Glycine-MS [1000]	1 ml/l
5. Iron-MS [500]	5 ml/l
6. Inositol-MS [500]	5 ml/l
7. MES, pH 5.8	5 g/l
8. Sucrose	10 g (modified)
9. Gelrite	0.3 %
10. ddH2O	Up to 1 l

7.2.2 Macronutrients-MS 10 concentration.

Composition	Amount (g/l)
1. NH_4NO_3	16.5
2. KNO_3	19
3. $CaCl_2.2H_2O$	4.4
4. $MgSO_4.7H_2O$	3.7
5. KH_2PO_4	1.7

7.2.3 Micronutrients-MS 1000 concentration.

Composition	**Amount (g/l)**
1. H_3BO_3	620
2. $Na_2MoO_4.2H_2O$	25
3. KI	83
4. $MnSO_4.H_2O$	1000
5. $ZnSO_4.7H_2O$	860
6. $CoCl_2$.6H2O	2.5
7. $CuSO_4.5H_2O$	2.5

7.2.4 Vitamins-MS 1000 concentration.

Composition	**Amount (mg/100 ml)**
1. Nicotinic acid	50
2. Pyridoxine-HCl	50
4. Thiamine-HCl	10

7.2.5 Glycine-MS 1000 concentration.

Composition	**Amount (mg/100 ml)**
1. Glycine	200

7.2.6 Fe-Solution-MS 500 concentration.

Composition	**Amount (mg/100 ml)**
1. EDTA ferric sodium salt	734

7.2.7 Inositol-MS 500 concentration.

Composition	**Amount (mg/100 ml)**
1. EDTA ferric sodium salt	2000

7.3 Primer pairs used for *knox* mutant PCR genotyping

SALK Number	Locus	Oligo Name	Sequences	Length (bp)
SALK_109159	AT1G70510	*knat2 (LP)*	GAGTTTGTCCTTGCCTTCATG	21
SALK_109159	AT1G70510	*knat2 (RP)*	TCCAGCTAGTTCTTATCAGGTGG	23
SALK_099837	AT1G70510	*knat2-5 (LP)*	CAGAGAAAATCCTACCCACCG	21
SALK_099837	AT1G70510	*knat2-5 (RP)*	GGAATT TTACATGTATTCATCGTCG	25
SALK_136464	AT5G25220	*knat3(LP)*	TCTCCTTCAATCATTTCACCG	21
SALK_136464	AT5G25220	*knat3 (RP)*	ACATCTAATCCCCCATCGAAC	21
SALK_020216.	AT5G11060	*knat4 (LP)*	AACTTTAGAAGCCGCTCAAGG	21
SALK_020216	AT5G11060	*knat4 (RP)*	TGACAAGTTCTTGGTTGATTGG	22
SALK_116798	AT4G32040	*knat5 (LP)*	TTCGGAGATGCAAAATACTGG	21
SALK_116798	AT4G32040	*knat5 (RP)*	TTGATGTACCATTGGAGCTTG	21
SALK_117904	AT1G23380	*knat6 (LP)*	TTATCCCTCTCTGGTTCGGTC	21
SALK_117904	AT1G23380	*knat6 (RP)*	GCAGATAAGAGTGGCCACTTG	21
SALK_110899	AT1G62990	*knat7 (LP)*	TTGCCACCAATT TTTCAAGAC	21
SALK_110899	AT1G62990	*knat7 (RP)*	TGCCGTGAAATTGAGAACAAC	21
	T-DNA	LBa1	TTGTTCACGTAGTGGGCCATC	21

7.4 PCR reaction for identification of homozygous *knox* mutants

Composition	Amount (µl)
1. Sterile deionized water	13.4 µl
2. 10x taq buffer	2 µl
3. 2 mM dNTP mix	0.5 µl
4. Left Primer (LP)	0.5 µl
5. Right Primer (RP)	0.5 µl
6. Taq DNA Polymerase	0.1 µl
7. 25 mM MgCl2	1 µl
8. Template DNA	2 µl
Total Volume	20 µl

Adopted from www.fermentas.com

7.5 Primer pairs used for *expression* analyses using qRT-PCR.

No.	Locus	Oligo Name	Sequences	Length (bp)
1.	At3g18780	*Actin2 (LP)*	TGGGATGAACCAGAAGGATG	20
2.	At3g18780	*Actin2 (RP)*	AAGAATACCTCTCTTGGATTGTGC	24
3.	At4g08150	*KNAT1 (LP)*	TCCCATTCACATCCTCAACA	20
4.	At4g08150	*KNAT1 (RP)*	CCCCTCCGCTGTTATTCTCT	20
5.	At1g62360	*STM1 (LP)*	TCCTCACCTTCCTCTTTCTCC	21
6.	At1g62360	*STM1 (RP)*	GCAAGAGCTGTCCTTTAAGCTC	22
7.	AT1G70510	*KNAT2 (LP)*	CAGCGTCTGCTACAGCTCTTT	21
8.	AT1G70510	*KNAT2 (RP)*	TCATCCGCTGCTATGTCATC	20
9.	AT5G25220	*KNAT3 (LP)*	GAAGAACAAACGCAAAAGGTG	21
10.	AT5G25220	*KNAT3 (RP)*	CTAAAACCCTGCTTTCAAATCC	22
11.	AT5G11060	*KNAT4 (LP)*	CAGTCGCTTCAAAGTTTTACAGG	23
12.	AT5G11060	*KNAT4 (RP)*	TTGCTCATCTTCATCCTCAGAC	22
13.	AT4G32040	*KNAT5 (LP)*	AATGGCCATACCCAACTGAG	20
14.	AT4G32040	*KNAT5 (RP)*	TGACGTGGAAGAGTTGCTGT	20
15.	AT1G23380	*KNAT6 (LP)*	GTCTGCCAGGGGAGTTTCT	19
16.	AT1G23380	*KNAT6 (RP)*	GCTACCTCATGATCACCTCCA	21
17.	AT1G62990	*KNAT7 (LP)*	TTGCCGTGAAATTGAGAACA	20
18.	AT1G62990	*KNAT7 (RP)*	TCATCCTCATCCTCCGACAT	20
19.	At1g62360	*STM2 (LP)*	CAAATGGCCTTACCCTTCG	19
20.	At1g62360	*STM2 (RP)*	GCCGTTTCCTCTGGTTTATG	20

7.6 GUS staining solution

Composition	Final Concentration	Amount
1.1 M Sodium phosphat buffer pH 7.2	50 mM	600 µl
2. 0.1 M Ferrocyanide	5 mM	750 µl
3. 0.1 M Ferricyanide	5 mM	750 µl
4. H_2O	-	12.6 ml
5. 100 mM X-Gluc 5. H_2O	2mM	300 µl
Total Volume		**15 ml**

X-Gluc (X-GlucA, Duchefa, Netherlands) stock : 2 ml N-N Dimethylformamide + 104 mg X-Gluc. Store at –20 °C. When the solution turns purple, it has gone bad. Ferricyanide stock: 1.65 g in 50 ml water. Store at –4 °C. Ferrocyanide stock: 2.2 g in 50 ml water. Store at –4 °C

7.7 Formaldehyde-Acetic acid-Ethanol (FAE) solution

Composition	**Amount** (ml/l)
1. Formaldehyde (37%) 2. Acetic acid (100%)	50
2. Acetic acid (100%)	50
3. Ethanol (70%)	900
Total Volume	1000 ml

7.8 Chloral Hydrate-glycerol solution

Composition	**Ratio**
1. Chloral Hydrate	8 (w)
2. Glycerol	3 (w)
3. H_2O	1 (w)

7.9 Fixation and embedding of *Arabidopsis* hypocotyls in paraffin.

Embedding Solution	**Temperature**	**Time**
1. FAE	RT	1-2 h
2. 70% Ethanol	RT	30 min
3. 80% Ethanol	RT	30 min
4. 90% Ethanol	RT	30 min
5. 96% Ethanol	RT	30 min
6. 96% Ethanol : Isopropanol (1:1)	RT	30 min
7. Isopropanol	RT	30 min
8. Isopropanol : Roti-Histol (3:1)	RT	30 min
9. Isopropanol : Roti-Histol (1:1)	RT	30 min
10. Isopropanol : Roti-Histol (1:3)	RT	30 min

Continued

Embedding Solution	Temperature	Time
11. Roti-Histol	RT	30 min
12. Roti-Histol	RT	30 min
13. Roti-Histol	RT	30 min
14. Saturated paraffin in Roti-Histol (Cold)	RT	1-2 h
15. Saturated paraffin in Roti–Histol (Warm)	40°C	1-2 h
16. Melted pure paraffin	60°C	1-2 h
17. Melted pure paraffin	60°C	8-12 h

7.10 Protocol for gelatinized slides

1. Clean new slides in wash-machine (BANDELIN SONOREX SUPER 510 H) using detergent for overnight at room temperature.
2. Dry slides and put in a slide tray.
3. Prepare a gelatin solution from 0.125 g potassiumchrom-II-sulfate + 1.25 g of gelatin + 250 ml ddH2O in a erlenmeyer flask.
4. Immerse the slide in the gelatin solution individually using tweezers and put them back into the slide tray.
5. After the slides are dried, they are ready to use.

7.11 Toluidine Blue O (TBO) solution

Composition	Amount
Stock Solution:	
1. Toluidine blue O (Sigma)	1 g
2. Alcohol (70%)	100 ml
Sodium Chloride (1%)	
1. Sodium Chloride	0.05 g
2. Distilled water	50 ml
Adjust pH to 2.0~2.5 using glacial acetic acid or HCl	

Working Solution (pH 2.0~2.5)

1. Toluidine blue stock solution	5 ml
2. 1 % Sodium Chloride pH 2.3	45 ml

7.12. Primer pairs used for co-expression analyses experiment

No.	Locus	Oligo Name	Sequences	Length (bp)
1.	AT3g18780	ACTIN2 (LP)	TGGGATGAACCAGAAGGATG	20
2.	AT3g18780	ACTIN2 (RP)	AAGAATACCTCTCTTGGATTGTGC	24
3.	AT3G59010	PME61 (LP)	GCGGCTGGAATACTTACCAA	20
4.	AT3G59010	PME61(RP)	TCGAGCTATGAATCCATCTCC	21
5.	AT5g59310	LTP4 (LP)	GCAAAAGGGGTTAATCCAAGT	21
6.	AT5g59310	LTP4 (RP)	TCCCCACTTCACTTGATGG	19
7.	AT5G30170	FLA11(LP)	TCGTTATAGCCACTACTTATGGTCA	25
8.	AT5G03170	FLA11(RP)	CGGTTATGTTCGTTGGACCT	20
9.	AT4G18780	CesA8, IRX1 (LP)	TTTGCCTCTTGTTGCTTACTGT	22
10.	AT4G18780	CesA8, IRX1 (RP)	CAGCATGCTTGCTAGGTTTG	20
11.	AT5G17420	CesA7, IRX3 (LP)	TGACATGAATGGTGACGTAGC	21
12.	AT5G17420	CesA7, IRX3 (RP)	CATCAAATGCTCCTTATCACCTT	23
13.	AT5G44030	CesA4, IRX5 (LP)	CTGTGGTTATGAAGAGAAGACTGAA	25
14.	AT5G44030	CesA4, IRX5 (RP)	TGCATTCTAAATCCAGTGAGGA	22
15.	AT5G15630	COBL4, IRX6(LP)	TAACTCCTTGCCCGTCTTGT	20
16.	AT5G15630	COBL4, IRX6(RP)	TGTGTTGAGACCTTTCTTGGTTAG	24
17.	AT1G51680	At4CL1(LP)	ATGCCAAACTCGGTCAGG	18
18.	AT1G51680	At4CL1(RP)	GCAAAACCTAACGACATTGCT	21
19.	AT2G37040	PAL1(LP)	ATTAACGGGGCACACAAGAG	20
20.	AT2G37040	PAL1(RP)	GTCTCCGCCGCATAACATAG	20
21.	AT4G39330	CAD1(LP)	CCTCTTGTTCTCGGAAGGAA	20
22.	AT4G39330	CAD1(RP)	GGAGGGCTCAAGGAGTTAGC	20
23.	AT3G21770	Peroxidase (LP)	AAAAACCAAGGCCTTAATCTCA	22
24.	AT3G21770	Peroxidase (RP)	GAACAATGTGAGACGCCAATC	21
25.	AT4G32880	ATHB-8 (LP)	CTCAAGAGATTTCACAACCTAACG	24
26.	AT4G32880	ATHB-8 (RP)	TCACTGCTTCGTTGAATCCTT	21
27.	AT1G32770	SND1 (LP)	CAAGCTTGAGCCTTGGGATA	20
28.	AT1G32770	SND1 (RP)	TGGTCCCGGTTGGATACTT	19

Continued

No.	Locus	Oligo Name	Sequences	Length (bp)
29.	AT4G28500	SND2 (LP)	CCCTTCTTGTGGCCATAACTT	21
30.	AT4G28500	SND2 (RP)	GCCTTCAAGATGCTCCAAGA	20
31.	AT2G46770	NST1(LP)	GATGTCACCGTTCATGAGGTC	21
32.	AT2G46770	NST1(RP)	GGACTGTTTAGGGTTTTGTGAAG	23
33.	AT5G60450	ARF4 (LP)	GGTTAATGTCCAGTTGCTTGCT	22
34.	AT5G60450	ARF4(RP)	CCCCATTTAGCATCGAAAAC	20
35.	AT4G29080	IAA27(LP)	GATGTCCCTTGGGAAATGTTTA	22
36.	AT4G29080	IAA27(RP)	TCCTGCTTCTGCACTTCTCC	20
37.	AT5G54690	GAUT12, IRX8(LP)	CTTACTATCATTGGCTTGACGAGA	24
38.	AT5G54690	GAUT12, IRX8(RP)	ACATGACCGTGGAAAGCAAT	20
39.	AT2G38080	Laccase, IRX12(LP)	AATGAGAAAGTCACTGTTCTAGGTG	25
40.	AT2G38080	Laccase, IRX12(RP)	CCAGACTTAAGCGCCTCATTA	21
41.	AT3G16920	CTL2/GH19(LP)	TCAAGGGATGAAGGAAGTCG	20
42.	AT3G16920	CTL2/GH19(RP)	CTGTTGCAACCCCGTACC	18
43.	AT3G42950	GH28/Polygalacturonase(LP)	CGCTGAGAATCTTGCTCTTCA	21
44.	AT3G42950	GH28/Polygalacuronase(RP)	CGAGGTCCATGATGCTCTCT	20
45.	AT3G10340	PAL4(LP)	GCCATGGCTTCTTATTGCTC	20
46.	AT3G10340	PAL4(RP)	TGGACATGGTTGGTCACG	18
47.	AT5G02030	BELL (LP)	TTCGATCATTTCTTGCATCCT	21
48.	AT5G02030	BELL(RP)	TTCGATACCTGATTTCTGGAGAG	20

Publication

Sunaryo W and Fischer U (2009). *In silico* expression analysis of the *Arabidopsis KNAT1* gene and its homologs in poplar. Review of forests, wood products and wood biotechnology of Iran and Germany - Part III (Ali Reza Kharazipour, Christian Schöpper, Cora Müller and Markus Euring, Eds.). Universitätsdrucke Göttingen. P:293-302

In silico expression analysis of the Arabidopsis *KNAT1* gene and its homologs in poplar

Widi Sunaryo and Urs Fischer
University of Göttingen, Büsgen-Insitiute, Forest Botany and Tree Physiology, Büsgenweg 2, 37077 Göttingen, Germany
Corresponding author: ufische@gwdg.de

1 Introduction

Plant development requires a tightly controlled balance between undifferentiated dividing cells and cells, which are subjected to undergo differentiation. In the shoot apical meristem, this process is governed by a complex signaling network involving several classes of transcription factors, which are often expressed in highly distinct patterns (Shani et al., 2006). Key-players of differentiation control are the *KNOX* genes (*Knotted-1* like genes; e.g. *KNAT1*, *KNAT2*, *STM*), which comprise a small gene family with eight members in *Arabidopsis thaliana*. *KNOX* genes can be divided into two subclasses, class I and II *KNOX* genes, based on phylogenetic analyses (Scofield and Murray, 2006). A well-characterized member of the class I *KNOX* genes is *SHOOT MERISTEMLESS* (*STM*), which is expressed in the centre of the shoot apical meristem (SAM) but not in the newly formed leaf primordia and in the incipient leaf (Long et al., 1996). Loss-of-function mutations in *STM* lead to premature differentiation of meristematic cells and eventually to cessation of the SAM (Long et al., 1996); but its simultaneous over-expression together with the homeodomain transcription factor *WUSCHEL* induces meristem formation at ectopic places (Lenhard et al., 2002). Taken together these findings indicate that *STM* is a critical regulator of differentiation, whose expression is required to keep cells in an undifferentiated state. The other characterized members of the class I *KNOX* genes fulfill partly redundant functions to *STM* and are generally suggested to be involved in preventing differentiation of the tissue where they are expressed (Scofield and Murray, 2006) . In contrast to the class I *KNOX* genes, the members of class II *KNOX* genes are only scarcely described and functional data is mostly lacking.

In the vascular cambium similar decisions as in the SAM have to be taken; an equally tight balance between meristematic cells and cells, which undergo differentiation, is required. Some daughter cells of the cambial meristem differentiate into xylem or phloem, whereas others stay undifferentiated and maintain the pool of meristematic cells. In the model tree poplar, functional evidence for an involvement of *KNOX* genes in controlling differentiation of cambial daughter cells is still lacking. However, high resolution transcript analyses of the poplar cambium showed several *KNOX* genes with strong cambial expression (Hertzberg et al., 2001; Schrader et al., 2004). Furthermore, the poplar *KNOX* gene *ARBORKNOX1* (*ARK1*), which is a close homolog of the Arabidopsis *STM*, was shown to be expressed in the cambium (Groover et al., 2006). Over-expression of *ARK1* leads to an inhibition of differentiation of vascular cells. This is in line with the proposed role for *KNOX* genes of keeping cells undifferentiated. However, it has not been shown that the endogenous *ARK1* function is required for the indeterminate state of cambial cells.

The current understanding of the regulation of differentiation in vascular development was greatly enhanced by the study of Arabidopsis mutants in the *KNAT1/BP* (*BREVIPEDICELLUS*) gene (Mele et al., 2005). The *bp* mutants show among various developmental defects an increase in lignification of the cambial daughter cells; whereas over-expression of *KNAT1* leads to a decrease in lignin deposition, which is a hallmark of terminal differentiation. These results show that *KNAT1* is regulating the lignification of pro-cambial derivates and that it is playing a similar role as a repressor of differentiation processes in the procambium as *STM* in the shoot apical meristem.

Cell walls of woody plants constitute an important resource of fixed carbon, and are the base for a manifold of products as paper and panels. Secondary cell wall formation contributes to a large extent to the biomass of wooden tissues. The major compounds of secondary cell walls are cellulose, hemicelluloses and lignin of which the latter is unwanted for many industrial downstream processes. The wood of poplar trees typically consists of 45 % of cellulose, 25 % hemicelluloses and 20 % of lignin (Timell et al., 1969; McDougall et al., 1993). Upon gravistimulation however, the lignin content is drastically lowered and the S2 and S3 layer are replaced by the so called G-layer (gelatinous-layer), which is characterized by highly crystalline cellulose and greatly reduced lignin content. The resulting wood is called tension wood and can contain up to 20 % more cellulose and correspondingly lower levels of lignin and hemicelluloses (Timell et al., 1969). Especially the lignin content is remarkably reduced in gravistimulated wood; albeit if lignin deposition in secondary cell walls of tension wood is completely absent is still a matter of debate (Joseleau et al., 2004). A very similar syndrome of hypo-lignification, as observed during tension wood formation, occurs in a *35S::KNAT1* over-expressor (Mele et al., 2005). However, whether *KNAT1* up-regulation is required during tension wood formation is not known. Here, we identified the putative homologs of *KNAT1/BP* in poplar and reanalyzed publicly available microarray data in order to test if differential regulation of *KNAT1* genes can explain the repression of lignin deposition during tension wood formation in poplar.

2 Materials and Methods

Amino acid sequence alignments were performed with the help of ClustalW (http://ch.embnet.org; Thompson et al., 1994) and phylogenetic trees were drawn with Treeview (http://taxonomy.zoology.gla.ac.uk/rod/treeview.html) and afterwards graphically modified with Adobe Illustrator. Sequences were retrieved from the TAIR (www.arabidopsis.org) or form the JGI (http://genome.jgi-psf.org/Poptr1_1/Poptr1_1.home.html) websites. For alignments the amino acid sequences were used over their entire length. Opening and ending gap penalties were set to the value of 10, extending and separation gap penalties to 0.05 and "blocks substitution matrix" (BLOSUM) was used as a scoring matrix. BLAST searches were done on the JGI server (http://genome.jgi-psf.org/Poptr1_1/Poptr1_1.home.html), with a word size of 3 and BLOSUM62 matrix.

For clustering of the Arabidopsis expression data GENEVESTIGATOR (Zimmermann et al., 2004) was used. The Pearson Correlation was applied to estimate the distance between nodes. Expression data for the poplar *KNOX* genes was obtained form the UPSC BASE (Sjödin et al., 2006) or directly from the respective publications.

3 Results and Discussion

In order to identify sequences homologues to the Arabidopsis *KNAT1* gene we performed a BLAST search with the *KNAT1* amino acid sequence on the entire annotated *Populus trichocarpa* genome (Tuskan et al., 2006). The BLAST search resulted in 15 poplar gene models with an e-value < 10-15 (data not shown). These sequences and the Arabidopsis *KNOX* sequences were aligned and a phylogenetic tree calculated (Figure 1A.) The topology of the tree showed two different clades separating the class I form the class II *KNOX* genes, with nine poplar gene models classified as class I *KNOX* genes. Interestingly, the clade of *KNAT2/KNAT6* contains six poplar homologs, indicating a recent gene amplification in poplar. In contrast, *KNAT1* only pairs with one poplar gene model; favoring the idea that one of the paralogs got deleted after the recent whole genome duplication (salicolid duplication, Tuskan et al., 2006) in poplar.

Publicly available microarray of Arabidopsis gene expression studies was used to determine which *KNOX* genes are expressed in the developing xylem, a place where lignification takes place (Figure 1B). Strongest expression was found for *KNAT1* and *STM*, whereas *KNAT7* reached half of their expression levels (data not shown). The other *KNOX* genes were hardly expressed in the Arabidopsis xylem. Surprisingly, clustering of the expression data including 3110 arrays grouped *KNAT7* together with the class I *KNOX* genes (Figure 1B), suggesting that its regulation is more similar to class I than class II *KNOX* genes. Interestingly, the *KNAT7* mutant *irregular xylem11* (*irx11*) shows collapsed xylem elements in the inflorescence (Brown et al., 2005) indicating that *KNAT7* together with *KNAT1* are required for proper xylem differentiation. If the collapsed xylem elements are due to impaired lignification is however not yet clear.

In order to study the gene expression of *KNOX* genes in poplar we identified nine ESTs (expressed sequence tags) within 17 345 poplar gene models in the UPSC BASE (Sjödin et al., 2006). The nine ESTs correspond to six different gene models (Figure 2D). We made use of a recent high resolution microarray analysis of the poplar vascular cambium (Schrader et al., 2005) in order to test the expression patter of these *KNOX* genes. Two different expression clusters could be identified (Figure 2A), genes with high expression in the cambium but low in zone of secondary wall formation (group I) and an inverse complementary expression pattern, representing genes with low cambial expression but high expression in the zone of secondary wall formation (group II). Group I genes constitute of class I *KNOX* genes only, whereas the group II expression cluster contains both class I and II *KNOX* genes. Interestingly, the two groups are also reciprocally expressed in the zone of final cell maturation, where programmed cell death is induced. The finding that group II genes are up-regulated at sites of terminal differentiation is in sharp contrast to what is known of class I *KNOX* genes in several other plant species. Normally, class I *KNOX* genes are highly expressed in undifferentiated dividing cells and have partly redundant function (Scofield and Murray, 2006; Byrne et al., 2002). It will be interesting to see if the group II genes work additively to the group I genes or antagonistically by e.g. competing for the same binding sites on target genes and therefore enhance the effect of down-regulation of group I genes.

At the site of lateral organ formation, *KNAT1* and *KNAT2* expression is repressed by the MYB domain transcription factor *ASYMMETRIC LEAF1* (*AS1*; Byrne et al., 2002). This mechanism allows cells in the flank of the meristem to differentiate and to give rise to lateral organs. The group I genes behaved similarly than *KNAT1* and *KNAT2* in respect of their down-regulation in the zone of terminal differentiation (Figure 2A). We could identify four different *AS1/2* ESTs in the UPSC BASE of which only *PU12615* gave readable results on the microarrays performed by Schrader et al. (2005). Intriguingly, *PU12615* is reciprocally regulated to the group I genes and therefore a candidate for their repression, suggesting a similar mechanism of transcriptional control as *AS1*performs over *KNAT1* and *KNAT2*.

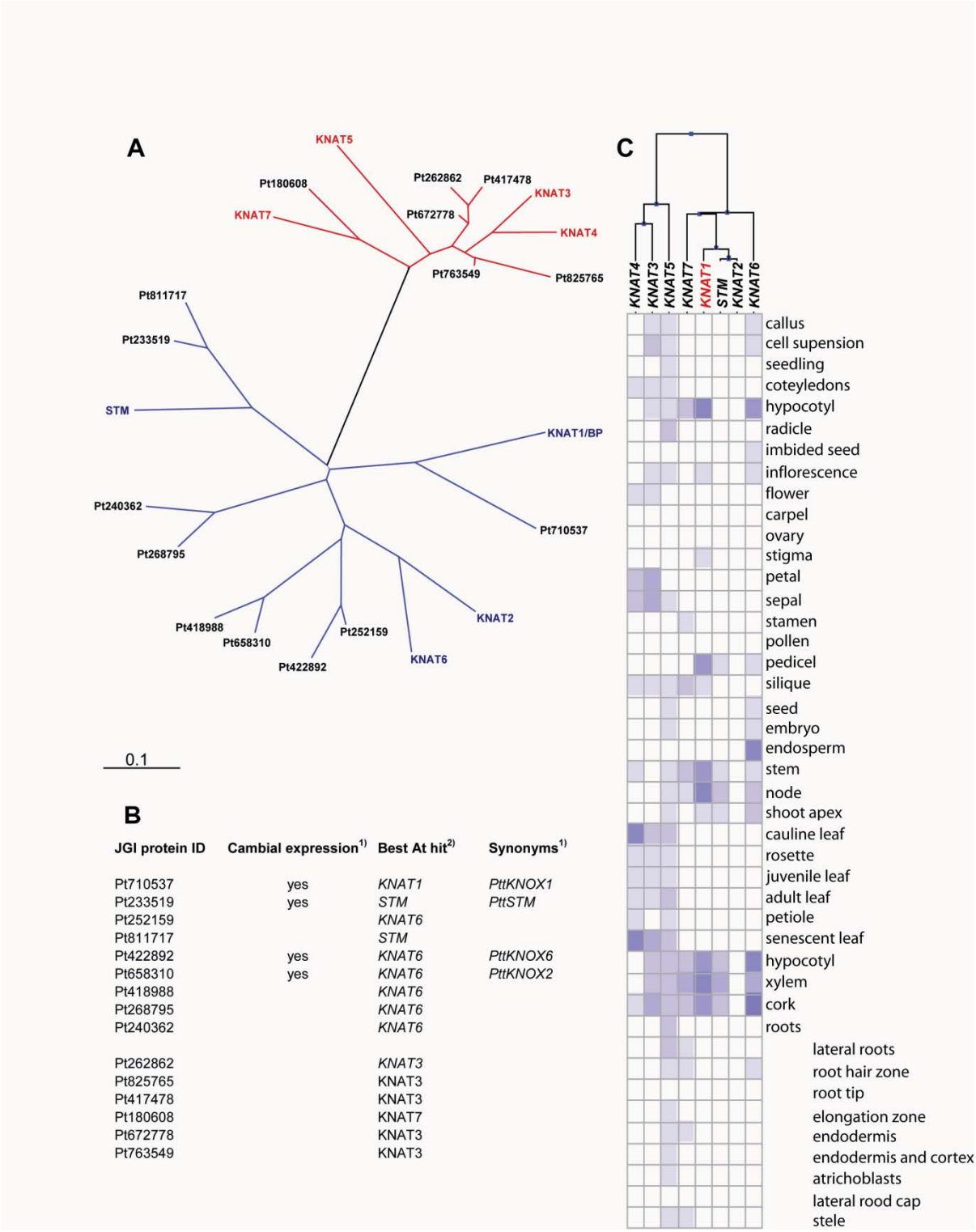

B

JGI protein ID	Cambial expression[1)]	Best At hit[2)]	Synonyms[1)]
Pt710537	yes	*KNAT1*	*PttKNOX1*
Pt233519	yes	*STM*	*PttSTM*
Pt252159		*KNAT6*	
Pt811717		*STM*	
Pt422892	yes	*KNAT6*	*PttKNOX6*
Pt658310	yes	*KNAT6*	*PttKNOX2*
Pt418988		*KNAT6*	
Pt268795		*KNAT6*	
Pt240362		*KNAT6*	
Pt262862		*KNAT3*	
Pt825765		KNAT3	
Pt417478		KNAT3	
Pt180608		KNAT7	
Pt672778		KNAT3	
Pt763549		KNAT3	

Figure 1. A) Phylogenetic tree of all *KNOX* genes of Arabidopsis and poplar. Class I *KNOX* genes are in blue. Class II *KNOX* genes in red. B) Protein models of the identified poplar *KNOX* homologs. Cambial expression and synonyms (1) according to Scharder et al. (2005). (2) refers to best hit in a BLAST search. C) Clustering of microarray data including more than 3000 microarray slides.

The closest poplar homolog of *KNAT1* is strongly down regulated in the zone of secondary cell wall formation (group I expression pattern); the place where the major lignification takes place. Given the role of *KNAT1* in the Arabidopsis vascular tissue as a repressor of lignification, a similar function can be proposed for the poplar *KNAT1* homolog. In order to test if the expression *KNOX* genes within the group I expression cluster correlates with the repression of lignification in tension wood; we re-analyzed the microarray data published by Andersson-Gunnerås et al. (2006). The authors of this study induced tension wood formation by leaning poplar trees to the side under greenhouse conditions. RNA was extracted form tension wood and compared to un-induced wood on the opposite side of the place of tension wood formation. We analyzed the above identified *KNOX* ESTs on their expression in tension wood. None of the group I genes, which are down-regulated during lignification in cambial derivates, was differentially expressed in tension wood (Figure 2B). However, two of the group II genes showed regulation. *PU09838* was down-regulated and, more interestingly, *PU07724* showed a significant up-regulation in tension wood (Figure 2B). A role of *PU07724* in repression of lignification is nevertheless unlikely, since under un-induced conditions it shows low cambial expression and strong expression in the zone of secondary cell wall formation, where lignin is deposited (Figure 2B, C).

The initially formulated hypothesis that repression of lignification during tension wood formation could be due to up-regulation of *KNAT1* homologs can be rejected on the basis of the analyzed data. Nonetheless, it should be kept in mind that only about half of the poplar *KNOX* genes could be analyzed in this work. Additional experiments will be required to finally show if default lignification in cambial derivates and repression of lignin deposition during tension wood formation is co-regulated by the activity of *KNOX* genes. In order to gain a conclusive picture of *KNOX* action on lignification, it will be essential to extent the comparative study of gene expression to functional analyzes. Gene knock-down strategies but also over-expression of the *AS1/2* homolog *PU12615*, which we identified as a putative repressor of group I *KNOX* genes, will provide a handle to achieve better understanding of regulatory networks governing lignification.

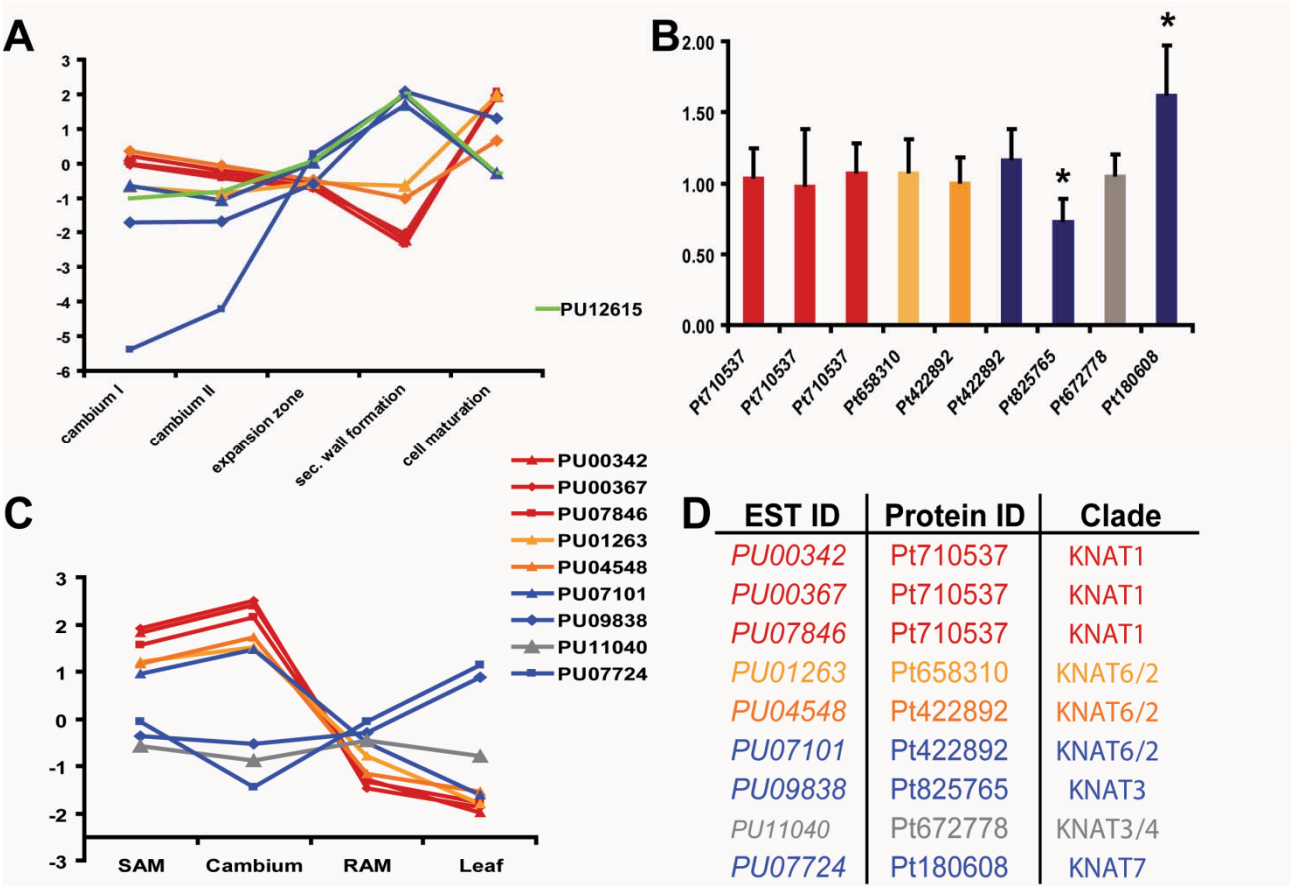

EST ID	Protein ID	Clade
PU00342	Pt710537	KNAT1
PU00367	Pt710537	KNAT1
PU07846	Pt710537	KNAT1
PU01263	Pt658310	KNAT6/2
PU04548	Pt422892	KNAT6/2
PU07101	Pt422892	KNAT6/2
PU09838	Pt825765	KNAT3
PU11040	Pt672778	KNAT3/4
PU07724	Pt180608	KNAT7

Figure 2. Scales *log*(2). A) Expression of *KNOX* genes in the vascular cambium and its derivates, data re-analyzed (Schrader et al., 2005). Genes corresponding to the group I expression cluster are in red. Group II genes in blue. The *AS1/2* homolog *PU12615* behaved like a group II gene and is shown in green. B) *KNOX* gene expression during tension wood formation, data re-analyzed (Andersson-Gunnerås, et al., 2006). Red bars correspond to group I genes, blue bars to group II. C) *KNOX* gene expression in different tissue, data from Schrader et al. (2005). D) Poplar protein models, corresponding EST numbers and phylogenetic clade.

4 References

Andersson-Gunnerås S, Mellerowicz EJ, Love J, Segerman B, Ohmiya Y, Coutinho PM, Nilsson P, Henrissat B, Moritz T, and Sundberg B (2006). Making cellulose enriched tension wood in *Populus*: global analysis of transcripts and metabolites identifies biochemical and developmental regulators in secondary wall biosynthesis. The Plant Journal, 45, 144–165.

Brown DM, Zeef LA., Ellis J, Goodacre R and Turner SR (2005). Identification of novel genes in Arabidopsis involved in secondary cell wall formation using expression profiling and reverse genetics. Plant Cell, 17, 2281–2295.

Byrne ME, Simorowski J and Martienssen RA (2002). *ASYMMETRIC LEAVES1* reveals knox gene redundancy. Development, 129,1957 -1965.

Groover AT, Mansfield SD, DiFazio SP, Dupper G, Fontana JR, Millar R and Wang Y (2006). The *Populus* homeobox gene *ARBORKNOX1* reveals overlapping mechanisms regulating the shoot apical meristem and the vascular cambium. Plant Molecular Biology, 61, 917-932.

Hertzberg M, Aspeborg H, Schrader J, Andersson A, Erlandsson R, Blomqvist K, Bhalerao R, Uhlen M, Teeri TT, Lundeberg J, Sundberg B, Nilsson P, and Sandberg G (2001). A transcriptional roadmap to wood formation. Proceedings of the National Academy of Sciences of the United States of America, 98, 14732-14737.

Joseleau JP, Imai T, Kuroda K and Ruel K (2004). Detection in situ and characterization of lignin in the G-layer of tension wood fibres of *Populus deltoides*. Planta, 219, 338–345.

Lenhard M, Jurgens G and Laux T (2002). The *WUSCHEL* and *SHOOTMERISTEMLESS* genes fulfil complementary roles in Arabidopsis shoot meristem regulation. Development, 129, 3195-3206.

Long JA, Moan EI, Medford JI and Barton MK (1996). A member of the *KNOTTED* class of homeodomain proteins encoded by the *STM* gene of Arabidopsis. Nature, 379, 66-69.

McDougall GJ, Morrison IM, Stewart D, Weyers JDB and Hillman JR (1993). Plant fibres: botany, chemistry and processing for industrial use. J. Sci. Food Agric., 62, 1–20.

Mele G, Ori N, Sato Y and Hake S (2003). The *knotted1*-like homeobox gene *BREVIPEDICELLUS* regulates cell differentiation by modulating metabolic pathways. Genes & Development, 17, 2852-2852.

Schrader J, Nilsson J, Mellerowicz E, Berglund A, Nilsson P, Hertzberg M and Sandberg G (2004). A high-resolution transcript profile across the wood-forming meristem of poplar identifies potential regulators of cambial stem cell identity. Plant Cell, 16, 2278-2292.

Scofield S and Murray JAH (2006). *KNOX* gene function in plant stem cell niches. Plant Molecular Biology, 60, 929-946.

Shani E, Yanai O, and Ori N (2006). The role of hormones in shoot apical meristem function. Current Opinion in Plant Biology, 9, 484-489.

Sjödin A, Bylesjo M, Skogström O, Eriksson D, Nilsson P, Ryden P, Jansson S and Karlsson J (2006). UPSC-BASE –*Populus* transcriptomics online. The Plant Journal, 48, 806–817.

Thompson JD, Higgins DG, and Gibson TJ (1994). CLUSTAL W: improving the sensitivity of progressive multiple sequence alignment through sequence weighting, position-specific gap penalties and weight matrix choice. Nucleic Acids Research, 22, 4673-4680.

Timell TE (1969). The chemical composition of tension wood. Svensk papperstidning, 72, 173–181.

Tuskan GA, DiFazio S, Jansson S, Bohlmann J, Grigoriev I, et al. 2006. The genome of black cottonwood, Populus trichocarpa (Torr & Gray ex. Brayshaw). Science, 313,1596–1604.

Zimmermann P, Hirsch-Hoffmann M, Hennig L, and Gruissem W (2004). GENEVESTIGATOR: Arabidopsis Microarray Database and Analysis Toolbox. Plant Physiology, 136, 2621-2632.

Acknowledgements

الحمد لله رب العالمين

This dissertation would not have been accomplished without the help and support from many people: my supervisors, colleagues, friends and family. Therefore, I would like to thank to those who have contributed to the completion of my study.

First, I would like to express my sincere gratitude to Prof. Dr. Andrea Polle and Dr. Urs Fischer for accepting me as a PhD student, for the outstanding supervision and guidance throughout my doctoral study, for supporting and help in every step of my work.

I am thankful to PD Dr. Thomas Teichmann for the willingness to be my co-referee and to Prof. Dr. Holger Kreft for kindly accepting to be a member of the examination committee.

I am particularly grateful to Xu Jin for valuable help in conducting quantitative real time PCR. I deeply thank to Thomas Klein, Christine Kettner, Marianne Smiatacz, and Bernd Kopka for technical help in laboratory and greenhouse. I also thank all my colleagues at the Department of Forest Botany and Tree Physiology for the pleasant atmosphere.

My deepest gratitude to all expatriated friends from Indonesia who made me feels at home in Göttingen, especially for Wak Tini and family Klein, Mbak Atiet Engel, Ukhti Rita, Essy, Pak Yudi, Mbak Diah, Pak Condro, Mbak Ira, Pak Dadan, Teh Hani and Pak Ichsan. Thank you very much for your kind support in many ways and for the beautiful friendship throughout this time.

My immeasurable thanks to my wife Dr. Nurhasanah, my sons: M. Ariq Athallah Sunaryo and M. Ammar Nurfaza Sunaryo, and also my lovely newborn daughter Alma Sumayyah Sunaryo for being a part of my life and give me strength in difficult moments.

This project was supported by the DFG (Pappelgruppe) to which I am highly indebted. I thankfully acknowledge to the Directorate of General and Higher Education of Indonesia, the Ministry of National Education of Indonesia for the scholarship that made this study possible.

Curriculum Vitae

Personal Data

Name	:	Widi Sunaryo
Date of birth	:	2 April 1973
Place of birth	:	Blitar, Indonesia
Nationality	:	Indonesian
Marital Status	:	Married to Dr. Nurhasanah (three children)
Current address	:	Hermann-Rein Straße 13/111, Göttingen, Germany (37075) E-mail : wsunary@gwdg.de or widi_sunaryo@yahoo.com
Phone	:	(HP)00491798782805

Education

Oct 2007- Nov 2010 : Doctoral studies at the Faculty of Forest Sciences and Forest Ecology, Department of Forest Botany and Tree Physiology
Georg-August-University Göttingen, Germany
Dissertation title: Secondary growth in the *Arabidopsis* hypocotyl
Advisors: Dr. Urs Fischer
Prof. Dr. Andrea Polle
Final grade: Magna Cumlaude

Sept 1998- Jan 2002 : Master in Biotechnology
Bogor Agricultural University, Indonesia
Thesis title: Somaclonal variation of Soybean (*Glycine max* L. Merril) derived from tissue culture and selection for drought tolerance using poly-thylene glycol (PEG)
Advisors: Prof. Dr. Sudarsono
Dr. Hajrial Aswidinnoor
Grade average: 3.92 (on a scale 4.0=excellent to 1.0=failed)

Aug1993 - Jun 1997 : Bachelor in Agronomy
Program study of agronomy, Faculty of Agriculture
Mulawarman University, Samarinda, Indonesia
Thesis title: The Effect of soil tillage and phosphor to the Growth and yield of Cowpea (*Vigna unguiculata* L. Walp)
Advisors: Prof. Dr. Soehartini Riyanto
Ir. Yetty Elidar
Grade average: 3.58 (on a scale 4.0=excellent to 1.0=failed)

Employment Record

1999-Present	:	Lecturer and Researcher, Mulawarman University, Faculty of Agriculture, Department of Agronomy, Samarinda, East Kalimantan, Indonesia.
1997-1998	:	Agricultural Extension Agent, Riotinto Foundation, Bigung Baru, East Kalimantan, Indonesia.

Scholarships

2009-2010	:	DIKTI, DEPDIKNAS, Jakarta, Indonesia
1998-2001	:	University Research Graduate Education (URGE) Batch V, World Bank.
1999-2000	:	Van Deventer Maas Foundation, Jakarta, Indonesia.
1994-1996	:	PT. Badak Bontang, LNG, Bontang, East Kalimantan, Indonesia.

Achievements

1. 2000. The excellent master student with the grade point average (GPA) 4.00 (excellent) for semester 3. Awarded by The Director of Postgraduate Program, Bogor Agricultural University. Bogor, Indonesia.

2. 1999. The excellent master student with the grade point average (GPA) 4.00 (excellent) for semester 2. Awarded by The Director of Postgraduate Program, Bogor Agricultural University. Bogor, Indonesia.

3. 1997. The best graduated bachelor student with the predicate *cumlaude*. Awarded by the Rector of Mulawarman University at the Annual Graduation Ceremony of Mulawarman University, 27 September 1997. Samarinda, Indonesia.

4. 1995. The best student. Awarded by the Dean of Faculty of Agriculture, at the annual selection of the best student, at Faculty of Agriculture, Mulawarman University. Samarinda, Indonesia.

Publications

1. Sunaryo W and Fischer U (2009). *In silico* expression analysis of the *Arabidopsis KNAT1* gene and its homologs in poplar. Review of forests, wood products and wood biotechnology of Iran and Germany - Part III (Ali Reza Kharazipour, Christian Schöpper, Cora Müller and Markus Euring, Eds.). Universitätsdrucke Göttingen, p: 293-301.

2. Sunaryo W, Raras E, Widoretno W, and Sudarsono (2005). Effectiveness of poly-ethylene glycol (PEG) to characterize the response of Soybean genotypes against drought stress. FRONTIER, 19(2): 29-35.

3. Sunaryo W and Sulichantini ED (2004). In vitro regeneration of pepper (*Piper nigrum* (L.). Mahakam Journal, III(2): 76-86.

4. Sunaryo W (2004). The assembling disease-resistant crop plants to endorse agribusiness using biotechnological approach (*Review*). MAPETA, 6 (3): 128-135.

5. Sunaryo W (2004). In vitro regeneration of Soybean via somatic embryogenesis. Buletin Bapeda Kaltim, VI(56): 18-30.

6. Sunaryo W (2003). The asssembling programs of pepper (*Piper nigrum* (L.) resistant to foot root disease caused by fungal *Pytophthora palmivora* Var. Pipperis using biotechnological approach (*Review*). Prosiding, Puslitbang Sosekta, Departemen Pertanian. p :71-175.

7. Sunaryo W (2002). Somaclonal variation of Soybean (*Glycine max* L. Merril) derived from tissue culture and selection for drought tolerance using poly-thylene glycol (PEG). Master thesis.

8. Sunaryo W (1997). The Effect of soil tillage and phosphor to the growth and yield of Cowpea (*Vigna unguiculata* L. Walp). Bachelor thesis.